

UNCLASSIFIED

| |
|---|
| |
| |
| |
| AD NUMBER |
| AD873576 |
| NEW LIMITATION CHANGE |
| TO Approved for public release, distribution unlimited |
| FROM Distribution authorized to U.S. Gov't. agencies and their contractors; Critical Technology; 26 FEB 1970. Other requests shall be referred to Air Force Rocket Propulsion Lab., Edwards AFB, CA. |
| AUTHORITY |
| AFRPL ltr, 20 Mar 1974 |

THIS PAGE IS UNCLASSIFIED

AD873576

Dr 20

A FEASIBILITY STUDY OF COMMAND CONTROL OF SOLID PROPELLANT BURNING RATE

L. H. CAVENY AND M. SUMMERFIELD
PRINCETON UNIVERSITY, DEPARTMENT OF
AEROSPACE AND MECHANICAL SCIENCES

AD NO. —
FILE COPY

TECHNICAL REPORT AFRPL TR-69-249
FEBRUARY 1970

DDC
RECEIVED
SEP 2 1970
RECEIVED

af B

THIS DOCUMENT IS SUBJECT TO SPECIAL EXPORT CONTROLS AND EACH TRANSMITTAL TO FOREIGN GOVERNMENTS OR FOREIGN NATIONALS MAY BE MADE ONLY WITH PRIOR APPROVAL OF AFRPL (APORT/STINFO), EDWARDS, CALIFORNIA 93523

**AIR FORCE ROCKET PROPULSION LABORATORY
AIR FORCE SYSTEMS COMMAND
UNITED STATES AIR FORCE
EDWARDS, CALIFORNIA**

AFRPL-TR-69-249

A FEASIBILITY STUDY OF COMMAND CONTROL
OF SOLID PROPELLANT BURNING RATE

L. H. Caveny and M. Summerfield

This document is subject to special export controls and each transmittal to foreign governments or foreign nationals may be made only with prior approval of AFRPL (APORT/STINFO), Edwards, California 93523.

FOREWORD

This is the final report issued under Contract FO611-69-C-0067. Reported herein is work performed over an eight (8) month period starting 1 April 1969, by the Aerospace and Mechanical Sciences Department of Princeton University located in Princeton, New Jersey. The final report was submitted on 26 February 1970 and was given Aerospace and Mechanical Sciences Department Report Number 893.

The work performed under this contract was monitored by the Air Force Rocket Propulsion Laboratory (AFRPL), Edwards, California. The Project Officer during the initial phases of the program was Captain Charles E. Payne, AFRPL/RPMCP. The Project Officer during the remainder of the program was Captain Leigh E. Stamets, AFRPL/RPMCP.

This technical report has been reviewed and is approved.

Leigh E. Stamets, Capt., USAF
Project Engineer

ABSTRACT

Analytical studies of twenty methods of command control of burning rate were performed to help establish which methods are most likely to be effective. Any method which offers a $\pm 5\%$ or greater throttleability is of interest. Since the study was not directed at a particular application, problems of implementation were not considered in detail. The approaches which received the greatest attention include: thermal radiation by injected particles and inserted intensifiers, acoustic energy, penetration of thermal wave by back flow of combustion gases into either perforated propellants or embedded porous elements, injection of burning rate catalysts, rammed propellant surfaces, and resistive heating. Other methods which were surveyed include: partial quenching, heating through vibration, induced unstable burning, dielectric heating, resistive wire networks, electrical and electromagnetic effects on flames and ingredient decomposition, acceleration forces, and utilization of photochemical processes. The thermal radiation methods should produce 10-50% increases in pressure level, but a practical radiation source is not apparent. The penetration of thermal waves into perforated propellants offers a wide range of control ($>10:1$), but feasibility of controlled burning is not established. The embedded porous element approach should produce $>8:1$ control in high performance systems with reasonable developmental risks. Injection of catalysts is dependent on finding a method of delivering micron size particles to the propellant reaction zones. Two propellants of dissimilar composition, when rammed together, may produce a very wide range of control. Radiation and electrical methods which accelerate the decomposition of some propellant ingredients are largely untried and offer potential. The results emphasize that the merit and practicality of each method is largely dependent on the application.

TABLE OF CONTENTS

| | <u>Page</u> |
|--|-------------|
| List of Figures | vii |
| List of Tables | xi |
| Nomenclature | xii |
| Section I Introduction | 1 |
| Section II Augmentation of Burning Rate by Radiation | 2 |
| A. Radiative Heating to the Propellant Surface | 2 |
| B. Injection of Particulate Matter into the Gas Phase | 7 |
| C. Insertion of Radiation Source to Concentrate Radiative Energy | 9 |
| D. Calculated Effects of Radiation on Burning Rate | 14 |
| Section III Control of Solid Propellant Burning Rates by Acoustic Energy | 22 |
| Section IV Control of Solid Propellant Burning Rate by Means of a Confining Pressure Plate | 34 |
| A. Background | 34 |
| B. Analysis | 38 |
| C. Calculated Effects of Energy Feedback by Means of Opposing Surfaces | 41 |
| Section V Penetration of Thermal Wave in Solid Phase by Back Flow of Combustion Gases into Perforated Propellants | 48 |
| A. Possible Motor Configurations | 49 |
| B. Analysis | 55 |
| C. Calculated Results for Perforated Propellants | 61 |

TABLE OF CONTENTS - (Cont'd.)

| | <u>Page</u> |
|--------------|---|
| Section VI | Embedded Porous Element Rocket Motor (EPERM) 71 |
| | A. Description of Concept 71 |
| | B. Analysis 76 |
| | C. Calculated Results 77 |
| Section VII | Injection of Burning Rate Catalysts via the Gas Phase 86 |
| Section VIII | Resistive Heating of Propellant Surface 89 |
| Section IX | Other Methods of Burning Rate Control 96 |
| | A. Partial Quench of a Propellant Near Its Extinguishment Point 96 |
| | B. Self Heating Through Vibration 96 |
| | C. Induced Unstable Burning as a Means of Increasing Mean Burning Rate 97 |
| | D. Description of Metal Film on Burning Propellant Surface 97 |
| | E. Dielectric Heating 98 |
| | F. Resistive Heating of Wire Network Buried in the Propellant 99 |
| | G. Electrical and Electromagnetic Effects on Solid Propellant Flames 99 |
| | H. Electric Currents to Enhance Decomposition of Certain Propellant Ingredients 100 |
| | I. Acceleration Forces to Alter Propellant Combustion 101 |
| | J. Utilization of Photochemical Process 103 |
| Section X | Conclusion 107 |
| References | 112 |
| DD Form 1473 | |

LIST OF FIGURES

| | <u>Page</u> |
|--|-------------|
| Fig. 1 Effect of Composition on the Flame Temperature of Aluminized AP Composite Propellants with Hydrocarbon Binders (PBCT) | 3 |
| Fig. 2 Radiative Heat Flux as a Function of Temperature and Emissivity | 4 |
| Fig. 3 Effect of AP Percentage on Products of AP Composite Propellants with a Hydrocarbon Binder (PBCT) | 6 |
| Fig. 4 The Trajectories of Individual Particles After They Are Injected Close to the Propellant Burning Surface | 8 |
| Fig. 5 Effect of Axial Position on the Concentration of Injected Particles and Radiative Heat Flux to the Propellant Surface | 10 |
| Fig. 6 Variation of Radiation Interchange Factor for Radiation Between Cylindrical Radiator and Cylindrical Burning Surface | 11 |
| Fig. 7 Semi-Log Plot of the Effect of Separation Distance on Burning Rate and on Radiation Shape Factor | 12 |
| Fig. 8 Burning Rate Increases Resulting From Increasing Radiative Heat Transfer to the Burning Propellant Surface | 18 |
| Fig. 9 Effect of Temperature Sensitivity of Burning Rate on the Burning Rate Enhancement due to Increasing Radiation | 19 |
| Fig. 10 Effect of Basic Propellant Burning Rate on the Burning Rate Enhancement due to Increasing Radiation | 20 |
| Fig. 11 Effect of Weight Mean Diameter on Burning Rate of AP Composite Propellant. | 24 |
| Fig. 12 Upper Limit of Burning Rate as Reduced AP Particle Size Eliminates Diffusional Mixing as a Rate Limiting Process | 25 |
| Fig. 13 Decay of Sound Wave Intensity with Distance From Sound Source (From Ref. 20) | 27 |
| Fig. 14 Effect of Sound Waves on Burning Rate (From Ref. 20) | 28 |

| | | |
|---------|--|----|
| Fig | Effect of Sound Waves on the Burning Rate of Various Propellants (From Ref. 20) | 29 |
| Fig. 16 | Effect of Sonic Irradiation and Helium Flow on Motor Operating Pressure (From Ref. 21) | 31 |
| Fig. 17 | Burning Rate Augmentation by Gas Flow and Sonic Irradiation (From Ref. 21) | 32 |
| Fig. 18 | Schematic Views of Disks Rammed Against Propellant Burning Surface to Produce Enhanced Burning Rates | 35 |
| Fig. 19 | Schematic Drawing of Burning Propellant Surfaces Being Rammed Together | 36 |
| Fig. 20 | Burning Rate Augmentation Resulting From Ramming Propellant With a Cluster of Hollow Tubes (From Ref. 31) | 37 |
| Fig. 21 | Control Volume Used in the Model to Analyze Burning of Propellant Surfaces Whose Pressure and Velocity Distributions are Influenced by an Opposing Surface | 39 |
| Fig. 22 | Static Pressure, Mach Number, and Separation Distance for Propellant Being Rammed by a Long Flat Ram | 42 |
| Fig. 23 | Effect of Ram Geometry on Pressure and Mach Number Across Propellant Surface | 45 |
| Fig. 24 | Effect of Ram Width on Ramming Force and on Increase in Chamber Pressure Produced by Ramming Propellant | 46 |
| Fig. 25 | Effect of Separation Distance at Ram Centerline on Ramming Force and on Increase in Chamber Pressure Produced by Ramming Propellant | 47 |
| Fig. 26 | Schematic Showing Perforated Propellant Grain in a Solid Propellant Rocket Motor | 50 |
| Fig. 27 | Transients During Constant Thrust Operation of Rocket Motor With Perforated Propellant Grain | 52 |
| Fig. 28 | The Type of Throat Area Response That Will Be Required to Make Continuous Corrections to Thrust | 53 |
| Fig. 29 | Response to Non-Uniform Burning of Motors With Vented Head-Ends and Closed Head-Ends | 54 |

| | <u>Page</u> |
|---|-------------|
| Fig. 30 Idealized Model of Fluid Flow and Thermal Zones in Burning Perforated Propellant Showing a Single Perforation | 56 |
| Fig. 31 Pressure and Temperature Along Perforation for Datum Case Conditions | 64 |
| Fig. 32 Gas Velocity and Convective Heat Transfer Coefficient Along Perforation for Datum Case Conditions | 65 |
| Fig. 33 Perforated Propellant Burning Rate and Mass Flow Rate into Perforation as a Function of Chamber Pressure | 66 |
| Fig. 34 Effect of Perforation Diameter on Mass Flow Rate and Burning Rate | 67 |
| Fig. 35 Burning Rate and Mass Flow Rate as a Function of Head-End Pressure | 69 |
| Fig. 36 Burning Rate as a Function of Grain Length | 70 |
| Fig. 37 New Rocket Motor Configuration That Contains Porous Axial Elements That Have Very High Gas Flow Resistances | 72 |
| Fig. 38 Rocket Motor Containing Thin Wall, Metal Tubes Embedded Axially in the Propellant | 74 |
| Fig. 39 Analytical Model for Steady State Burning of Propellant Along an Embedded Tube With Bleed Flow | 75 |
| Fig. 40 Analytical and Experimental Burning Rates vs Bleed Flow | 75 |
| Fig. 41 Effect of Propellant Composition on Tube Burning Rate | 75 |
| Fig. 42 Burning Rate Along Embedded Porous Element as a Function of Mass Flow Rate of Hot Combustion Gases | 78 |
| Fig. 43 Parameters of Embedded Porous Element Rocket Motor upto an 8:1 Pressure Modulation Ratio | 79 |
| Fig. 44 Pressure at the Head-End of a Porous Element with Chamber Pressure, Flow Rate, and Spherical Packing Diameter as Parameters | 80 |
| Fig. 45 Pressure Differential Between Combustion Chamber and Head End Plenum With Porosity of Embedded Element as a Parameter | 82 |

| | <u>Page</u> |
|---|-------------|
| Fig. 46 Pressure Differential Between Combustion Chamber and Head End Plenum With Diameter of Spherical Packing as a Parameter (Porosity = 0.5) | 83 |
| Fig. 47 Pressure Differential Between Combustion Chamber and Head End Plenum With Diameter of Spherical Packing as a Parameter (Porosity = 0.4) | 84 |
| Fig. 48 Rocket Motor Configuration to Obtain Uniform Distribution of Injected Catalyst by Means of a Piccolo Tube Injector | 87 |
| Fig. 49 Resistive Heating of Propellant Surface | 90 |
| Fig. 50 Effect of Temperature on Volume Resistivity of Various Plastics (From Ref. 44 and 45) | 91 |
| Fig. 51 Effect of Electrical Heating on Propellant Burning Rate for Propellants with Typical Temperature Sensitivity of Burning Rate | 94 |
| Fig. 52 Effect of Electrical Heating on Propellant Burning Rate for Propellants With Moderately High Temperature Sensitivity of Burning Rate | 95 |
| Fig. 53 Schematic Design Showing Propellant Rod Which Can Be Either Rotated or Oscillated About its Longitudinal Axis in the Combustion Chamber | 102 |
| Fig. 54 Effect of Propellant Rod Angular Velocity on Removal of Aluminum and Aluminum Oxide From Propellant Surface | 104 |

LIST OF TABLES

| | | <u>Page</u> |
|---------|--|-------------|
| Table 1 | Effect of Radiator Distance from Propellant Surface on Propellant Burning Rate (Ref. 11) | 13 |
| Table 2 | Datum Case Values for Evaluating Effect of Radiative Heating on Propellant Burning Rate | 17 |
| Table 3 | Datum Case Values Used in Opposing Slab Calculations | 43 |
| Table 4 | Datum Case Values Used in Perforated Propellant Calculations | 62 |
| Table 5 | Effects of Outward-Directed Radial Acceleration Fields on Burning Rates | 105 |
| Table 6 | Methods of Obtaining Command Control of Burning Rate- Conclusions and Summary | 108 |

NOMENCLATURE

| | | |
|-------|---|----------------------------|
| a | coefficient of aP^n burning rate law | |
| a | chemical kinetic reaction time parameter in Granular Diffusion Flame model | |
| A_b | propellant burning surface area | cm^2 |
| A_p | cross-sectional area of port | cm^2, in^2 |
| A_t | throat area | cm^2 |
| A_v | discharge area of valve that vents head-end plenum to the atmosphere | cm^2 |
| b | diffusional mixing time parameter in Granular Diffusion Flame model | |
| c | specific heat | cal/g K |
| c | acoustic velocity | cm/sec |
| c | exponent in erosive burning law $r = r_o (M/M_{\text{crit}})^c$ | |
| C_F | thrust coefficient | |
| c^* | characteristic velocity of combustion products | cm/sec |
| D | diameter | in, cm |
| d_e | diameter of embedded porous element | cm |
| D_i | inside diameter of tube | cm |
| d_m | mean diameter of oxidizer particles | μ |
| d_m | mean diameter of spherical particles that make up porous element | cm |
| E | voltage | volts |
| f | friction factor | |
| F | thrust; overall radiation interchange factor from combustion products to propellant surface | |
| g | gravitational constant | |

| | | |
|-------------|---|---------------------------|
| h | separation distance | in |
| h | convective heat-transfer coefficient | cal/cm ² sec K |
| k | thermal conductivity | cal/cm sec K |
| L | length | cm |
| M | Mach Number | |
| \dot{m} | mass rate of gas flow | lbm/sec, g/sec |
| \bar{m}_g | average molecular weight | g / g - mole |
| n | exponent of aP^n burning rate law | |
| P | pressure | atm, psia |
| p_s | sound pressure | atm |
| q | heat flux | cal/cm ² sec |
| r | burning rate | cm/sec |
| r | radius | in, cm |
| R | electrical resistance | ohms |
| R | universal gas constant | 1.9867 cal/g-mole K |
| r_b | burning rate of propellant adjacent to embedded element without back flow of combustion gases | cm/sec |
| r_e | burning rate of propellant adjacent to embedded porous element with back flow of combustion gases | cm/sec |
| r_o | basic burning rate of propellant without enhancement | in/sec, cm/sec |
| r_t | burning rate of propellant adjacent to an embedded thin wall aluminum tube <u>with</u> a back flow of hot combustion gases | cm/sec |
| r_{to} | burning rate of propellant adjacent to an embedded thin wall aluminum tube <u>without</u> a back flow of hot combustion gases | cm/sec |
| r_w | radius of wall of perforation | cm |
| t | time | sec |

| | | |
|------------|--|---------------------|
| T | temperature | K |
| u_r | gas velocity in radial direction | cm/sec |
| u_z | gas velocity in axial direction | cm/sec |
| V | volume | cm ³ |
| w | mass flow rate | lbm/sec |
| x | distance normal to axial coordinate, z | in, cm |
| y | ratio of the forward component of velocity of injected gases to the main stream velocity | |
| z | distance in axial direction | in, cm |
| α | decay coefficient of a sound wave | |
| ϵ | emissivity of source radiating to propellant surface | |
| ϵ | porosity | |
| δ | thickness of acoustic boundary layer | cm |
| γ | ratio of specific heats | |
| ρ | density | g / cm ³ |
| σ | Stefan-Boltzmann's constant | |
| σ_p | temperature sensitivity of burning rate at constant pressure | %/K |
| τ_w | shear stress at the wall | |
| τ_w | wall thickness | |
| μ | viscosity | g / cm sec |
| ζ | particle displacement in a traveling acoustic wave | cm |
| ω | angular frequency | rad/sec |

Subscripts

| | |
|----|---------------|
| c | motor chamber |
| cl | center line |

| | |
|-------|---|
| crit | critical condition for onset of erosive burning |
| cyl | cylinder |
| dis | discharged through nozzle |
| e | porous element |
| elect | electrical heating |
| end | end of perforation |
| F | flame |
| g | gas |
| gen | generated by propellant combustion |
| h | head-end plenum |
| i | initial condition |
| ign | ignition |
| K_n | constant burning surface area to throat area ratio, A_b/A_t |
| o | reference conditions |
| p | propellant, pressure |
| per | perforation |
| rad | radiation |
| ref | reference temperature |
| s | propellant surface |
| t | embedded thin wall metal tube |
| v | valve |
| w | wall of perforation |

SECTION I

INTRODUCTION

The objective of this study was to perform investigations of the design concepts and basic principles relating to command control of solid propellant burning rates. The results of this study are to be used to help establish those methods which are most likely to be effective and thus warrant further investigation. Previous analytical and experimental studies have shown that thrust magnitude and pressure level control can be achieved mechanically by such means as varying the throat diameter, exposing more propellant surface, and injecting mass. The more attractive direction, in principle, is to modulate the propellant burning rate directly. Various ideas have been presented in the past for doing this and exploratory experiments have been performed in various laboratories. Partial success has been achieved in some cases, but none of the approaches have achieved wide acceptance.

We believe that this lack of success may be attributed, in part, to an incomplete understanding of the solid propellant burning process. Since the knowledge of how solid propellants burn has greatly increased in the last few years, the re-examination of previously suggested concepts and a search for new methods is timely.

In this report twenty possible methods are broadly surveyed. In almost all instances, a statement of the scheme, acknowledgment of previous work, and a discussion of the physical basis is given. For several of the concepts we have offered physical models and used them to approximate the extent of the burning rate control that can be achieved. For other concepts, we had difficulty finding a plausible mechanism to justify any optimism, and we proceeded to point out the limitations that we saw.

In this study any approach which offers a $\pm 5\%$ or greater range of throttleability was considered to be of interest. Since the study was not directed at a particular type of rocket motor, the practicality of the various concepts in terms of such items as mass fraction penalty, specific impulse, response time, and power required were not to be evaluated. Thus a concept that is absolutely inconceivable as part of a high performance sustainer may be quite practical for use in a small warm gas generator.

The discussions and analyses in this report are the result of a very small study program and, as a consequence, merely introduce the very interesting subject of command control of burning rate. Many of the concepts discussed in this report should be the subject of more extensive studies and should be evaluated experimentally.

SECTION II

AUGMENTATION OF BURNING RATE BY RADIATION

Since for most propellants radiative heating from the flame provides part of the heat required to decompose the propellant surface, burning rate control can be obtained by controlling the radiative heat flux to the burning propellant surface. Two methods of increasing the radiative heat flux to the solid propellant surface will be discussed: the injection of particulate matter into the combustion chamber and the insertion of a radiative device into the combustion chamber.

For purposes of this report, the prediction of the effectiveness of using radiative means to control burning rate will be considered in two inter-related parts: (1) a discussion of the radiative heat flux to the propellant surface and (2) the effect of radiation on burning rate.

A. Radiative Heat Flux to Propellant Surface

The following methods of intensifying radiative heating to the propellant surface were investigated:

1. Inject into the combustion chamber a particulate matter that radiates with a high effective emissivity.
2. Insert into the combustion chamber a device that is heated by the hot combustion gases and re-radiates to the propellant surface.
3. Place adjacent to the burning surface a device that is heated by an external power supply.*

Radiation as a means of obtaining burning rate control appears to offer little promise for propellants that use metal fuel additives. The primary difficulty is that metal fuel additives, such as aluminum, are only partially reacted when they leave the propellant surface and, thus, form a cool (between 900 and 1400K) layer of partially oxidized metal particles in the gas layer immediately above the propellant surface. This layer of metal and metal oxide particles tends to absorb and block from the propellant surface the radiant energy that originates in the combustion chamber. This inherent characteristic of metallized propellants is unfortunate since the very high flame temperatures achieved by metallized propellants (see Fig. 1) could produce very high heat fluxes. Fig. 2 shows the range of radiative heat fluxes that correspond to the range of propellant flame temperatures. The radiative

*The addition of external energy will increase the flame temperature and the thrust generated by the nozzle.

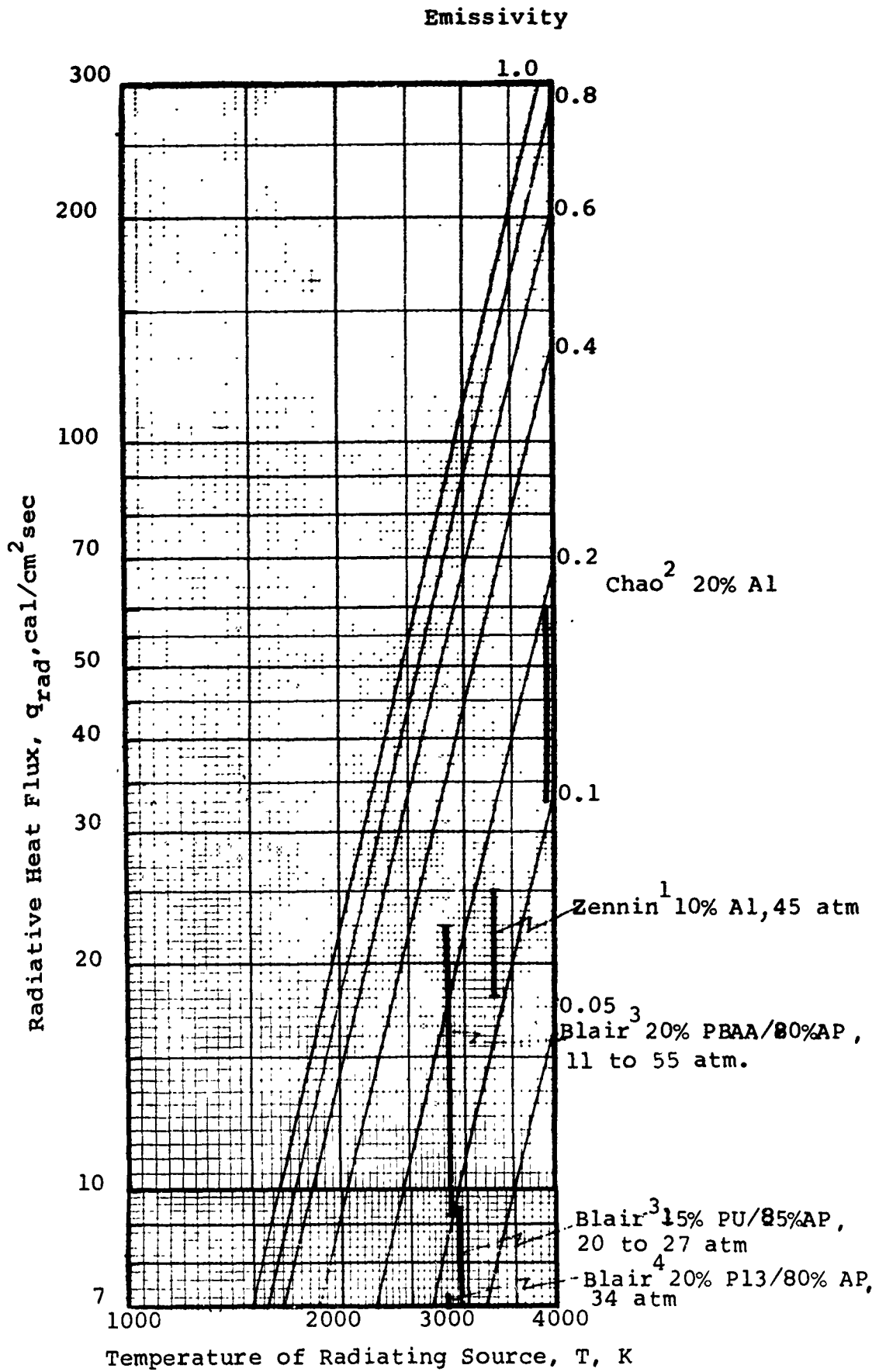


Fig. 2 Radiative Heat Flux as a Function of Temperature and Emissivity

heat flux from an aluminized propellant with a flame temperature of approximately 3500K is several times that of typical non-metallized propellants with flame temperatures usually less than 2500K.

Included in Fig. 2 are values of radiative heat flux reported in the literature for non-metallized and aluminized propellants. Since the flame temperatures of the various propellants are known, the measured heat fluxes give an indication of the effective emissivity of the gas and particle clouds. The results of Zennin¹ are consistent with those reported by Chao² in that the effective emissivity of the alumina cloud is approximately 0.2. Blair³ recently reported the effective emissivity of non-metallized AP composite propellants and suggested that radiative heat flux is strongly influenced by binder type and pressure. Also included in Fig. 2 are the data obtained at Princeton⁴. The data reported by Zennin are consistent with the approximate calculations for radiation from H₂O and CO₂ that were made using the techniques of Hottel and Safofim⁵.

An examination of the effect of aluminum fuel additives on propellant burning rate provides evidence that the relatively cool aluminum and alumina clouds block radiation from the burning surface. Ref. 6 discusses a series of experiments where the ratio of AP to binder was held constant as the aluminum content of the propellants was varied, from 0 to 15%. As indicated in Figure 1, the increase in aluminum content increases the theoretical flame temperature from 2050 to 2930 K. Even though it is reasonable to conclude that the increase in flame temperature produces a corresponding increase in the radiative heat flux from the flame, the data of Ref. 6 show that as the aluminum content is increased from 0 to 15% the burning rate decreases by as much as 15%. The effect of flame temperature and emissivity on the radiative heat flux is given by Fig. 2. Admittedly, the interactions between such items as the heat required to melt the aluminum, the increase in flame temperature, and the amount of thermal radiation blocked by the particles are complex; however, the data provide absolutely no encouragement to the notion that the addition of either particles which radiate with a higher emissivity than aluminum oxide or other radiation sources will be an effective means of burning rate control for metallized propellants. Thus it appears that if radiation is to be effectively used as a means of burning rate control, the propellant should not contain metal fuel additives.

Non-metallized propellants produce gaseous products which re-radiate to the propellant surface. But as indicated on Fig. 2 the heat flux from the relatively low flame temperature products produce correspondingly low radiative heat fluxes to the burning surface. Fig. 3 shows the combustion products of AP composite propellants. These results were calculated using the thermochemical program described in Ref. 7. The gaseous products H₂O and CO₂ are the primary sources of radiant energy from the combustion products⁵. These products are relatively transparent to thermal radiation and will not

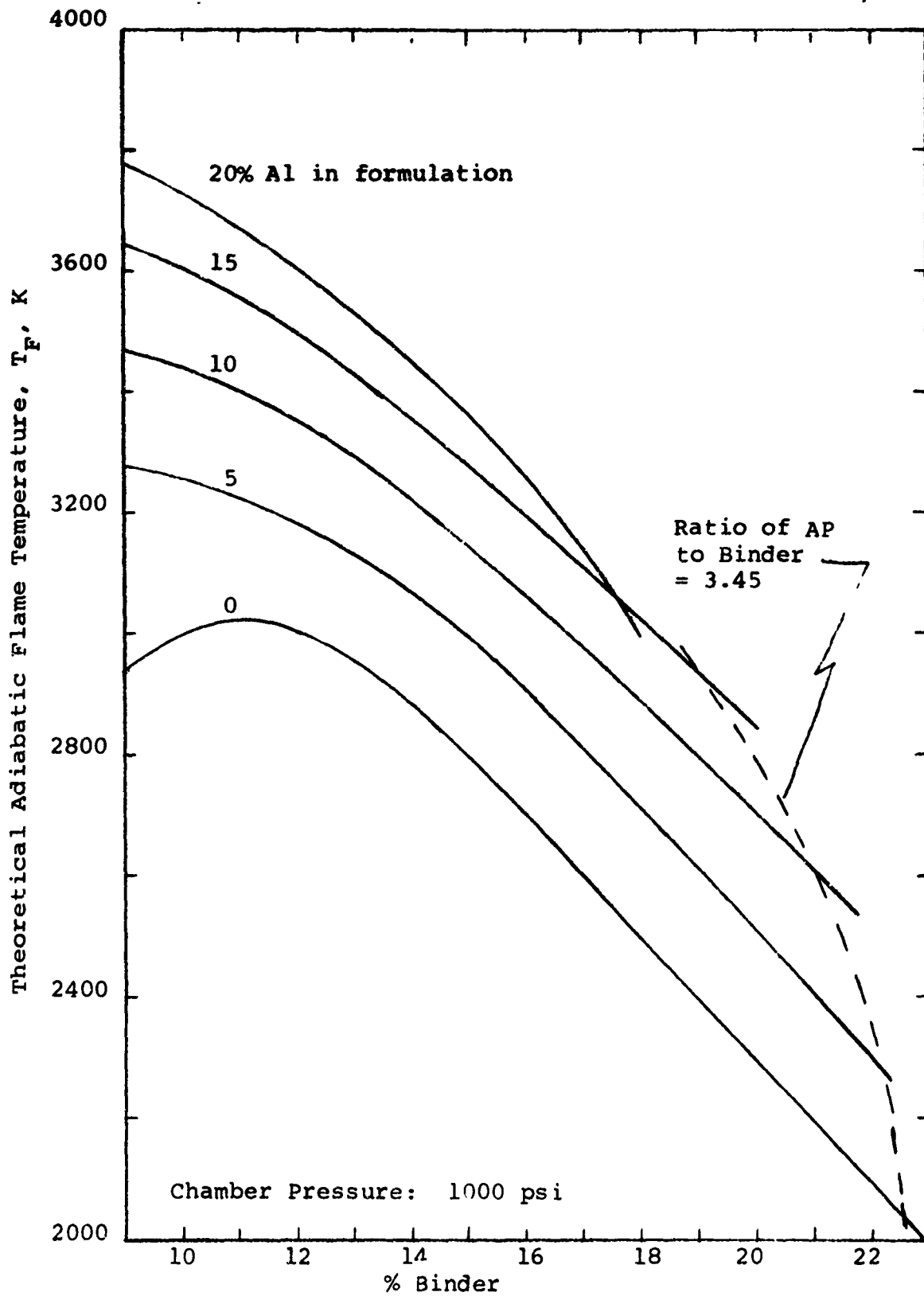


Fig. 1 Effect of Composition on the Flame Temperature of Aluminized AP Composite Propellants with Hydrocarbon Binders (PBCT)

heat flux from an aluminized propellant with a flame temperature of approximately 3500K is several times that of typical non-metallized propellants with flame temperatures usually less than 2500K.

Included in Fig. 2 are values of radiative heat flux reported in the literature for non-metallized and aluminized propellants. Since the flame temperatures of the various propellants are known, the measured heat fluxes give an indication of the effective emissivity of the gas and particle clouds. The results of Zennin¹ are consistent with those reported by Chao² in that the effective emissivity of the alumina cloud is approximately 0.2. Blair³ recently reported the effective emissivity of non-metallized AP composite propellants and suggested that radiative heat flux is strongly influenced by binder type and pressure. Also included in Fig. 2 are the data obtained at Princeton⁴. The data reported by Zennin are consistent with the approximate calculations for radiation from H₂O and CO₂ that were made using the techniques of Hottel and Safofim⁵.

An examination of the effect of aluminum fuel additives on propellant burning rate provides evidence that the relatively cool aluminum and alumina clouds block radiation from the burning surface. Ref. 6 discusses a series of experiments where the ratio of AP to binder was held constant as the aluminum content of the propellants was varied, from 0 to 15%. As indicated in Figure 1, the increase in aluminum content increases the theoretical flame temperature from 2050 to 2930 K. Even though it is reasonable to conclude that the increase in flame temperature produces a corresponding increase in the radiative heat flux from the flame, the data of Ref. 6 show that as the aluminum content is increased from 0 to 15% the burning rate decreases by as much as 15%. The effect of flame temperature and emissivity on the radiative heat flux is given by Fig. 2. Admittedly, the interactions between such items as the heat required to melt the aluminum, the increase in flame temperature, and the amount of thermal radiation blocked by the particles are complex; however, the data provide absolutely no encouragement to the notion that the addition of either particles which radiate with a higher emissivity than aluminum oxide or other radiation sources will be an effective means of burning rate control for metallized propellants. Thus it appears that if radiation is to be effectively used as a means of burning rate control, the propellant should not contain metal fuel additives.

Non-metallized propellants produce gaseous products which re-radiate to the propellant surface. But as indicated on Fig. 2 the heat flux from the relatively low flame temperature products produce correspondingly low radiative heat fluxes to the burning surface. Fig. 3 shows the combustion products of AP composite propellants. These results were calculated using the thermochemical program described in Ref. 7. The gaseous products H₂O and CO₂ are the primary sources of radiant energy from the combustion products⁵. These products are relatively transparent to thermal radiation and will not

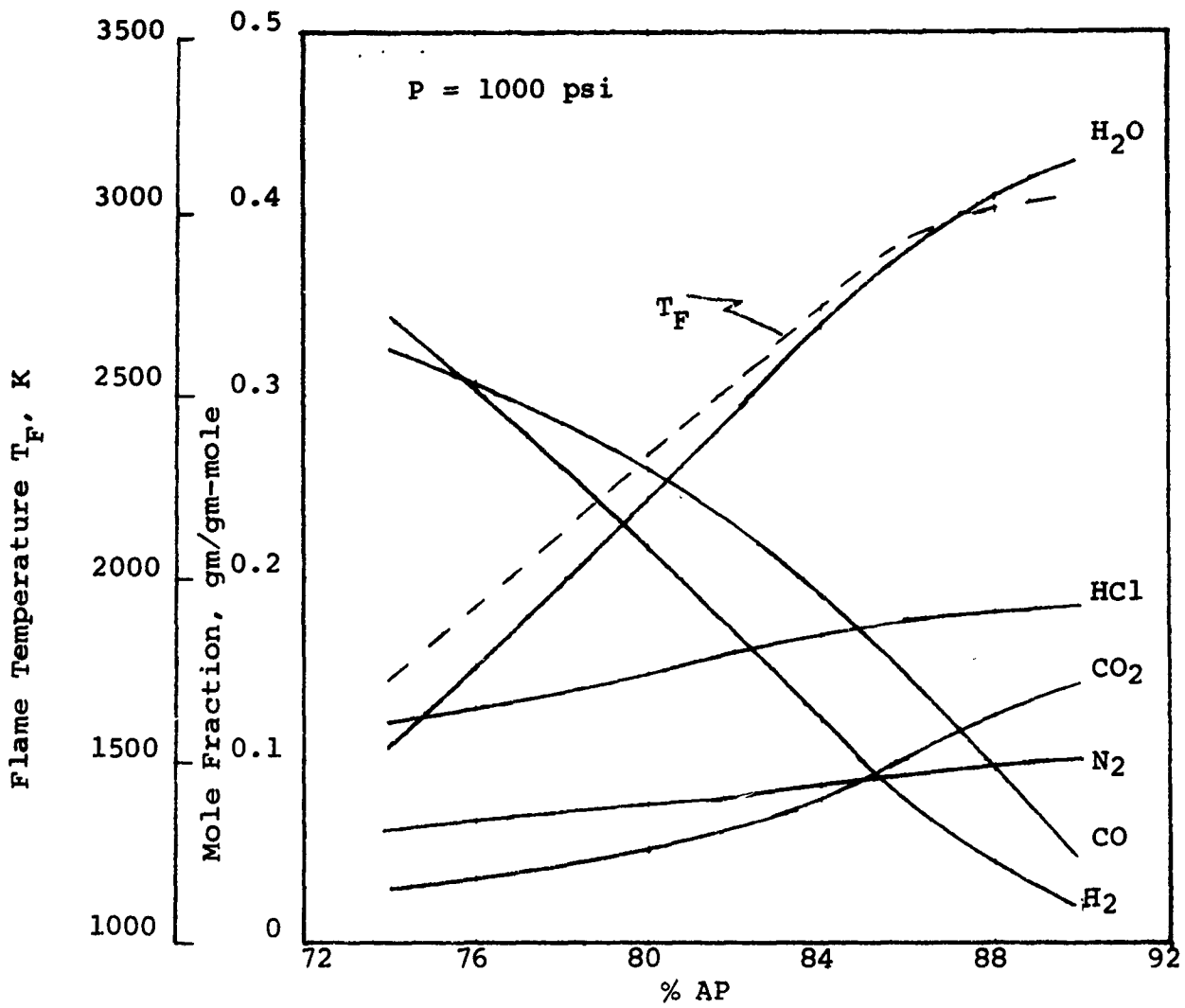


Fig. 3 Effect of AP Percentage on Products of AP Composite Propellants With a Hydrocarbon Binder (PBCT) and Without Metal Fuel Additives

prevent thermal radiation from reaching the burning propellant surface . Thus when additional radiative energy sources are placed in the combustion chamber, a large portion of the radiative energy should reach the burning surface. Based on results in Ref. 8 and 9, clouds of carbon particles can be made to radiate with an effective emissivity of greater than 0.8. Thus carbon particles should be effective in Method 1. A device that radiates more nearly as a black body can be inserted into the combustion chamber (Method 2). Depending on the application, such a device may be more attractive from a weight standpoint than the methods using injected particles that are continuously discharged from the combustion chamber. As indicated in Fig. 2, increasing the temperature of the radiating body greatly affects the heat flux level. Devices which are heated to temperatures higher than flame temperatures (Method 3) may be attractive in systems where relatively large onboard electrical power supplies are available.

When small propellant strands are burned in a bomb, the heat transfer by radiation can have compensating effects. Radiant energy feedback from the flame augments the heat conduction from the gas phase to the solid phase. But an equally significant reduction in flame temperature occurs because of heat loss from the flame to the relatively cool walls of the bomb. When propellant is burned in a radial-burning motor, the combustion products near the propellant surface do not see cold walls and the heat is retained in the combustion products indicating that motor radiation data, rather than strand radiation data, will be required to accurately evaluate radiation effects on burning rate.

B. Injection of Particulate Matter into the Gas Phase

Injection of particulate matter into the gas phase (Method 1) was considered as a means of altering the heat feedback to the propellant surface. It is not likely that particulate matter will appreciably alter the chemical reactions at the propellant surface. However, injected particulate matter could affect the heat transfer to the propellant surface, either by changing the radiative properties of the combustion gases or by affecting the energy level of the combustion products. Particulate matter has been injected into rocket motors to achieve extinguishment¹⁰; this use as an energy-spoiling coolant is a penalty too severe for practical burning rate control. Similarly, if an injectant were used to increase the energy level of combustion products, the technology would approach that of the hybrid rocket motors.

An important consideration in predicting the radiative heat transfer from the injected particulate matter and, thus, the effects caused by injecting particulate matter is the particle cloud density as a function of distance from the burning surface. If the particles are injected at the head-end as indicated in Fig. 4, the particle cloud density will not be uniform along the grain.* Also, the gases leaving the propellant surface will continuously displace the injected particles

*For steady state conditions, it is recognized that the number of particles that passes through a transverse cross-section of the port does not vary with longitudinal distance.

-- -- Velocity profiles

▲ □ ○ Individual particles (or droplets) shown at different points along their trajectories

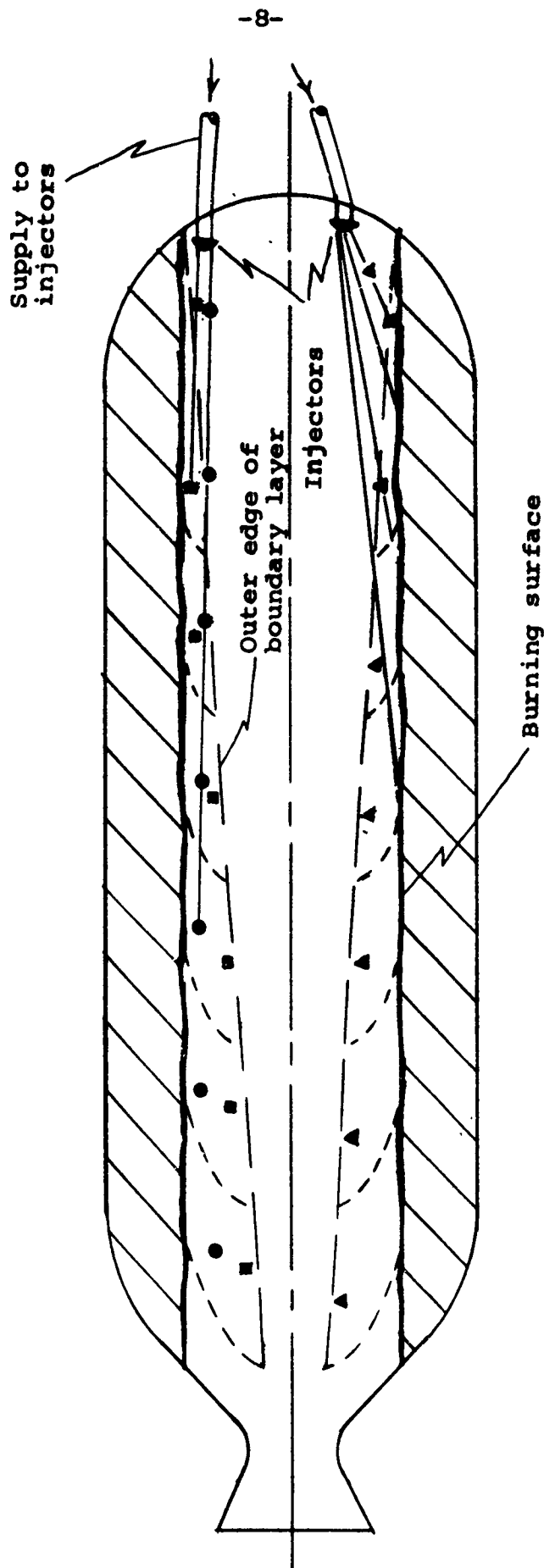


Fig.4 The Trajectories of Individual Particles After They are Injected Close to the Propellant Burning Surface.

away from the burning surface. As indicated in Fig. 5, the increasing gas velocity in the direction of flow decreases the particle cloud density and, as a consequence, decreases the particle residence time per unit length of propellant burning surface. Also, propellants which contain metal fuel additives and other radiation absorbers form clouds above the burning surface which tend to prevent radiation from the injected particles from reaching the propellant surface. This discussion of the nonuniformity of injected particle clouds not only points out factors that complicate analyses to predict the degree of burning rate control, but also casts serious doubt on the practicality of approaches that use injected particles.

C. Insertion of Radiation Source to Concentrate Radiative Energy.

The concept of a device that is inserted into the combustion chamber and heated by the hot combustion gases for the purpose of intensifying the radiant heating to the propellant was considered. Depending on the motor geometry several such devices can be envisioned. For example, to achieve the uniform radiant heating along an internal burning propellant configuration, the radiation source is extended along the entire length of the grain. The radiation source would achieve a temperature somewhat less than the flame temperature and re-radiate to the propellant surface with an effective emissivity higher than that of the combustion gases. Since the radiant energy that arrives at the burning surface increases as the diameter of the radiation source increases (see Fig. 6), burning rate control can be achieved by adjusting the diameter of the radiation source. Of course, the practicality of fabricating such a light weight and expendable radiation source is doubtful.

The use of a radiant heat source to modify the burning rate of solid propellant was the subject of a patent issued to Gessner¹¹ (assigned to the Phillips Petroleum Company). He provided for a mechanical drive system whereby either a hot plate or another burning propellant surface could be brought arbitrarily close to the propellant surface. A series of experimental results for ammonium nitrate propellants (these propellants did not have metal fuel additives) were reported in the patent. These results are shown in Fig. 7 and Table 1. Attempts were made to provide a mechanism that explains the burning rate changes in terms of the distance separating the opposing propellant surfaces. At present, the source of effective radiant heating is unclear. For instance, in the case of the opposing propellant surfaces, it is unlikely that one relatively cool solid propellant surface provides appreciable radiant heating to the other. It is more likely that the hotter gaseous emitters such as H_2O and CO_2 are the important radiant heat sources. If this is

* Reradiation increases flame temperature on the propellant side of the reradiator but as combustion gases heat the reradiator they return to normal flame temperature. The reradiator temperature depends on the heat transfer rate from the combustion gases to the reradiator.

- Particles injected at head-end to intensify radiative heating to the propellant surface

- Alumina particles

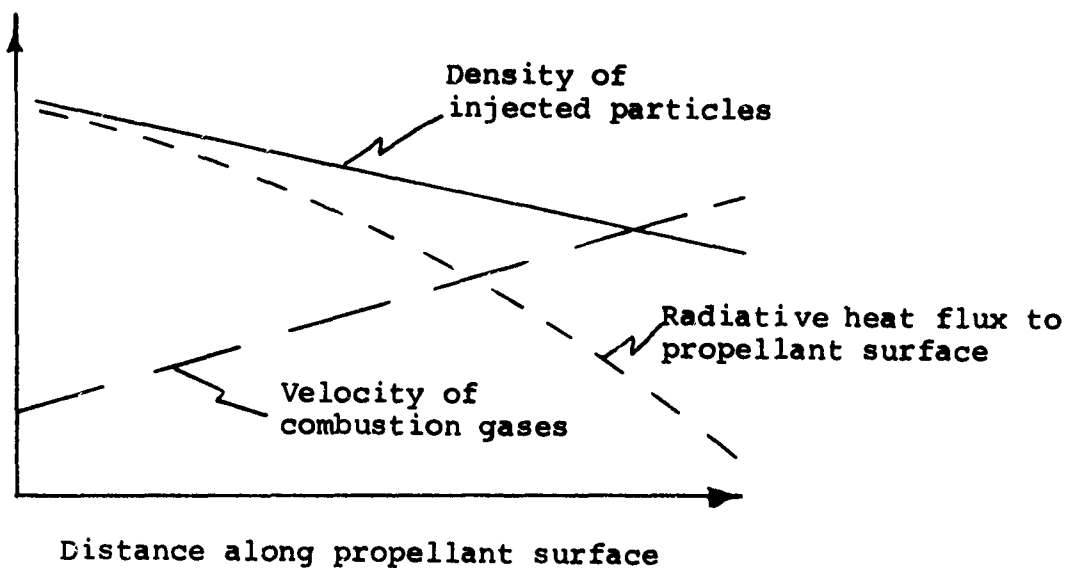
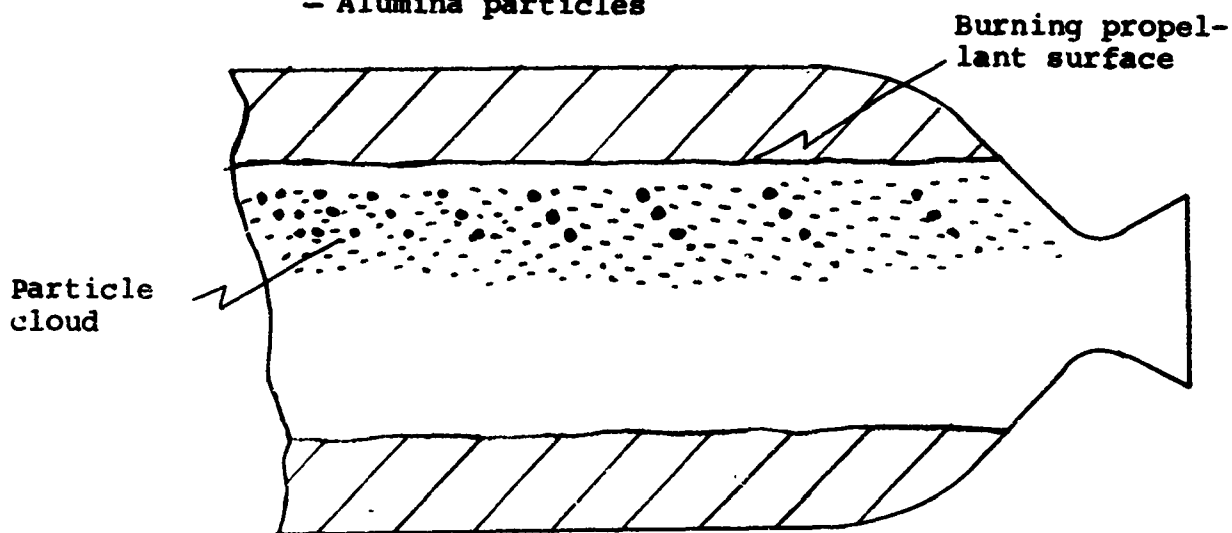


Fig. 5 Effect of Axial Position on the Concentration of Injected Particles and Radiative Heat Flux to the Propellant Surface

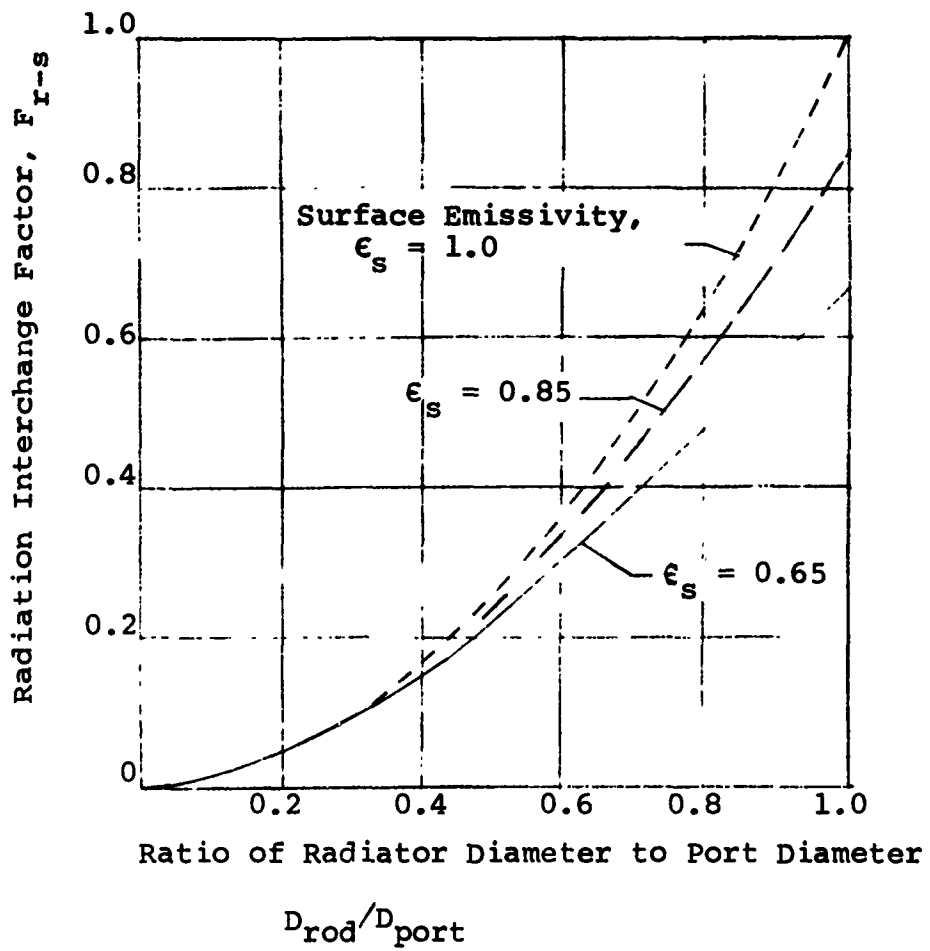
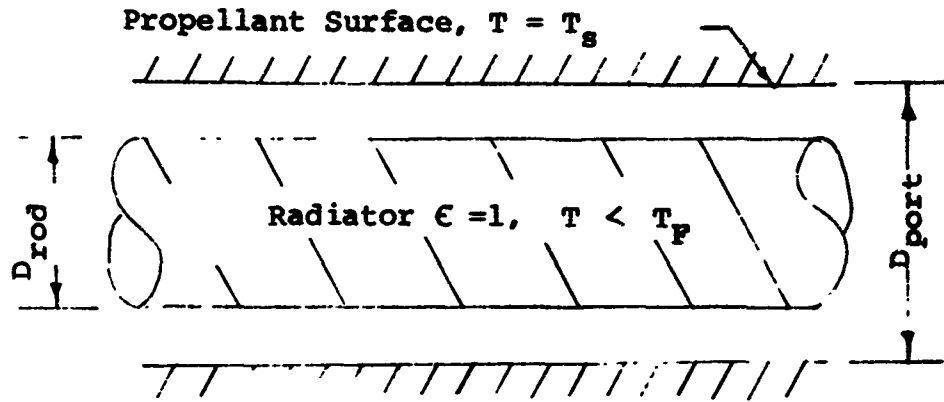


Fig. 6 - Variation of Radiation Interchange Factor for Radiation between Cylindrical Radiator and Cylindrical Burning Surface.

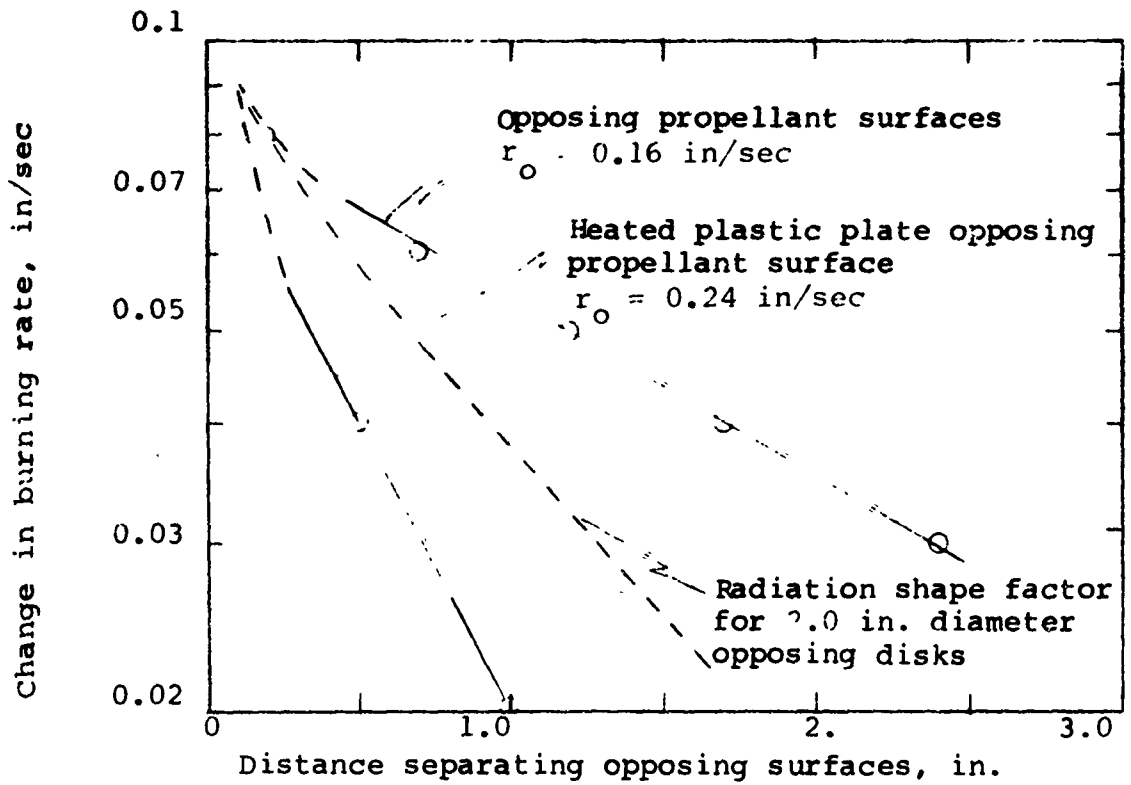


Fig. 7 Semi-log Plot of the Effect of Separation Distance on Burning Rate and on Radiation Shape Factor

TABLE I

Effect of Radiator Distance from Propellant Surface
on Propellant Burning Rate (Ref. 11)

Propellant A

| <u>Distance from</u> <u>Surface, in</u> | <u>r₆₀₀, in/sec</u> |
|--|--------------------------------|
| 0.1 | 0.33 |
| 0.2 | 0.30 |
| 0.5 | 0.28 |
| 1.0 | 0.26 |
| 2.0 | 0.24 |

Propellant B

| <u>Distance from</u> <u>Surface, in</u> | <u>r₆₀₀, in/sec</u> |
|--|--------------------------------|
| 0.1 | 0.25 |
| 0.4 | 0.23 |
| 1.2 | 0.21 |
| 2.5 | 0.19 |
| 5.7 | 0.17 |
| 10.0 ⁺ | 0.16 |

the case, then it is difficult to explain the distance effect in terms of the very low absorptivity of the hot combustion gases separating the two propellant surfaces. Indeed, it appears that other effects may be important. For instance, the radiation interchange factor is also a function of separation distance. To illustrate this effect, the shape factor of 2.0 in. diameter opposing disks is included in Fig. 7. Note that the functional dependence of the data in Gessner's patent and the shape factor are similar.

The data in the patent¹¹ were discussed with Mr. Gessner,¹² who is no longer employed by the Phillips Petroleum Company. It is interesting to note that Mr. Gessner considers erosive burning and crack burning to be the modes by which his invention can most effectively control burning rate. But since the dimensions of the propellant samples used in the Phillips Petroleum Co. experiments are not available, the relative importance of the burning effects and radiative heating effects can not be established.

Also it is interesting to note that high-loading density motors with star-point tips that are separated by less than 0.25 inches have not produced evidence of large increases in burning rate as a result of the close proximity of the burning surfaces. Indeed, there is no reason to expect such motors to have unusual propellant burning characteristics.

Additional attention will be given in Section IV to evaluating another mechanism by which opposing propellant surfaces can produce increased solid propellant burning rates.

D. Calculated Effects of Radiation on Burning Rate

Predictions of the effect of radiation on burning rate must account for the complex interplay between the increased mass generation rate resulting from the radiation and the changes in the gas phase produced by the increased rate of mass generation at the propellant surface. Glick¹³, in his discussion of the effects of temperature sensitivity of solid propellant burning rate, used the granular diffusion flame model to show that small increases in burning rate increase the thickness of the granular diffusion flame zone, which, in turn, decreases the heat conduction from the gas phase to the solid phase. In a similar manner, Ref. 14 discusses an analytical expression for the inverse relationship between burning rate and heat feedback to the solid phase from the gas phase. Either of these theories can be used to estimate radiation effects on burning rate. A conventional approach would be to calculate the heat feedback from the gas phase to the solid phase, using a flame theory such as Ref. 14 and 15 and to incorporate a term that accounts for an additional radiative source that heats the propellant surface. Such a theory would be applicable to a wide range of non-metallized, composite propellants, but would not necessarily apply to some

double base propellants and to propellants with binders that melt. However, as the details of this approach were being carried out, a direct method for approximating radiation effects on burning rate for a wide range of propellants became apparent. In the approach presented here, we will avoid the uncertainties in the complex gas phase by using measured data for the temperature sensitivity of burning rate.

For steady state burning, the increased energy transferred to the propellant by enhancing radiative heating can be expressed in terms of an equivalent increase in initial propellant temperature. The increase in radiant heat transfer to the propellant surface may be expressed as

$$q_{\text{rad}} = \sigma \Delta F T_{\text{rad}}^4 \quad (1)$$

where ΔF is the effective increase in the overall radiation interchange factor. Under steady state burning conditions, the added radiative heat transfer produces an effect equivalent to increasing the initial propellant temperature by an amount

$$\Delta T_i = \Delta q_{\text{rad}} / r \rho c \quad (2)$$

The influence of initial propellant temperature on burning rate under constant pressure conditions is usually correlated by the following empirical relationship

$$r/r_0 = \exp [\sigma_p (T_i - T_{i,\text{ref}})] \quad (3)$$

where r_0 is the burning rate at the reference temperature, $T_{i,\text{ref}}$. The factor σ_p is referred to as the temperature sensitivity of burning rate at constant pressure and is defined as

$$\sigma_p = \left. \frac{\partial \ln r}{\partial T_i} \right)_p \quad (4)$$

Values for σ_p have been measured for most solid propellants; for many propellants σ_p is nearly constant over broad ranges of chamber pressure and initial temperature.* Thus to a good approximation an implicit expression for the effect of radiation on burning rate for constant pressure conditions is

$$r/r_0 = \exp [\sigma_p (\Delta q_{\text{rad}} / r \rho c)] \quad (5)$$

Eq. (5) accounts for the complex interaction between burning rate and heat feedback from the gas phase by substituting the measured propellant property σ_p for a mathematical description of the gas phase.

For most applications, changes in burning rate are amplified by the closely interrelated change in pressure. For the normal motor conditions, differentiating the logarithm of the burning rate law

$$r = aP^n \quad (6)$$

* It is not uncommon for σ_p to be reasonably constant over pressure ranges of greater than 300 psi and initial temperature changes in excess of 60K.

yields
$$\frac{\partial \ln r}{\partial T_i} = \frac{\partial \ln a}{\partial T_i} + n \frac{\partial \ln P}{\partial T_i} \quad (7)$$

At constant pressure,

$$\left. \frac{\partial \ln r}{\partial T_i} \right|_P = \frac{\partial \ln a}{\partial T_i} \quad (8)$$

and the measured value of temperature sensitivity is

$$\sigma_P = \frac{\partial \ln a}{\partial T_i} \quad (9)$$

An expression for equilibrium pressure using Eq. 6 as the burning expression is

$$P = (c^* \rho a A_b / g A_t)^{1/(1-n)} \quad (10)$$

Differentiating the logarithm of Eq. 10 when A_b and A_t are constant yields

$$\left. \frac{\partial \ln P}{\partial T_i} \right|_{K_n} = \frac{1}{1-n} \left[\frac{\partial \ln a}{\partial T_i} + \frac{\partial \ln c^*}{\partial T_i} \right] \quad (12)$$

Assuming that σ_P does not vary with r and the method of increasing radiation does not influence the value of c^* , results in

$$\left. \frac{\partial \ln P}{\partial T_i} \right|_{K_n} = \frac{1}{1-n} \sigma_P \quad (13)$$

For the conditions of constant throat area and surface area, $P \propto r$ and

$$r/r_0 = P/P_0 = \exp \left[\frac{1}{1-n} \sigma_P (\Delta q_{rad} / r \rho c) \right] \quad (14)$$

Burning rate predictions were made by considering that the added radiative heat transfer is from a source that is at the actual flame temperature of the propellant[‡] and by considering the added radiant heating source in terms of an increase in the effective emissivity, $\Delta \epsilon$, above the effective emissivity of the gaseous combustion products.

Figures 8 through 10 are results of a parametric study to show the range of burning rate control that can be obtained. For completeness the parameters extend somewhat beyond those which can be obtained in practice. The ranges for typical high energy propellants are indicated by the shaded areas. The set of datum case values is given in Table 2. As previously discussed, the burning rate results are meaningful only for non-metallized propellants. The temperature

[‡] This is an idealistic situation for a reradiator since the reradiator temperature will only approach flame temperature as the heat transfer from the combustion gases to the reradiator increases.

TABLE 2

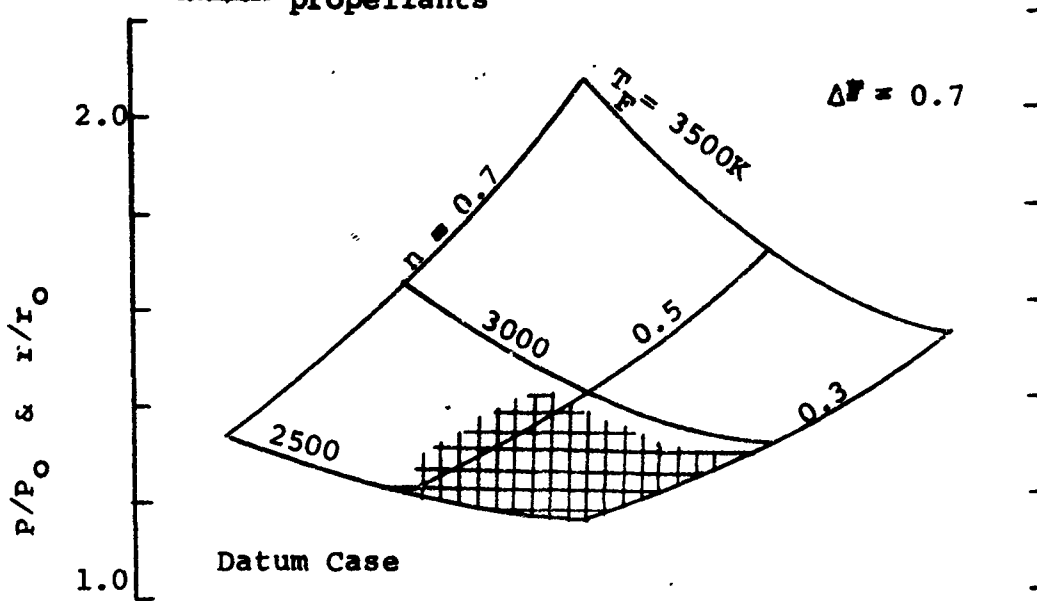
DATUM CASE VALUES FOR EVALUATING
EFFECT OF RADIATIVE HEATING
ON PROPELLANT BURNING RATE

| | |
|--|----------------|
| Burning Rate, r_o , cm/sec | 1.0 |
| Increase in effective overall radiation interchange factor, ΔF | 0.7 |
| Temperature sensitivity of burning rate at constant pressure $(\partial \ln r / \partial T_i)_p \times 100, \% / K$ | 0.135 |
| Propellant type | Non-metallized |
| Radiative heating does not produce* an increase in the flame temperature | |

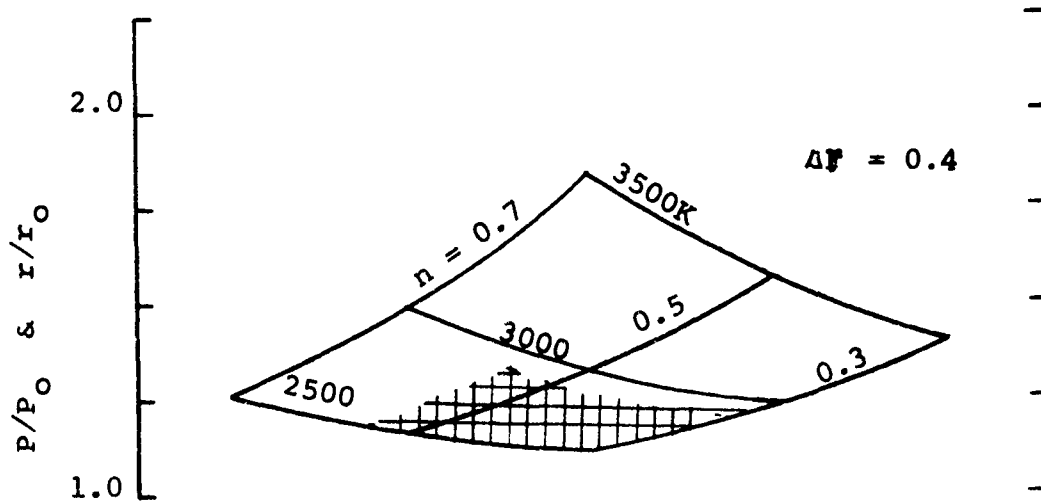
* Of course, the assumption that the method of increasing radiation does not influence T_F is not valid when the radiant energy is supplied by an external source (Method 3). The external energy increases the flame temperature which in turn increases c^* . The increase in c^* produces an increase in $(\partial \ln P / \partial T_i)_{K_n}$ on the order of $0.005/(1-n)\% / K$ for most propellants.

$\bar{G}_p = 0.135 \text{ \%}/\text{K}$
 $r'_0 = 1.0 \text{ cm}/\text{sec}$

 Region of typical non-metallized propellants



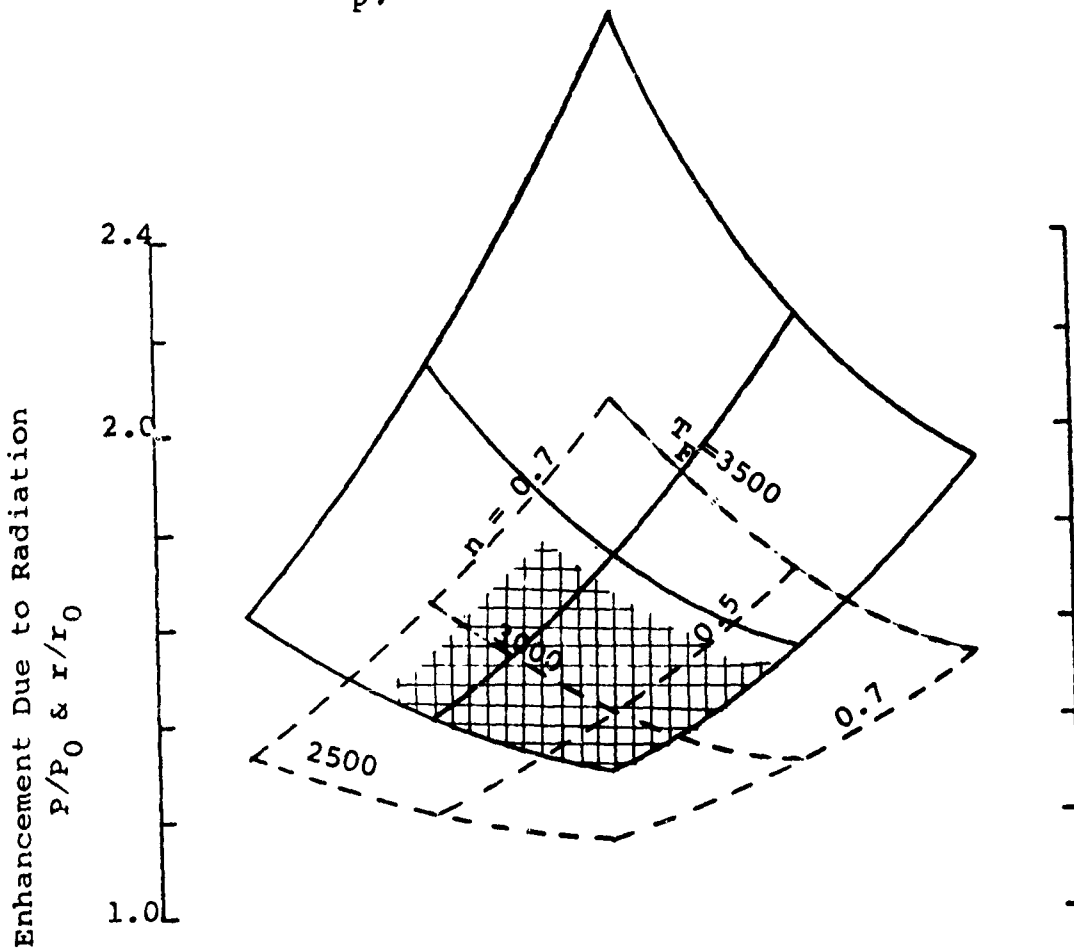
NOTE: Results include the effect of increasing pressure on burning rate



Method of increasing radiation does not increase flame temperature.

Fig.8 Burning Rate Increases Resulting From Increasing Radiative Heat Transfer to the Burning Propellant Surface

- Datum case except $\bar{v}_p = 0.27 \text{ \%}/\text{K}$
- - - Datum case
- Region of typical non-metallized propellants (without regard to practicality of increasing \bar{v}_p)



Method of increasing radiation does not increase flame temperature.

Fig. 9 Effect of Temperature Sensitivity of Burning Rate on the Burning Rate Enhancement due to Increasing Radiation.

———— Datum case except $r_o = 2.0$ cm/sec
- - - Datum case
Region of typical non-metallized propellants

Method of increasing radiation does not increase flame temperature.

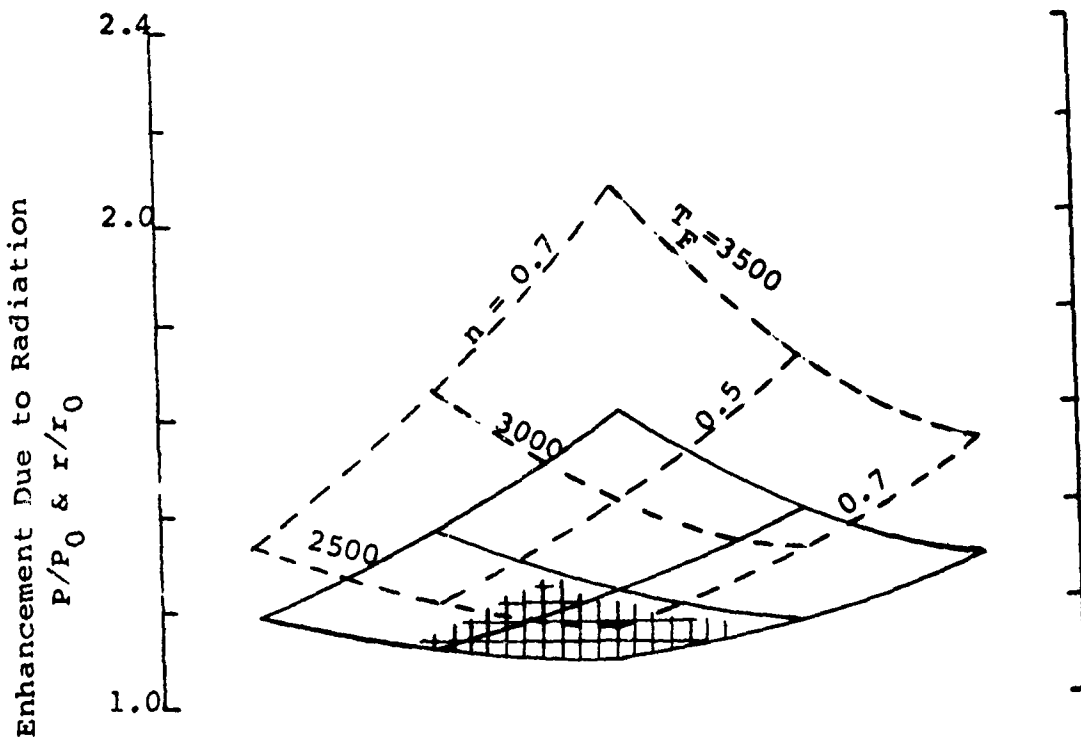


Fig.1⁰ Effect of Basic Propellant Burning Rate on the Burning Rate Enhancement due to Increasing Radiation

sensitivity value of 0.135%/K is typical of many composite propellants that are in wide use. The results of Fig. 8 show that increasing flame temperature has a strong influence on the burning rate enhancement. As indicated by Eq. 14, equally significant increases in the burning rate enhancement can be achieved by using high exponent propellants. The effects of increasing the radiation from sources in the combustion chamber are shown on Fig. 8. The absorptivity of the propellant surface was considered to be 0.8 and the upper bound of the emissivity of added radiation sources is approximately 0.9. As indicated by the data on Fig. 2, the effective emissivity from the combustion products is relatively low, about 0.1. Accordingly, the increase in the radiation interchange factor is: $F \approx 0.8 \times (0.9 - 0.1) = 0.64$. The increase in the radiation interchange factor for the upper series of curves in Fig. 8 is 0.7. These results are optimistic and show the advantages that could be achieved if ways are found to increase radiative heating to the propellant surface. The smaller increase in the radiation interchange factor, 0.4, shown on the lower set of curves should be readily obtainable.

As expected, formulating propellants with burning rates that are unusually sensitive to changes in initial temperature is extremely attractive. Fig. 9 compares propellants with temperature sensitivities of 0.27 and 0.135%/K. Temperature sensitivity values as high as 0.27%/K are not uncommon.

An important consideration is the basic burning rate of the propellant. The lower burning rate propellants are influenced to a greater extent by thermal radiation. This is explained in part by Eq. 2 which shows that the effective initial temperature is inversely affected by burning rate. The results of Fig. 10 indicate that the use of radiation as a means of burning rate control may be particularly attractive for some of the slower burning rate propellants.

The burning rate predictions, Figs. 8 through 10, indicate that burning rate control of 20% is achievable.

The following items tend to increase the degree to which burning rate is increased:

- 1) increasing temperature sensitivity of burning rate
- 2) decreasing the amount of metal fuel additives
- 3) increasing the pressure exponent of burning rate
- 4) increasing flame temperature
- 5) decreasing the basic propellant burning rate
- 6) increasing the effective emissivity of the radiation source

SECTION III

CONTROL OF SOLID PROPELLANT BURNING RATES BY ACOUSTIC ENERGY

The linear rate at which a propellant burns is proportional to the rate of heat feedback from the hot gaseous combustion zone to the propellant surface. Thus methods which accelerate the reaction rates in the gaseous combustion zone and thereby produce a thinner combustion zone should produce steeper thermal gradients in this gaseous layer. The steeper thermal gradients correspond to higher conductive heat fluxes to the propellant surface, which in turn will produce higher propellant burning rates. In the case of the widely used heterogeneous (i.e., composite) propellants, the speed of the gaseous reaction is controlled by two rate processes: 1) the chemical kinetics of oxidation and 2) the physical interdiffusional of the unmixed oxidizer and fuel vapors. In the practical operating range of most composite propellants (>500 psi), the slower of these processes is the interdiffusional mixing. At low pressures, less than 100 psi, chemical kinetics limit the burning rate processes.

Any physical factor that can speed up the interdiffusional mixing process in the gaseous combustion layer will increase the burning rate. For example, the finer the oxidizer particle size, the smaller the degree of heterogeneity of the gas zone and the higher the propellant burning rate at rocket motor pressures.

The basis for modulating the burning rate of composite propellants with sound waves was discussed in 1959 by Summerfield¹⁶ and was the subject of patent issued to Rod¹⁷. Summerfield postulated that acoustic stirring hastens the gaseous reaction through improved mixing in the thin granular diffusion flame zone and thus increases the energy feedback to the propellant surface. The greater the mixing, the more burning rate increases to the limit controlled by the chemical kinetics of the reaction between premixed AP and binder vapors. The acoustic energy can be projected into the combustion zone by separately energized whistles or other generators. The direction of the movement caused by the acoustic wave is generally considered to be parallel to the burning surface. However, wave motion normal to the burning surface should also produce mixing of vapors with unequal densities. The idea of acoustic mixing has occupied the attention of the Princeton group for some time, mainly as a means of studying various burning rate theories and incidently as a practical means of controlling burning rates.

The granular diffusion theory¹⁴ applies to many ammonium perchlorate composite propellants and leads to the following rate equation:

$$\frac{1}{r} = \frac{a}{P} + \frac{b}{P^{1/3}} \quad (15)$$

In the extreme limit of instantaneous mixing, the diffusional mixing time parameter, b , vanishes. In this extreme limit, the effect of eliminating the diffusional mixing time should increase the burning rate by factors of between three and ten.

The effect of mixing the oxidizer and fuel vapors by acoustic energy can be partially evaluated in terms of the effects produced by reducing the oxidizer particle size in composite propellants. When the oxidizer particle size is decreased, the dimensions of the individual regions of oxidizer and fuel vapors are also decreased. The burning rate trends produced by decreasing the particle size while holding all other propellant variables constant are shown in Fig. 11. A quantitative prediction of the upper limit of the degree of burning rate control which is obtainable by acoustic stirring can be made for propellants which satisfy the granular diffusion flame theory. Fig. 12 shows the upper limit of several propellants in terms of the coordinate P/r and $p^{2/3}$. Note that when the b parameter in Eq. 15 becomes zero the upper limit is a horizontal line in the P/r and $p^{2/3}$ coordinates. The limit is also shown in terms of burning rate versus pressure plots in Fig. 12. It should be noted that such large burning rate increases have not been realized in practice. The reasons for the departure from the idealized theory will be discussed.

The consideration of acoustics as a means of increasing burning rate should include the following requirements:

1. The acoustic boundary layer should be sufficiently thin so that the gaseous diffusion reaction is accelerated very close to the burning propellant surface.
2. The frequency of the acoustic oscillations should be such that the fuel and oxidizer vapor undergo at least one cycle while they are in the gaseous reaction zone.
3. The effect of the acoustic energy should be uniform along the burning propellant surface.
4. The acoustic energy should not excite the various acoustic modes of the combustion chamber.

To estimate the necessary acoustic frequency, the details of the gas flow processes and the thin gaseous combustion layer were considered. The gases flowing from the surface move outward at typical velocities of 50 to 100 cm/sec and the region of the flame zone layer to be affected is approximately 50μ thick. The total thickness of the gas phase reaction zone is approximately 100 to 1000 μ ^{14, 18, 19}. An expression for particle displacement in a traveling wave is²⁵

$$\xi = p_s g / \rho c \omega \quad (16)$$

For a zone thickness of 50μ , a minimum frequency of 10 kc will insure exposure of the reacting gases to at least one cycle of

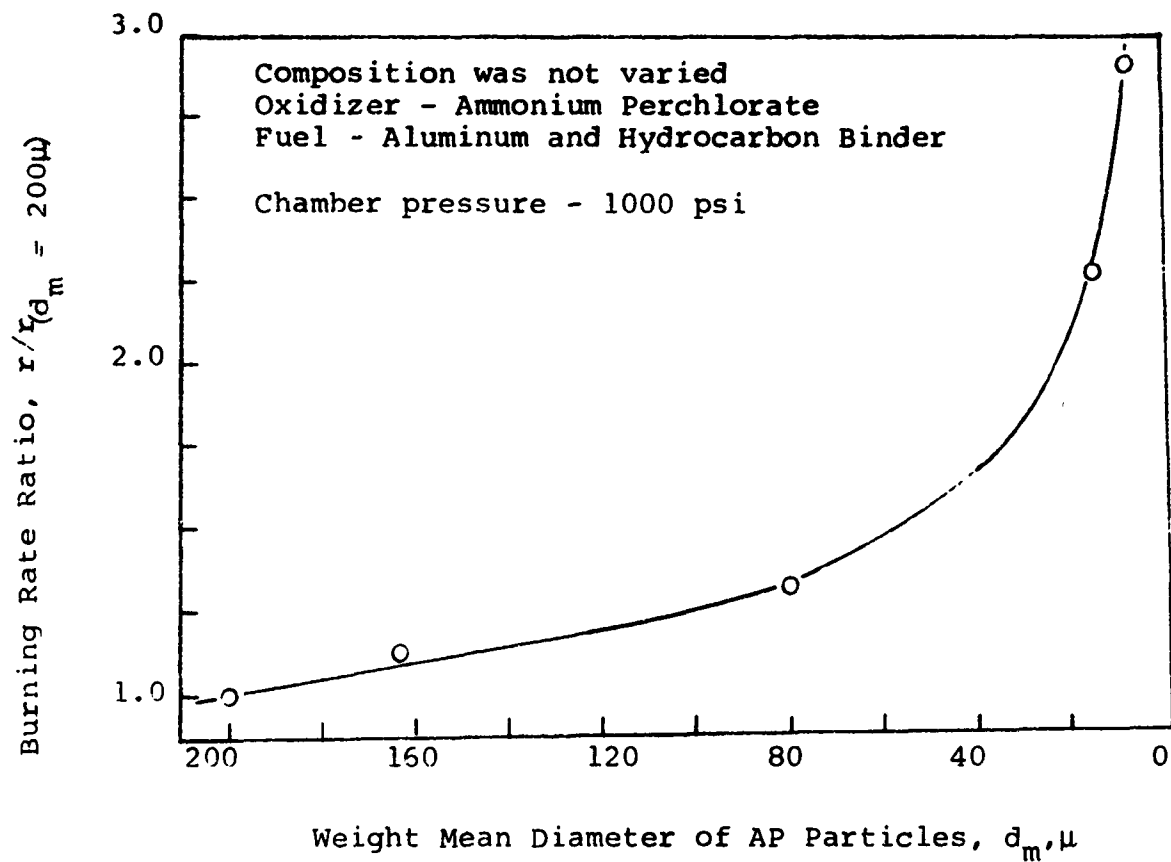


Fig. 11 Effect of Weight Mean Diameter on Burning Rate of AP Composite Propellant.

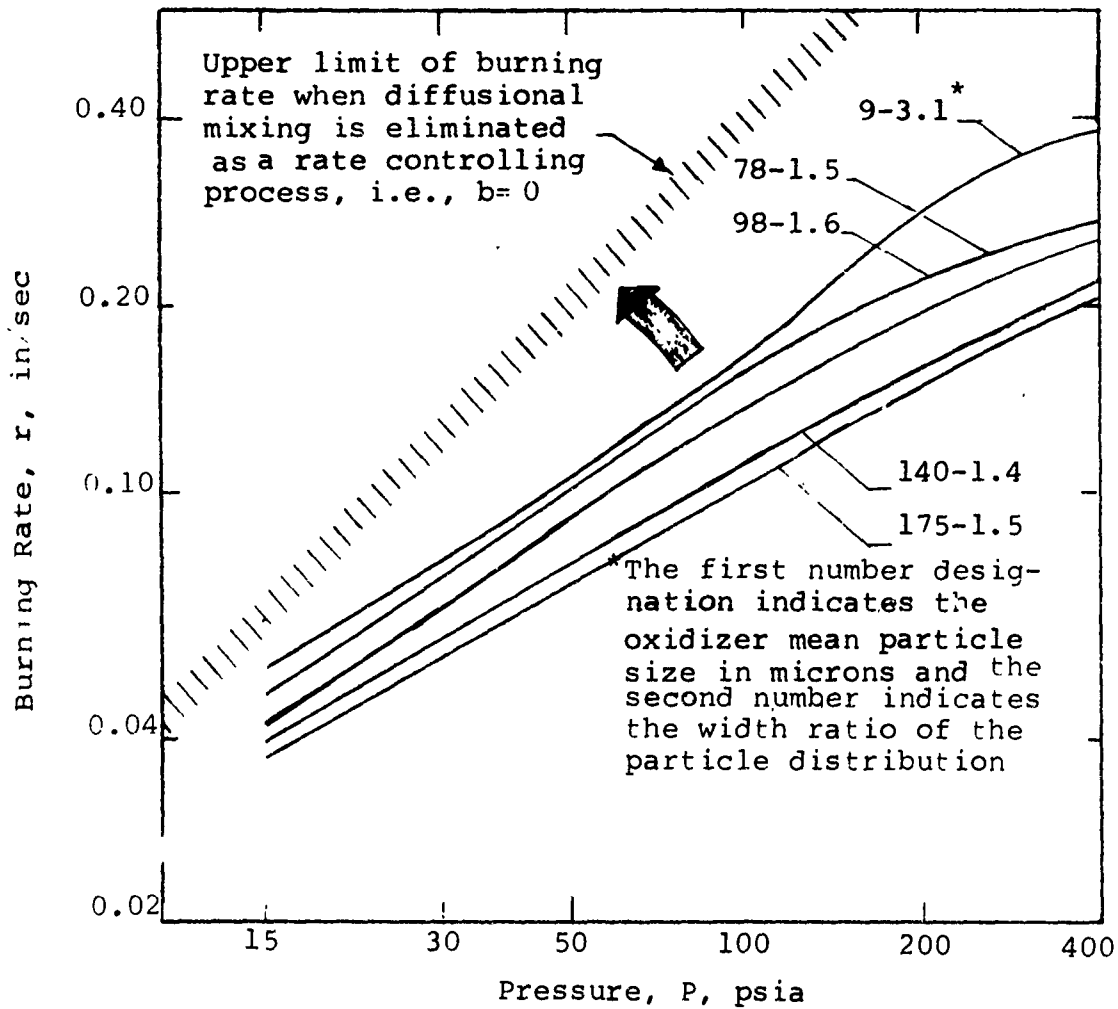
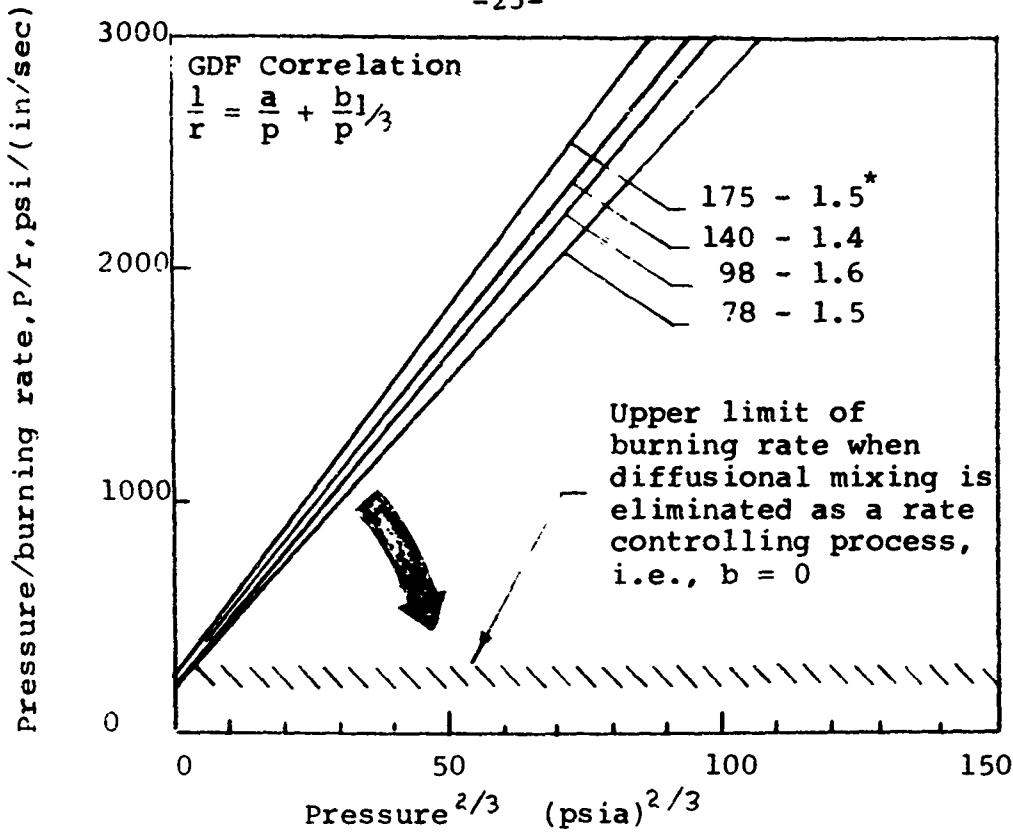


Fig.12 Upper Limit of Burning Rate as Reduced AP Particle Size Eliminates Diffusional Mixing as a Rate Limiting Process

oscillation. Using higher frequency should provide a greater degree of mixing of the gases.

Another consideration is the thickness of the acoustic boundary layer. For the method to be effective, the acoustic boundary layer must be considerably thinner than the gaseous reaction zone since the displacement attenuates to zero as the burning surface is approached. The thickness²⁵ of the acoustic boundary layer is given by the expression:

$$\delta = (2\nu/\rho\omega)^{1/2} \quad (17)$$

The 10 kc frequency results in a boundary layer thickness of approximately 20μ which probably represents a minimum frequency for effective mixing to occur near the burning surface.

The third consideration is the decay of the acoustic energy downstream of the energy source. Yamazaki²⁰ used the following expression for the decay coefficient of the sound wave being propagated into an infinite cylinder:

$$\alpha = (2\omega\nu/\rho)^{1/2} / 2 c r_{\text{cyl}} \quad (18)$$

Yamazaki²⁰ calculated the degree of decay in a cylinder with a 13 cm diameter and a pressure of 1 atm (see Fig. 13). Yamazaki²⁰ points out that the results for 1 atm are conservative for rocket motor pressures. Therefore, he concludes that the decay of sound waves in cylindrical rocket motor cavities is small and can be neglected. This result agrees with the measurements of Elias²¹.

Several series of experiments have been performed to evaluate the effectiveness of using acoustical energy to control solid propellant burning rate. Yamazaki²⁰ burned strands in a bomb which contained a tweeter placed below the strand. The center line of the strand was parallel to the center line of the tweeter. The output of the tweeter was 123 db. The results obtained by Yamazaki are summarized on Figs. 14 and 15. Fig. 14 shows moderate increases in burning rate and the unexpected trend that the most effective frequency decreases with increasing pressure. The very small increases in burning rate measured by Yamazaki may be a result of the low intensity sound waves used in his experiments. To achieve the degree of stirring and boundary layer thickness which was previously described, an intensity* of approximately 170 db is required.^{16,25} Also, Yamazaki may have produced relatively complex acoustic waves which moved primarily in a direction normal to the burning surface. Such waves may not be as effective as waves that travel parallel to the burning surface.

Small rocket motors with pneumatically driven sound generators have been tested at Princeton University^{22,23} and as part of a joint effort^{21,24,25} that involved Acoustica Associates and the Aerojet General Corporation. The Princeton experiment:

* The intensity is dependent on amplitude and frequency. Eqn. 17 establishes the minimum frequency and Eqn. 16 gives the amplitude.

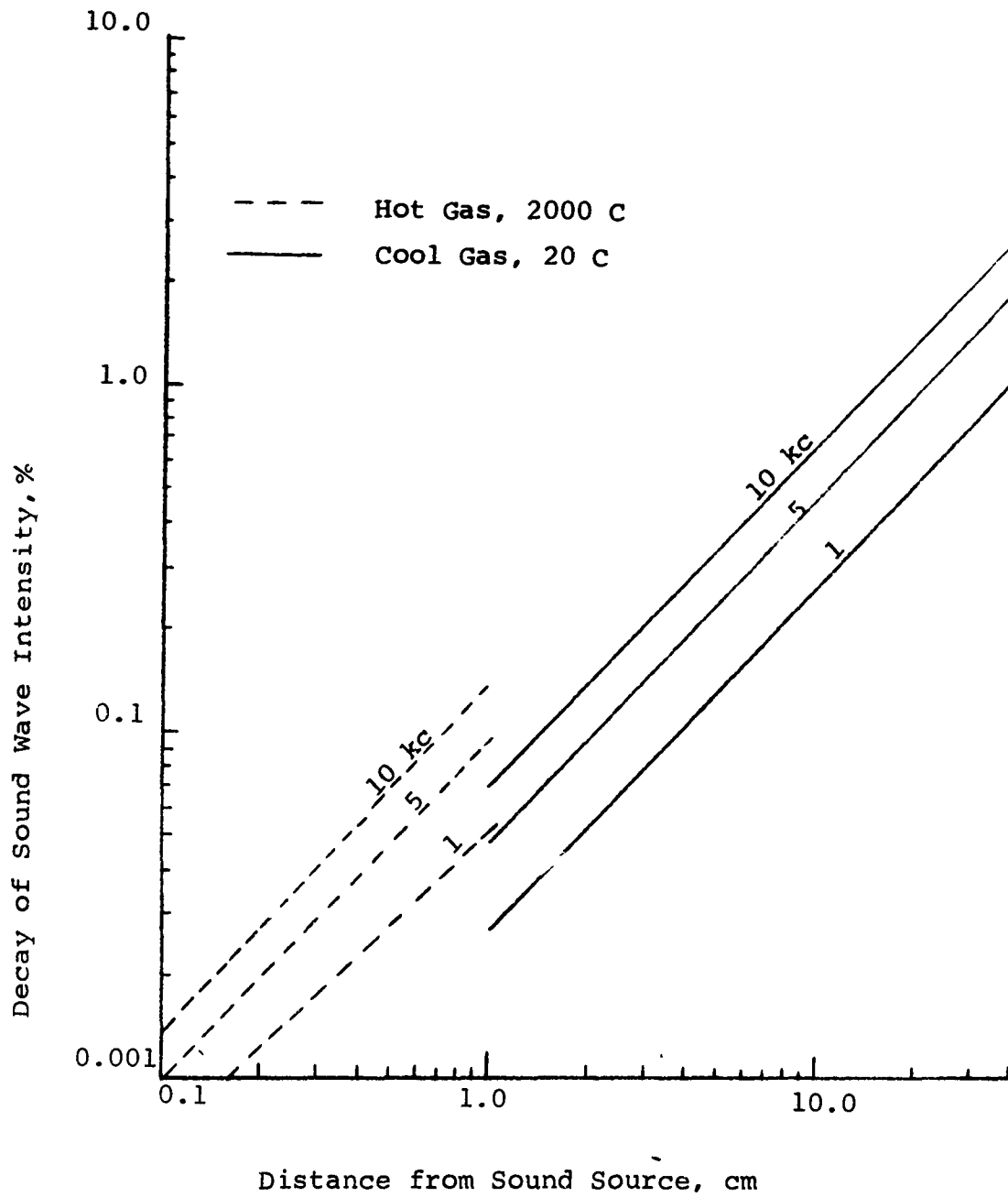


Fig. 13 Decay of Sound Wave Intensity versus Distance from Sound Source with Gas Temperature as a Parameter (From Ref. 20)

Propellant: Polysulfide Binder with 65% AP
Input to Tweeter: 30 watts

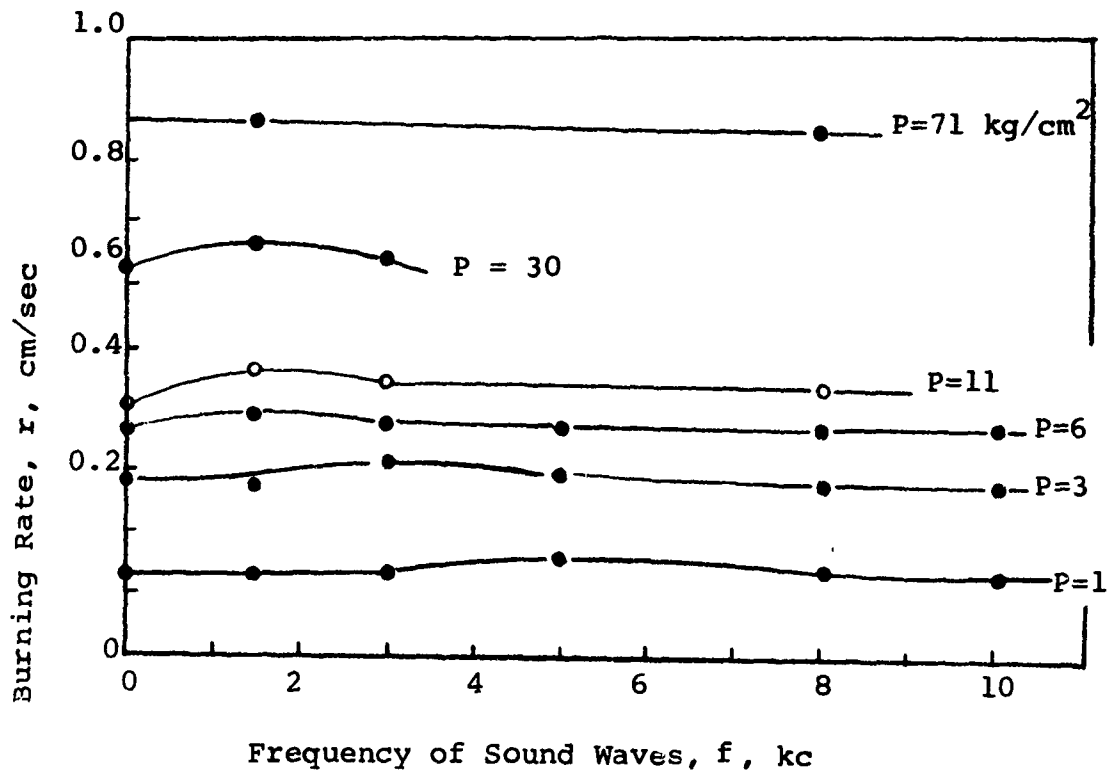


Fig. 14 Effect of Sound Waves on Burning Rate
(From Ref. 20)

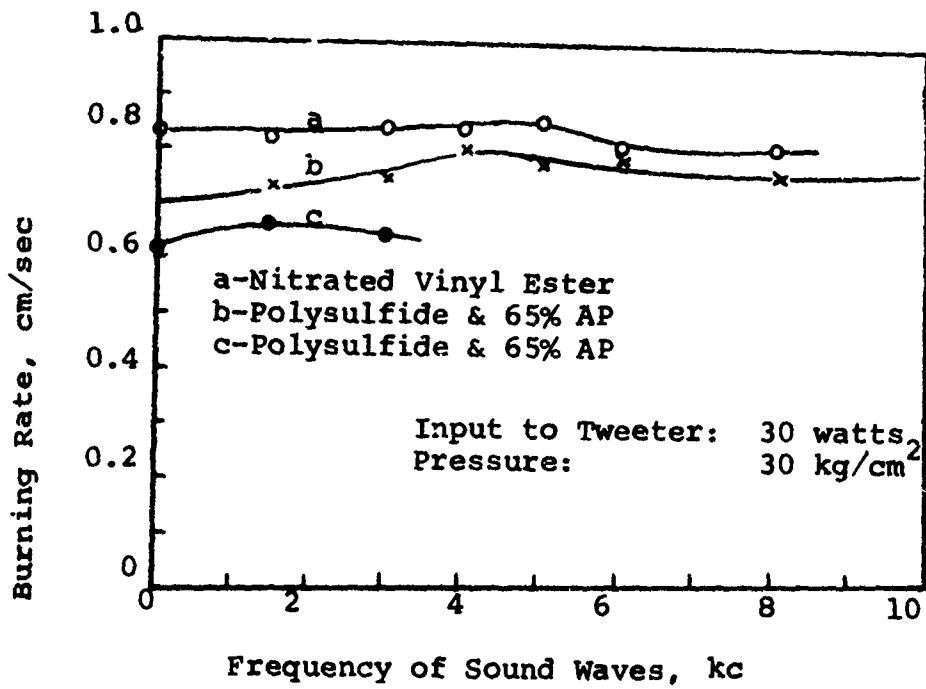


Fig. 15 Effect of Sound Waves on the Burning Rate of Various Propellants (From Ref. 20)

were run with a Hartmann-type whistle coupled to a small rocket motor. Frequencies as high as 15 kc and large amplitudes produced essentially negative results. The program conducted by Acoustica Associates and Aerojet General was an extensive program which involved a large number of motor tests. A Levasseur whistle was used for sound generation in these tests. Initially, the sound field was produced by exciting the whistle with nitrogen at 9.6 and 14 kc. At each frequency the whistle produced 174 db. Thirty-nine motor firings were made with essentially no effect on burning rate. After eliminating the sources of experimental error, the investigators decided that a gas having a cold acoustic velocity closer to that of the hot combustion gases would be needed to prevent the acoustic mis-matching and that the whistle should be operated at a higher frequency to reduce the acoustic boundary layer thickness. Helium gas, having a value of acoustic velocity closer to that of the combustion gases, was selected to provide a better acoustic match to reduce the degree of refraction from the boundary layer.

Acoustica and Aerojet made thirty-two firings with helium exciting the whistle at frequencies of 30 and 35 kc. Typical results from these firings are shown in Fig. 16. Included in the tests were tare firings for each batch of propellant as well as firings wherein an equal flow rate of helium was introduced into the chamber but without the sound generation. As shown in Fig. 16 an increase in burning rate was observed from these firings with helium flowing through a silent whistle. However, this increase was not nearly as large as when sound was being produced. The effect of the helium flow without sound was greater than could be accounted for on the basis of additional mass flow alone. It was postulated that the presence of helium caused an erosive effect through an increase in the molecular and eddy conductivities in the reaction zone.* The effect of helium flow alone is seen to diminish to zero as the propellant grain burns out because of the decreasing mass velocity of the helium with the increasing port area.

As shown in Fig. 16 and 17, the sonic irradiation produced marked burning rate increases during the early phases of motor operation, but these increases in burning rate tapered off to zero near burnout. A possible explanation for this includes the effects of two interacting items 1) the increased burning rate produced increased chamber pressures and gas velocities from the propellant surface and 2) the motor without acoustic excitation has a progressive pressure history. The first of these two items decreases the flame zone thickness which causes more of the rate controlling reactions to occur in the acoustic boundary layer and increases the velocity of the gas pockets moving through the flame zone which causes the gas pockets to experience fewer oscillations before they are consumed. Thus, the burning rate increases produced by a whistle of fixed frequency and power will tend to be self limiting. The increased pressure and burning rate produced by the second item decreases

* However, for the same reasons as described for the use of injected particles (pages 7-9), it is difficult to believe that the injected helium could uniformly reach the gaseous reaction zone.

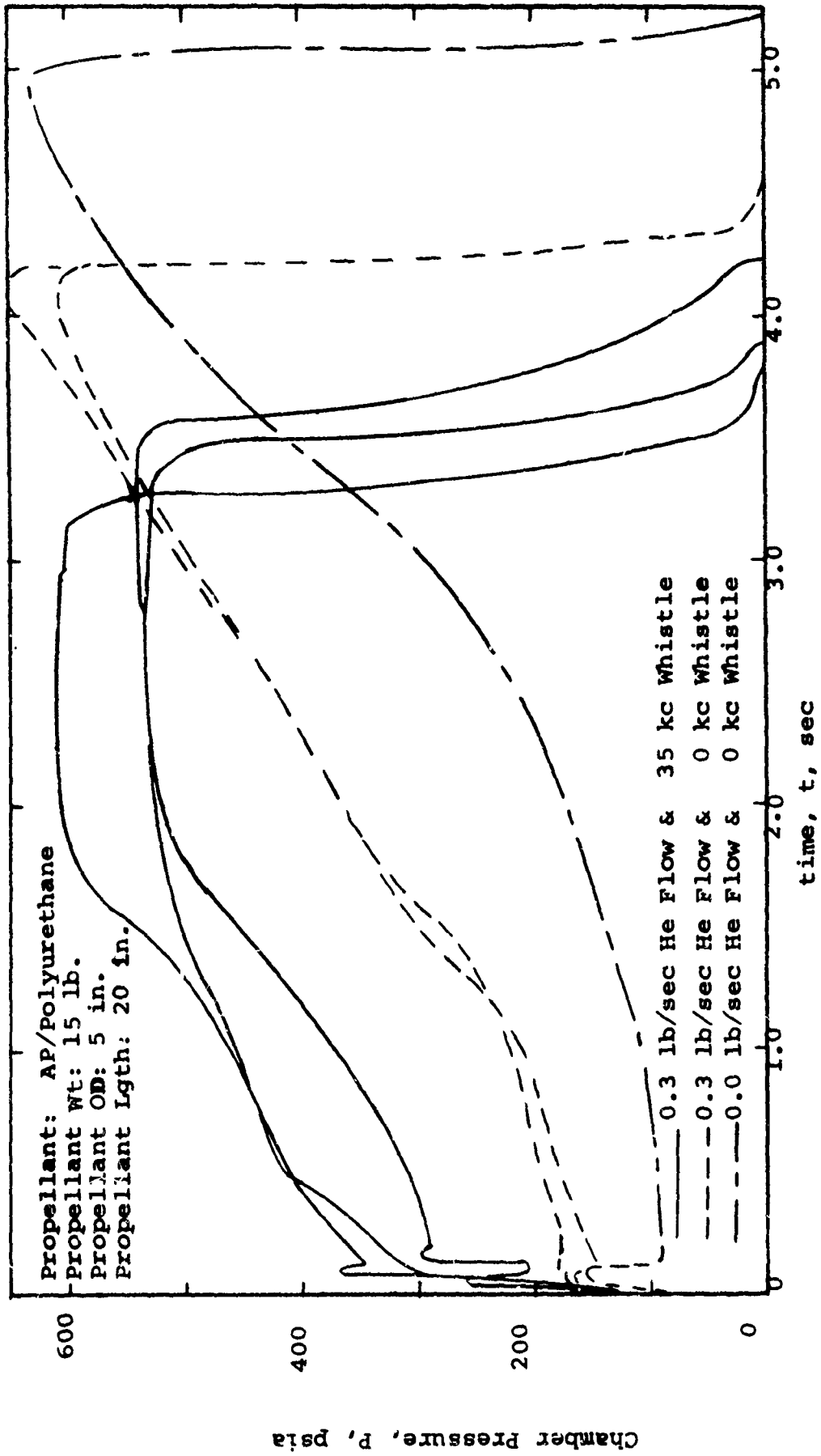


Fig. 16 Effect of Sonic Irradiation and Helium Flow on Motor Operating Pressure
(From Ref. 21)

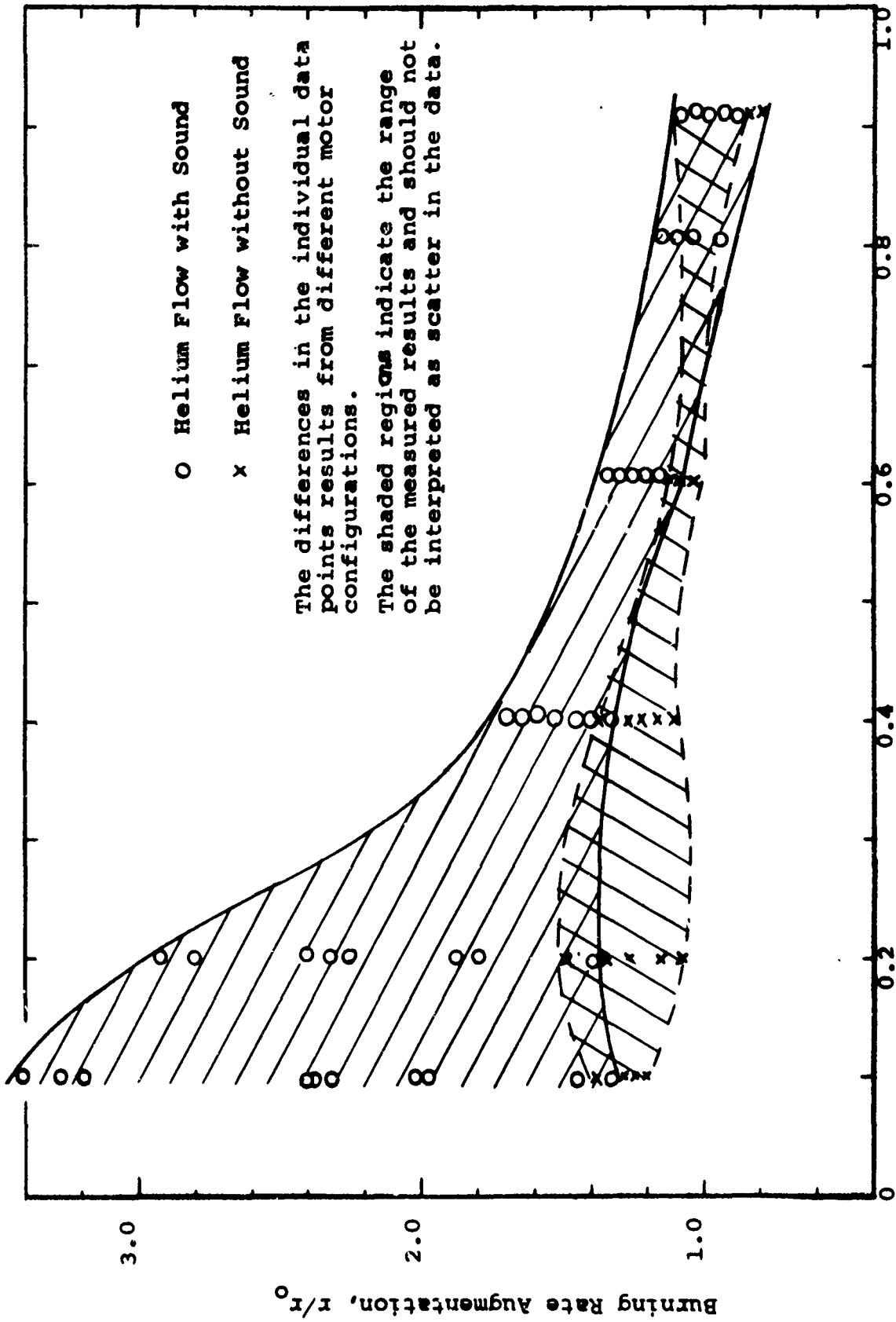


Fig. 17 Burning Rate Augmentation by Gas Flow and Sonic Irradiation.
(From Ref. 21)

the flame zone thickness, increases the velocity of the gas pockets and, thus, decreases the effectiveness of the acoustic stirring.

The sound field produced by the whistle in the Acoustica and Aerojet motor firings exhibited amplitudes of 10 to 30 psi from peak to peak which are considerably higher than the values of 5 psi obtained in the cold flow calibrations. This may indicate the presence of²¹ an acoustic-combustion interaction. However, it was noted²¹ that the whistle did not excite any acoustic modes in the motor. The reasonably sharp tail-offs on the measured pressure time traces indicate that the increase in burning rate is uniform along the length of the grain (see Fig. 16).

Based on the measurements of Acoustica and Aerojet General it can be concluded that a helium driven whistle can increase burning rate. However, the requirement that the driver gas be helium rather than nitrogen suggests that the means of burning rate control is strongly influenced by the sonic velocity of the gases used to drive the whistle. It is very important to note that the success of the experiments with helium suggests that other driver gases with high sonic velocities may also produce the desired degree of burning rate control. The practical limitations to using helium may be avoided by driving the whistle with a warm gas generator. The gas generator propellant should be selected so as to produce a gas with a relatively low average molecular weight and a flame temperature slightly below the melting point of the whistle components.

An externally mounted whistle driven by a warm gas generator could produce a very intense sound field on command and is consistent with the requirements for high performance rocket motors. The intensity of the sound field could be controlled on command either by movable components in the whistle or by using a state-of-the-art variable flow rate gas generator. Most importantly, the gas used to drive the whistle will also augment thrust.

As pointed out by Elias²⁵, much work has to be done to clarify the mechanisms of burning rate control. To date the types of experiments, the range of acoustic energy, and the motor geometry in the tests have been severely limited. Possibly a particular combination of motor geometry and propellant could produce a practical rocket motor. For example, a small spherical motor with a low burning rate, non-metallized propellant, a low chamber pressure, and a toroidal whistle around a deeply submerged nozzle may combine those characteristics which tend to make the method most effective.

The small pressure oscillations produced by acoustic sources may significantly increase the burning rate of propellants that contain porous ingredients^{26,27}. For example, either the oxidizer particles or the metal additives could be manufactured so as to have small (< 10 μ diameter) pores. As the pressure oscillated the pressure transients would cause the pores to breath in hot combustion gases and, thereby, increase the burning rate. The degree of burning rate increase should increase when pressure oscillations and frequency are increased.

SECTION IV

CONTROL OF SOLID PROPELLANT BURNING BY MEANS OF A CONFINING PRESSURE PLATE

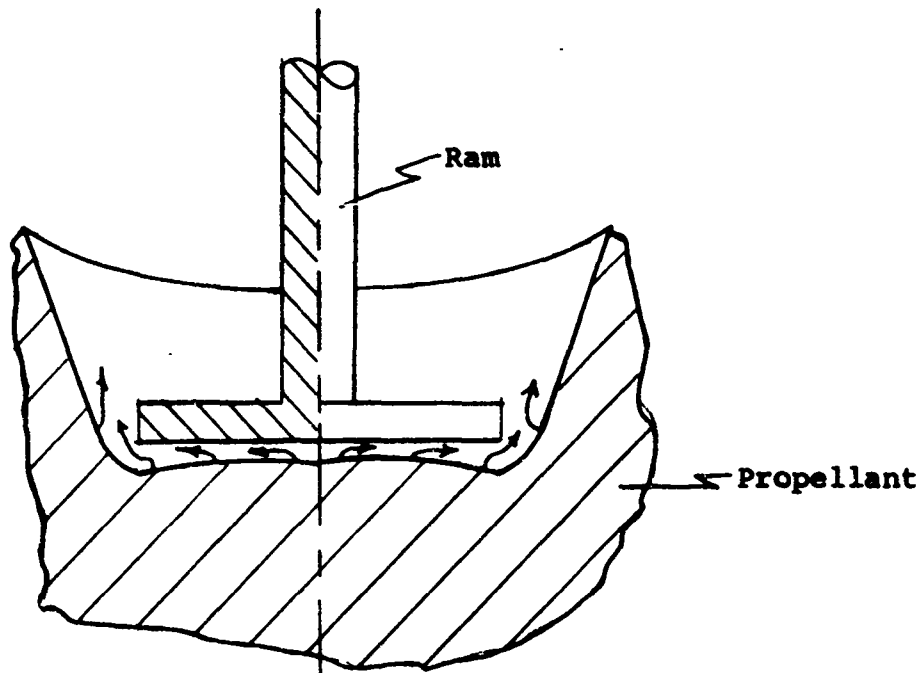
A. Background

Solid propellant burning rates can be increased by locally increasing the static pressure and gas velocity parallel to the burning surface. These local increases in static pressure and velocity can be produced on command either by bringing a ram very close to the burning surface (see Fig. 18a) or by forcing two burning propellant surfaces together (see Fig. 19). As the separation distance is decreased, the velocity of the gases flowing parallel to the burning surface increases because of two additive effects: a decreased flow area and an increased mass generation rate corresponding to the higher static pressure. Thus, for certain propellants burning rate enhancements can be obtained by locally varying the extent of the erosive burning.

The use of inert rams, as indicated in Fig. 18a, was the subject of a series of studies conducted at the Massachusetts Institute of Technology²⁸⁻³¹. A range of ram geometries and materials were evaluated using low flame temperature (approximately 1800 to 1900K) double base propellants. They³¹ found that burning rate could be increased from 0.07 in/sec to a maximum of 0.78 in/sec by pressing a tubular molybdenum "heat exchanger" ram against and into the burning surface (see Fig. 20). In many of the MIT tests, the leading edge of the thin walled, tubular ram was forced below the propellant surface and burning rate increases resulted from heat being transferred from the hot tube to the surrounding solid propellant. Tests conducted using rams with flat surfaces, as shown in Fig. 18a, demonstrated increases in rate of about 2:1. The investigators at MIT concluded from their analysis that this 2:1 increase in burning rate could not be explained in terms of the increases in local static pressure. However, no mention was made concerning the erosive burning effects. The devices studied at MIT were generally restricted to low flame temperature propellants because of the temperatures which the ram materials and drive mechanism could withstand.

The approach shown in Fig. 19 eliminates the problems of constructing a ram to withstand the combustion chamber environment. Possibly, two propellants with different burning characteristics opposite one another would produce the desired effects. For instance, steady state burning of a low burning rate, gas-generator propellant could be quickly established by opposing it with a high flame temperature conventional propellant. Also, the burning in close proximity of two dissimilar propellants may result in the burning rate of both propellants being enhanced because of the increased heat feedback resulting

a) Hot Ram



b) Ram With Ports for Injecting Burning Rate Catalysts

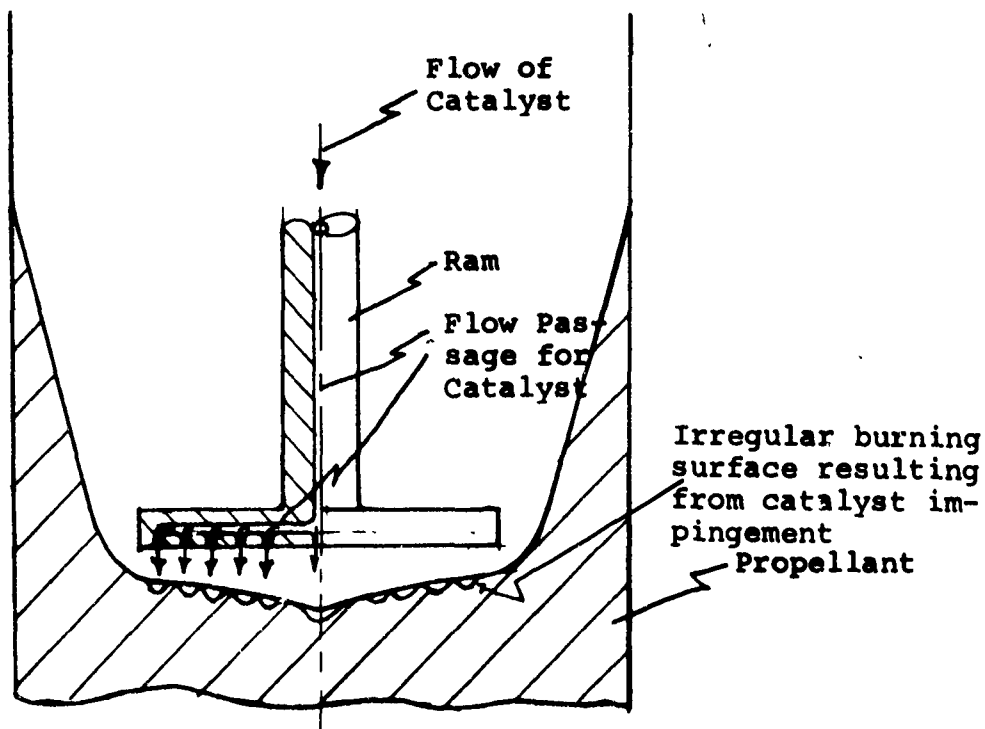
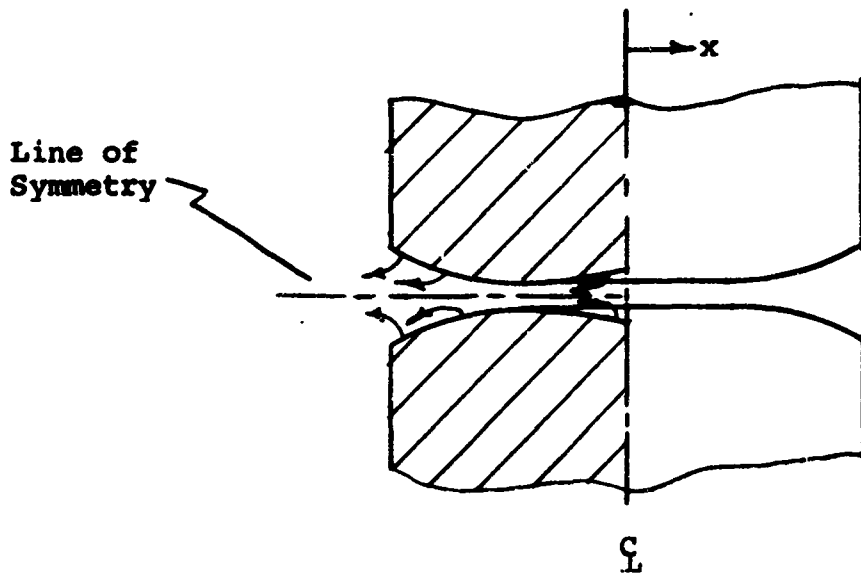


Fig. 18 Schematic Views of Disks Rammed Against Propellant Burning Surface to Produce Enhanced Burning Rates.

a) Two Identical Propellants Rammed Together



b) Two Dissimilar Propellants Rammed Together

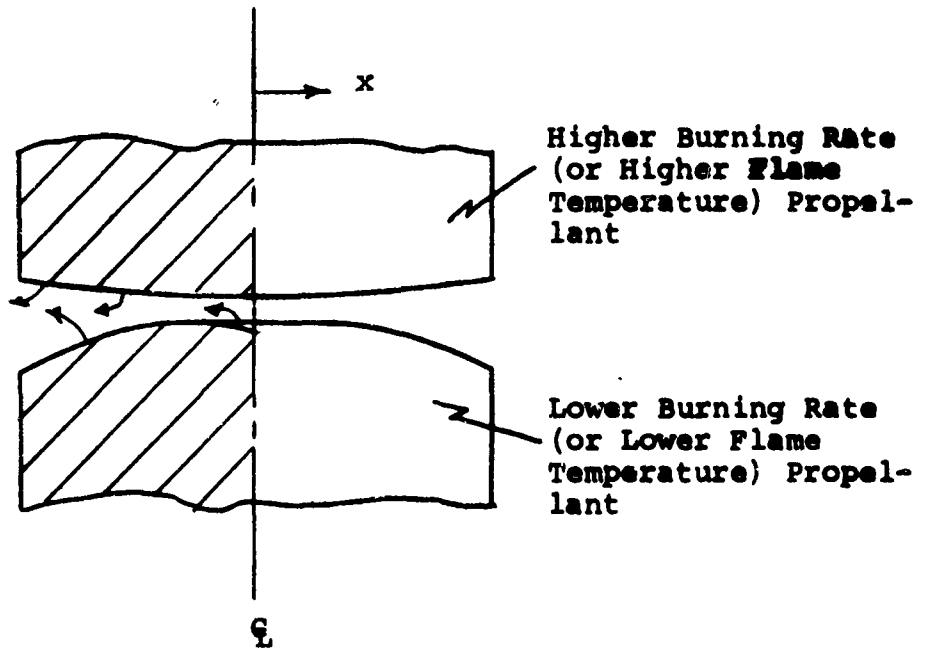


Fig. 19 Schematic Drawing of Burning Propellant Surfaces Being Rammed Together

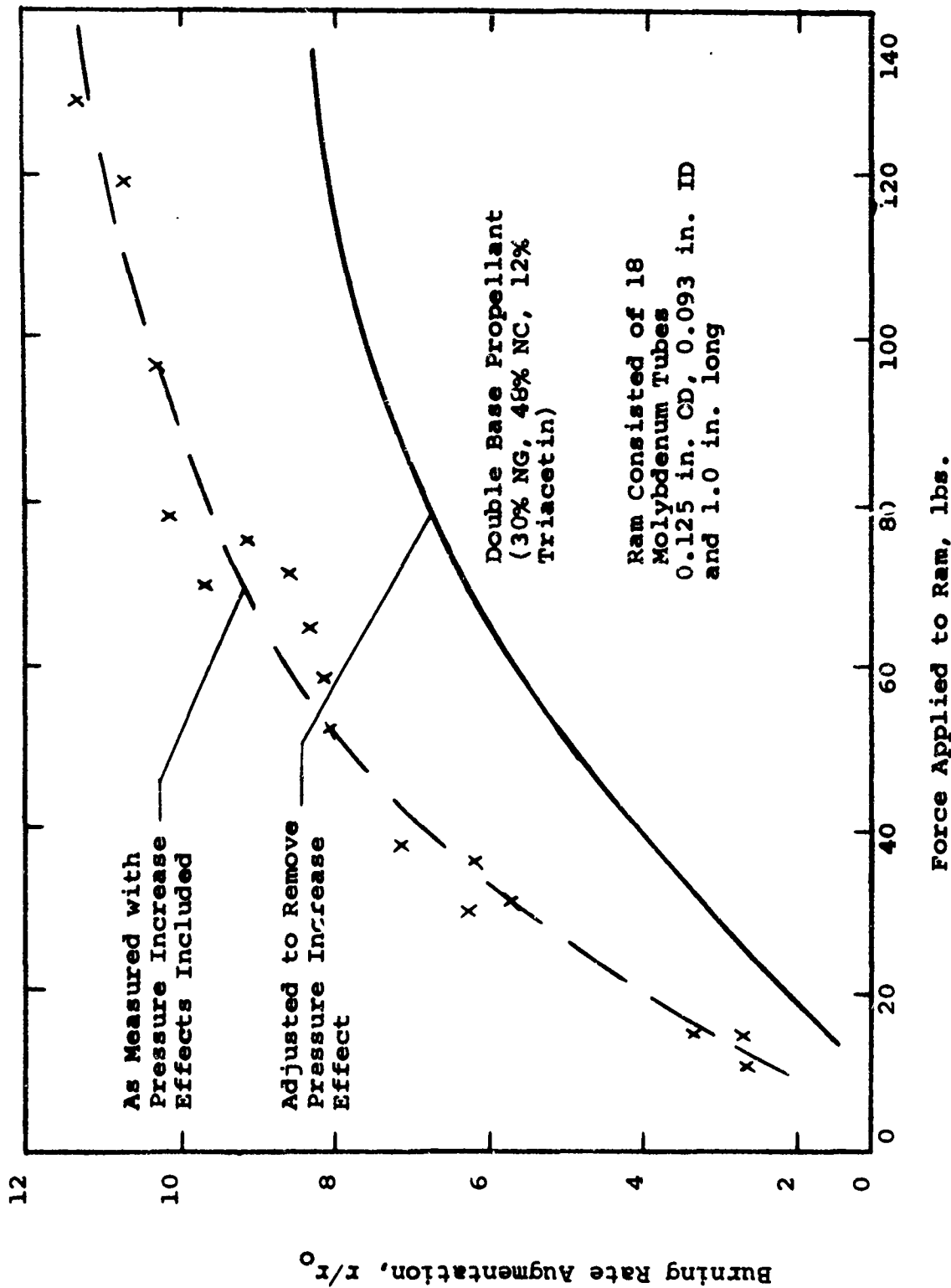


Fig. 20 Burning Rate Augmentation Resulting From Ramming Propellant With a Cluster of Hollow Tubes (From Ref. 31)

from an increased flame temperature. For example, a pressed ammonium perchlorate grain and a fuel rich, under-oxidized grain would burn slowly if they were separated; bringing them together will cause their combustion products to combine to produce a more intense flame. The heat feedback from the more intense flame would in turn cause more reactants to leave the surfaces of the individual grains, i.e. the burning rate is increased. An attractive possibility is that the effective lower deflagration pressure, P_{DL} , for the combination will be greater than atmospheric pressure. If that is the case, the gas generator can be extinguished by increasing the separation distance between the grains.

A variation on the ram approach is to inject burning rate catalysts through the face of the ram (see Fig. 18b). This eliminates the problems associated with one of the approaches to be considered (where catalysts must penetrate long distances through the hot combustion gases before they reach the propellant surface). One of the inconsistencies in this approach is that the catalyst must flow through the hot face of the ram. Thus, this approach may be limited to low flame temperature propellants.

B. Analysis

An analytical model was developed to analyze and predict the burning characteristics of propellants whose burning rates are affected by opposing surfaces.

The physical situation considered is shown in Fig. 21. The compressible flow model was formulated to account for the following:

- area change in the direction of flow
- non-normal mass addition
- a propellant surface opposed by an inert ram
- two opposing propellant surfaces with different burning rate laws
- radial or parallel gas flow
- friction at the ram and propellant surfaces

The assumptions in the model include:

- 1) the gases have a constant specific heat and constant average molecular weight
- 2) steady state flow
- 3) one-dimensional flow
- 4) erosive burning results obtained from rocket motor tests apply to the burning of opposing surfaces
- 5) chamber pressure is sufficiently high that if it increases, the pressure at the ram centerline increases.

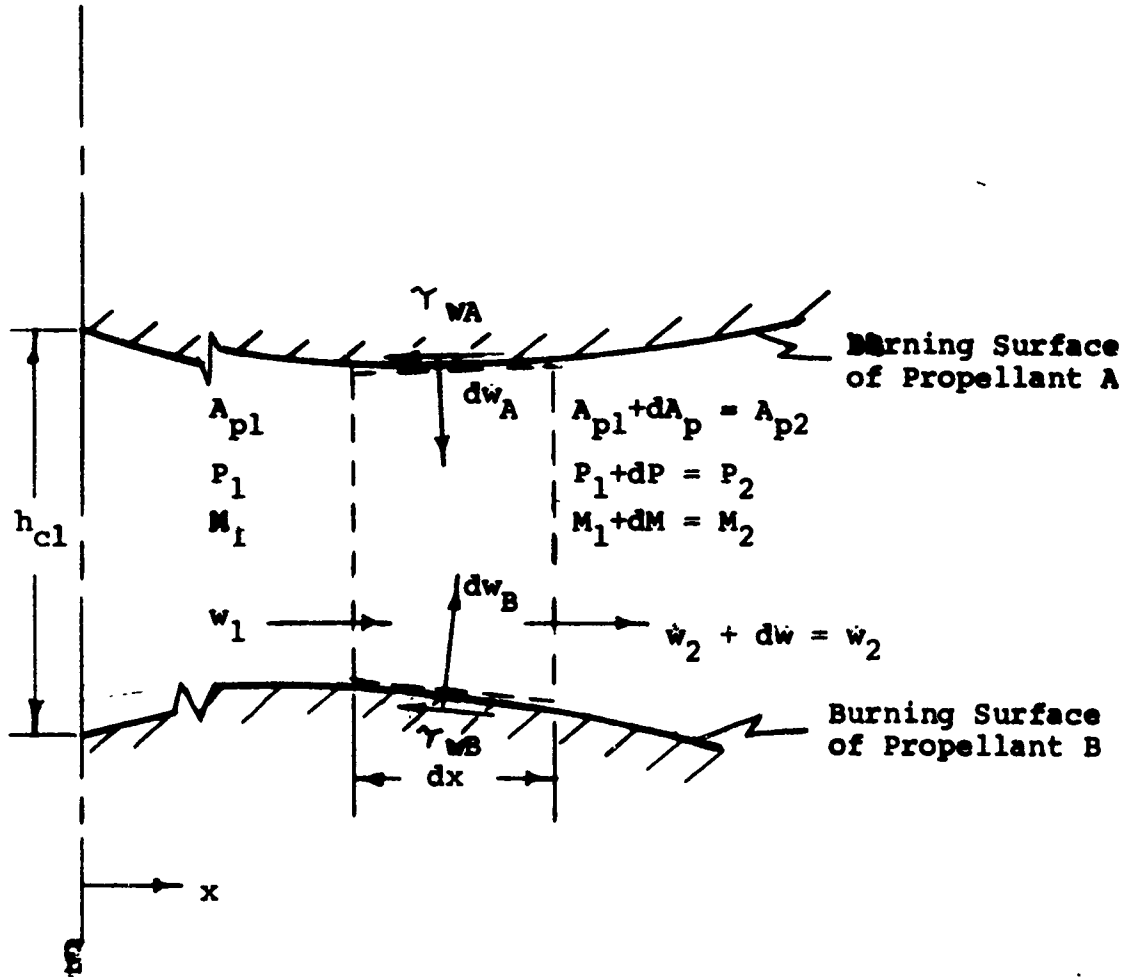


Fig. 21 Control Volume Used in the Model to Analyze Burning of Propellant Surfaces Whose Pressure and Velocity Distributions Are Influenced by an Opposing Surface.

The validity of assumption 3 must be evaluated in terms of the distance separating the surfaces and thickness of the flame zone. For very small separation distances, the flow is a complex developing compressible boundary layer flow. Such flows are common to all erosive burning situations. However, the use of experimentally obtained erosive burning data and friction factor data will to some extent negate the errors introduced by the one-dimensional flow assumption if the data are used in a manner that is consistent with the manner in which they were correlated.

Since the rate of mass generation from the opposing slabs of propellant is primarily controlled by the local pressure and Mach number, it was necessary to solve the differential form of the compressible flow equations for pressure and Mach number. For the high subsonic Mach numbers and rapidly changing flow conditions being considered here, the local pressures, Mach numbers, and burning rates are closely coupled; thus the differential equations for static pressure and Mach number were solved simultaneously. Shapiro³² arranged the compressible flow equations in terms of the independent variables and influence coefficients that are functions of Mach number. Shapiro's equation for Mach number can be multiplied through by M^2/dx to yield

$$\begin{aligned} \frac{d(M^2)}{dx} = & \frac{2M^2 \left(1 + \frac{\gamma-1}{2} M^2\right)}{A_p(1-M^2)} \frac{dA_p}{dx} + \frac{\gamma M^4 \left(1 + \frac{\gamma-1}{2} M^2\right)}{(1-M^2)} \left(\frac{4F}{D} - \frac{2\gamma}{w} \frac{dw}{dx}\right) \\ & + \frac{2M^2(1+\gamma M^2) \left(1 + \frac{\gamma-1}{2} M^2\right)}{w(1-M^2)} \frac{dw}{dx} \end{aligned} \quad (19)$$

Similarly Shapiro's equation for pressure when multiplied by P/dx becomes

$$\begin{aligned} \frac{dP}{dx} = & \frac{\gamma P M^2}{A_p(1-M^2)} \frac{dA_p}{dx} - \frac{\gamma P M^2 [1 + (\gamma-1)M^2]}{2(1-M^2)} \left(\frac{4F}{D} - \frac{2\gamma}{w} \frac{dw}{dx}\right) \\ & - \frac{2\gamma P M^2 \left(1 + \frac{\gamma-1}{2} M^2\right)}{w(1-M^2)} \frac{dw}{dx} \end{aligned} \quad (20)$$

Equations 19 and 20 are in a convenient form for integration using the Runge-Kutta method since

$$\frac{d(M^2)}{dx} = f_1(x, M, P) \quad (21)$$

$$\frac{dP}{dx} = f_2(x, P, M) \quad (22)$$

The mass generation rate is

$$w = \int_0^{A_b} \rho^b r(P, M) dA \quad (23)$$

The following erosive burning law suggested by Saderholm³³ was used:

$$r = aP^n \quad \text{when } M < M_{crit} \quad (24)$$

and

$$r = aP^n \left(\frac{M}{M_{crit}} \right)^c \quad \text{when } M \geq M_{crit} \quad (25)$$

The equations describing the compressible flow, surface regression, and the interactions between the compressible flow and the surface regression were solved using numerical techniques. An iterative method was used to establish the steady state condition, i.e., the burning rate component in the direction parallel to the center line was constant over the propellant slab. Results calculated by the major elements of the solution were compared to closed-formed solution results for several of the simple flow conditions.

C. Calculated Effects of Energy Feedback by Means of Opposing Surfaces.

A series of calculations was performed to investigate the conditions created when propellant burning rates are affected by opposing surfaces. Also, attention was given to finding those conditions which would produce an effective degree of burning rate control.

Fig. 22 compares the effects of propellant burning characteristics on the steady state flow conditions and the contour of the burning propellant surface. The results of Fig. 22 are for an adiabatic, rectangular ram that is 0.5 inches wide and very long in comparison to its width. The physical properties used in the calculations are given in Table 3. As the distance from the centerline of the ram increases, the velocity of the combustion gases increase (see Fig. 22b) to the extent that erosive burning becomes significant. The increased burning rates

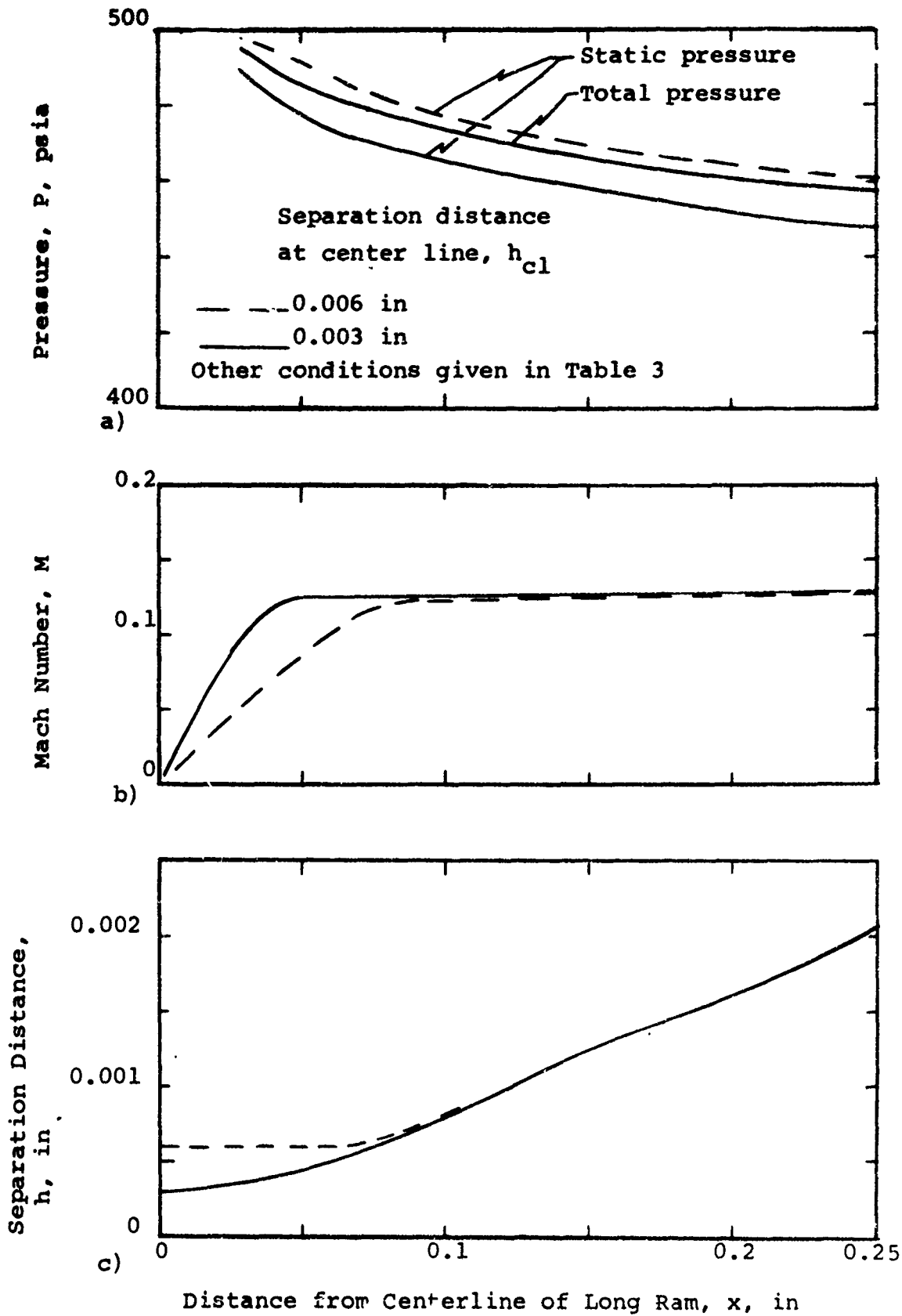


Fig. 22 Static Pressure, Mach Number, and Separation Distance for Propellant Being Rammed by a Long Flat Ram

TABLE 3

Datum Case Values Used in Opposing Slab Calculations

| | |
|--|--|
| Density of propellant, lbm/in ³ | 0.064 |
| Flame temperature, R | 6000. |
| Characteristic velocity, ft/sec | 4898. |
| Average molecular wt. of combustion gases, gm/gm-mole | 30.3 |
| Ratio of specific heats | 1.16 |
| Burning rate law: | |
| M < 0.12 | $r = 1.0(P/1000)^{0.27}$ |
| M ≥ 0.12 | $r = 1.0(P/1000)^{0.27} (M/0.12)^{0.23}$ |
| Pressure at center line of ram, psia | 500 |
| Separation distance at centerline of ram, in | 0.006 |
| Width of ram, in | 0.25 |
| Ram geometry | Length much greater than width |

cause the cross-sectional flow area to increase (see Fig. 22c) and, thereby, tend to limit the velocity of the combustion gases and the degree of erosive burning. Fig. 23 shows that the geometry of the ram affects the flow characteristics. For a given distance from the center line, the increasing cross-sectional flow area of the disk shaped ram results in smaller gas velocities than the long ram. Accordingly, the disk shaped ram results in a smaller degree of erosive burning and, thus, less burning rate augmentation.

Increasing the width of the ram increases the effect. But, as shown in Fig. 24, the wider ram also requires a greater ramming force.

It was hoped that by pressing the opposing slabs closer together very large changes in burning rate could be achieved. However, as indicated in Fig. 24, the separation distance at the center line has only a limited influence on the overall change in chamber pressure. This small degree of control is a direct result of the tendency of the erosive burning to increase the cross-sectional flow area and, thereby, to limit the changes that can be achieved by erosive burning. Fig. 25 illustrates that changing the pressure sensitivity of the propellant does not greatly change the degree of burning rate control.

The results of Figs. 24 and 25 indicate that the method can be used to achieve 2 to 5% increases in chamber pressure when either similar propellants are rammed together or when a conventional propellant is rammed by an inert ram. The results presented here do not establish if ramming together dissimilar propellants and propellant ingredients will produce a high degree of control. For example, a small gas generator could employ a pressed ammonium perchlorate grain and a fuel-rich grain which are brought into close proximity and ignited by injecting a fluid which would produce a hypergolic ignition. It is reasonable to expect that when the burning surfaces are close, volatilization of the individual grains can be sustained by heat feedback from the reacting volatiles and that the mass generation rate will be sensitive to separation distance.

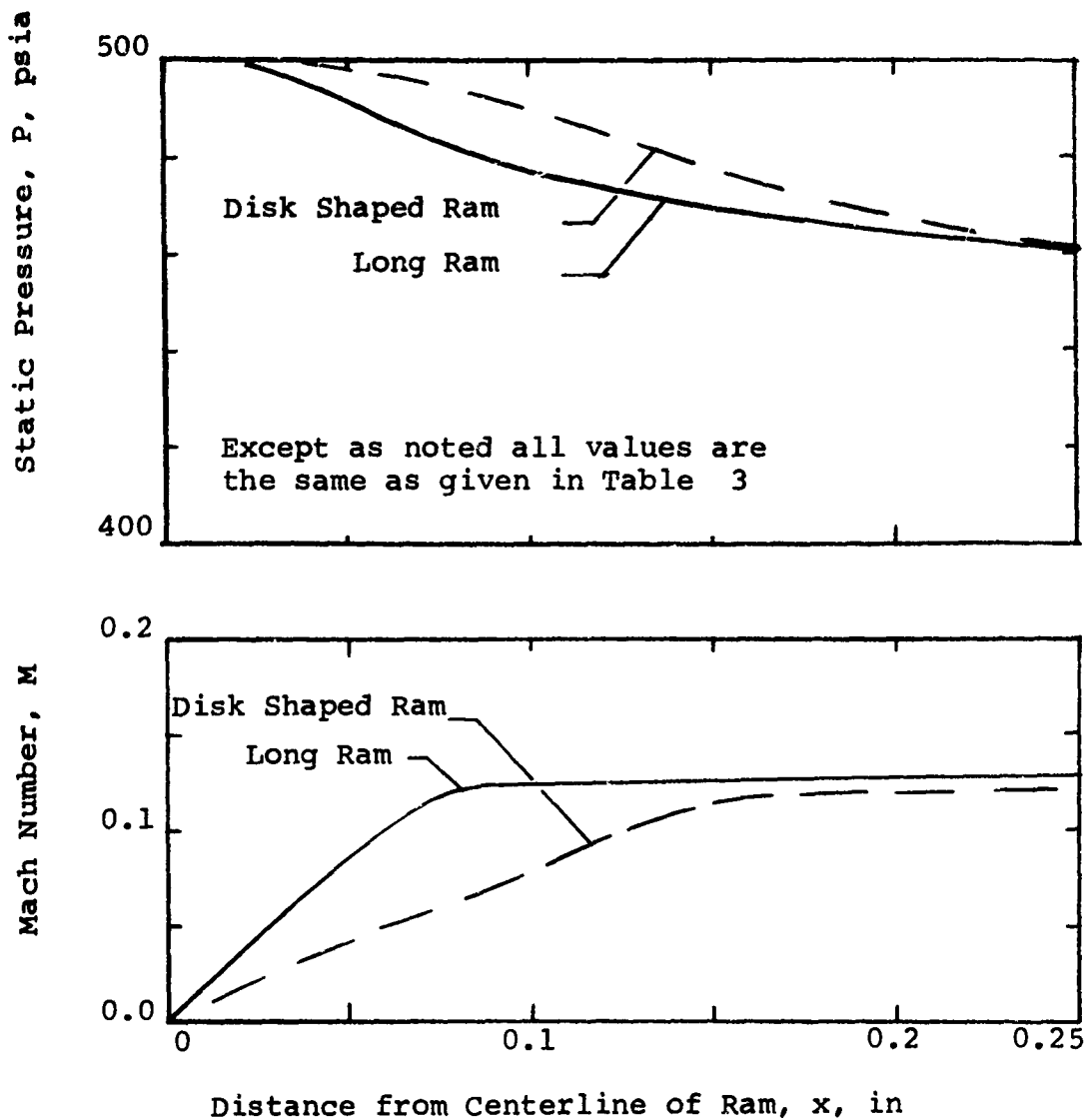


Fig. 23 Effect of Ram Geometry on Pressure and Mach Number Across Propellant Surface

Force per Length of Ram, lbf/in
and Increase in Chamber Pressure
Produced by Ram, P, psia

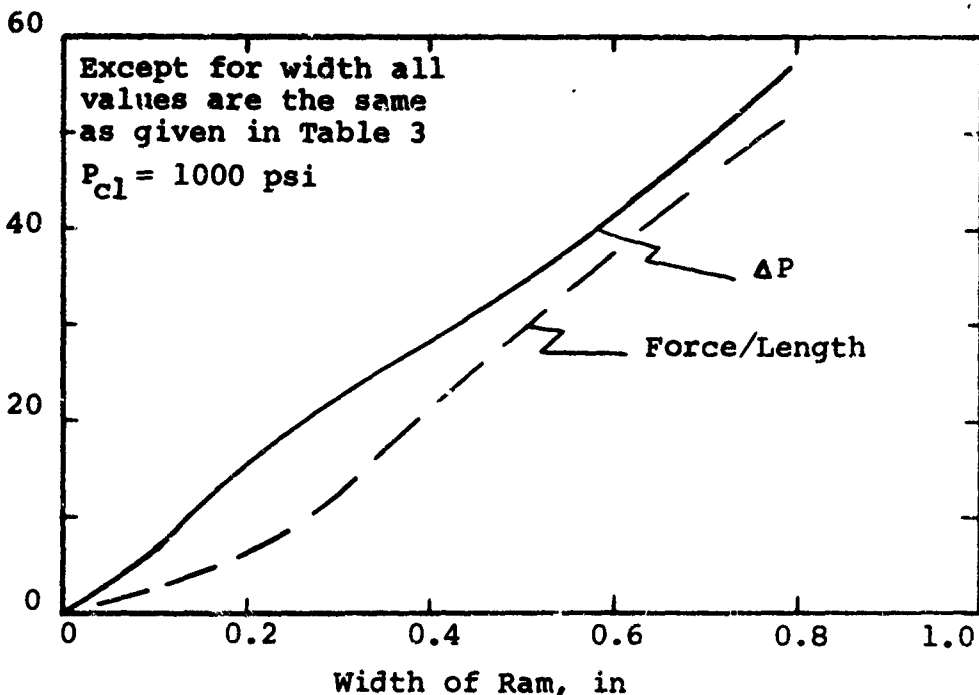


Fig. 24 Effect of Ram Width on Ramming Force and on Increase in Chamber Pressure Produced by Ramming Propellant.

Except for Separation Distance
All Values are the Same as Given
in Table 3.

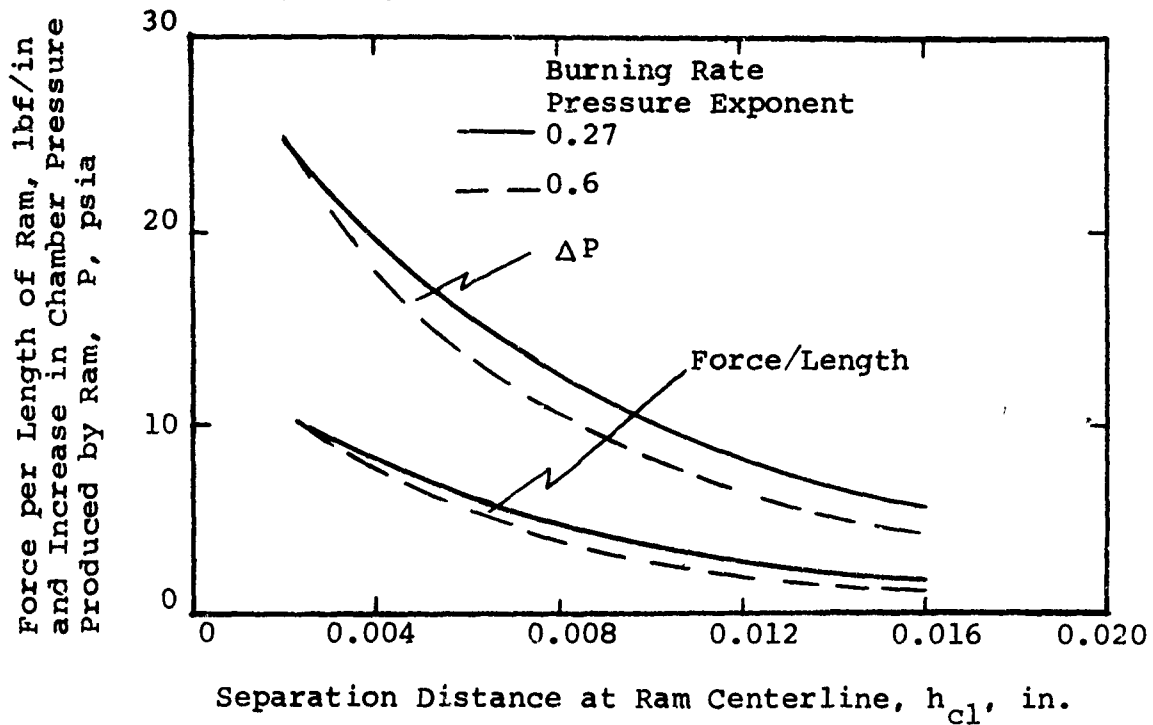


Fig. 25 Effect of Separation Distance at Ram Centerline on Ramming Force and on Increase in Chamber Pressure Produced by Ramming Propellant.

SECTION V

Penetration of Thermal Wave in Solid Phase by Back Flow of
Combustion Gases into Perforated Propellants

The burning rates of conventional high-energy solid propellants are usually limited by the net thermal energy that can be absorbed at the regressing solid surface (or for some propellants, the regressing liquid surface). Thus, the search for either controlled or enhanced solid propellant burning rates has often led to the consideration of methods to intensify the net heat transferred to the burning surface. This can be accomplished in two ways, 1) increase the heat flux to the surface and 2) increase on a microscopic level the exposed surface area. The effectiveness of increasing the effective burning rate by exposing additional burning surface area and subsurface voids is well established, primarily as a consequence of rocket motor malfunctions resulting from combustion phenomena associated with items such as:

1. Thermal cracking of large AP particles at high pressures (generally pressures greater than 3,000 to 5,000 psi).
2. Dewetting of oxidizer particles from the binder as a result of either thermal stresses or improper cure.
3. Propellants that contain many small voids (diameters less than about 0.05 cm) in a localized region.
4. Cracks and unbonds in the propellants.

When the combustion phenomena associated with the above items are viewed in terms of conventional rocket motor operation, they are considered as uncontrolled, nearly instantaneous, and often catastrophic events. However, when these events are viewed in terms of the requirements for ultra-high acceleration vehicles, they can be considered in a new light. In particular, it appears that the burning of porous propellants, propellants containing dewetted oxidizer particles, perforated propellants, and packed beds of propellant pellets, obeys readily formulated physical relationships in a predictable and usable manner. The primary departure from conventional propellant considerations is that we will be considering propellants with burning rates on the order of 50 in/sec. Thus, we will be considering deflagration velocities much higher than conventional burning rates but several orders of magnitude lower than detonation velocities.

A. Possible Motor Configuration

Figure 26 is a schematic drawing showing a solid propellant rocket motor with an end-burning, perforated propellant grain and a variable throat area nozzle. Depending on the manufacturing process used to produce the perforated propellant, the propellant grain could have conventional star point type of configurations. The variable throat area nozzle permits the chamber pressure to be continuously adjusted to maintain the desired pressure differential between motor chamber and the head end of the perforated propellant grain. As will be discussed in the following paragraphs, if control can be maintained over the pressure differential between the motor chamber and the propellant grain, the rate of flow of hot combustion gases into the perforations can be controlled. As a result, control over the propellant burning rate can be achieved. It must be emphasized that obtaining a prescribed thrust with a rocket motor containing perforated propellant is dependent on using a controllable throat area nozzle. Also, it is fully realized that the concept as presented may not be practical. Indeed the objective of this investigation is to explore the feasibility of propulsion systems that use perforated propellants.

Also, on Fig. 26 is a schematic drawing of a propellant section adjacent to the burning surface. Under a favorable pressure gradient, hot combustion gases flow into the perforations in the propellant grain and heat the propellant along the walls of the perforations. Since the cross sectional area of the perforations is necessarily small for a high-density and high-performance propellant, the hot combustion gases rapidly cool themselves and convectively heat the propellant. It is this convective heating that heats the normally subsurface propellant to its ignition temperature and, thereby, accelerates the combustion wave at a finite number of sites ahead of the normal burning surface.

Before beginning the more detailed discussions of internal ballistics and combustion, the following enumeration of the important physical processes required to achieve constant thrust operation* will help to indicate the interactions among the physical processes of the motor shown in Fig. 26:

1. Hot combustion gases pressurize the motor chamber.
2. The pressure differential between the motor chamber and head-end of the perforated propellant grain causes hot combustion gases to flow across the plane of the burning surface and into the perforated propellant grain.
3. The hot combustion gases flowing into the perforated propellant ignite the propellant along the walls of the perforation in the propellant.

*To a good approximation constant thrust operation corresponds to a constant mass generation rate; i.e., constant burning rate.

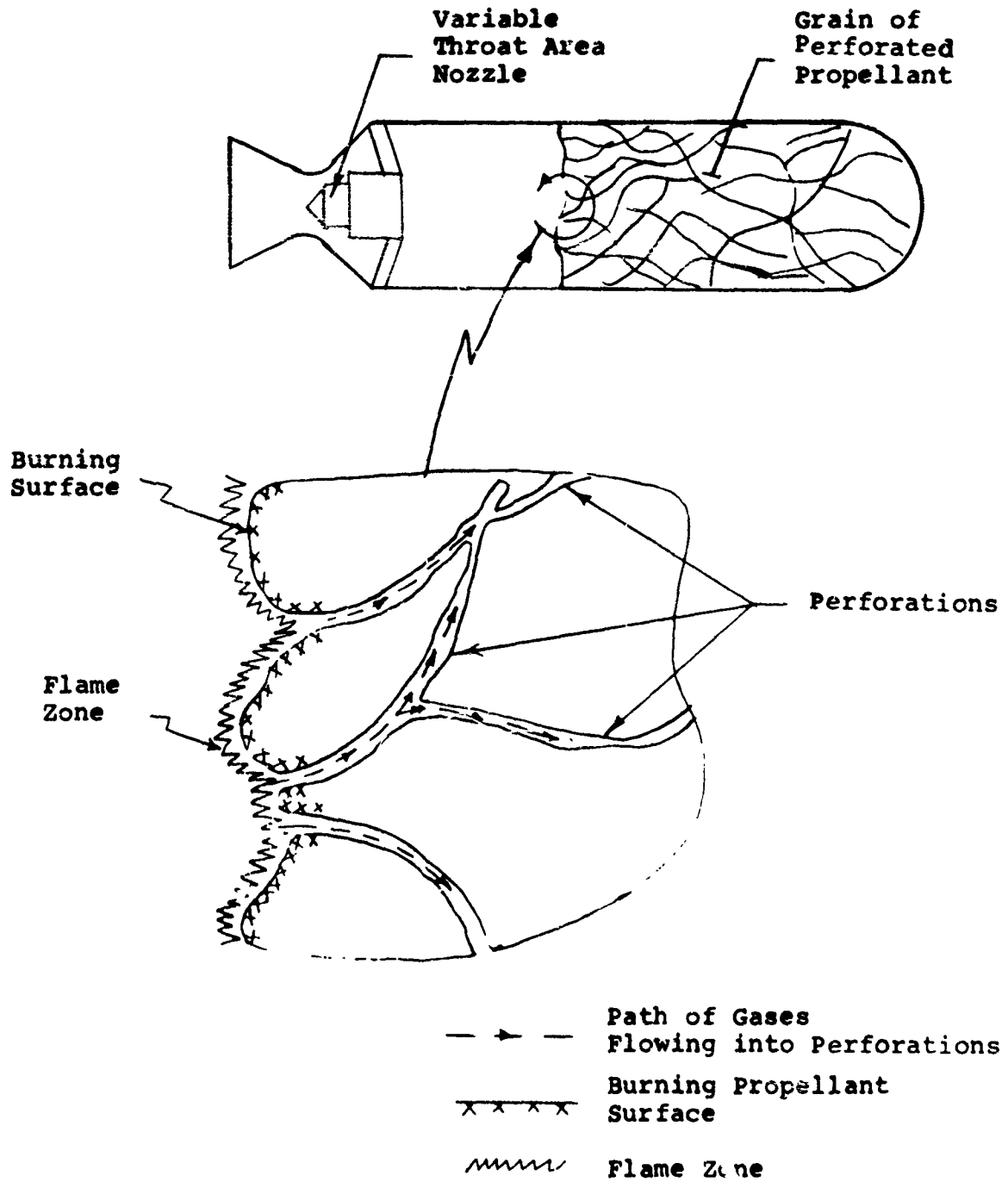


Fig. 26 Schematic Showing Perforated Propellant Grain in a Solid Propellant Rocket Motor.

4. As the hot combustion gases fill the cavities in the perforated propellant, a continuously increasing chamber pressure is required to maintain a constant mass flow rate across the burning surface (see Fig. 27).
5. To achieve the continuous increase in chamber pressure the throat area must be continuously decreased. However, because of the unsteady nature of the flow processes, it is most likely the throat area will be continuously increased and decreased based on commands from the feed-back control system that will be required to dynamically maintain the prescribed thrust level (see Fig. 28).

The foregoing processes are highly transient. For example, an 8-inch diameter rocket motor containing two hundred pounds of propellant would probably operate for less than one second. Thus, we are considering a rocket motor which is unsuitable for conventional sustainer type of operation. The rocket motor under consideration may be used for ultra-high acceleration booster type applications.

Because of the novelty of a controllable rocket motor that uses a perforated propellant, a number of questions immediately arise concerning its practicality. In principle, by developing a mathematical model that includes the interactions among the important processes, analytical investigations can:

1. Establish if stable operation is realistically attainable.
2. Determine the range of controlled burning rates that can be achieved.
3. Investigate the effects of variables such as number of perforations per unit volume, perforation cross-sectional area, perforation geometry, chamber pressure, and basic propellant burning rate.
4. Evaluate the requirements for manufacturing tolerances on the perforations.

One of the primary considerations will be the determination of whether the grain will burn in a uniform manner. Figure 29 illustrates how this consideration may influence the basic concept. Figure 29 shows a configuration where the pressure differential between the chamber and perforation propellant grain is maintained by venting the cooled combustion gas through the head-end dome. The pressure to which the grain is vented is not necessarily atmospheric pressure. In this configuration, if non-uniform burning occurs so as to reduce

———— Independent Variable or Prescribed Parameter
----- Dependent Variable

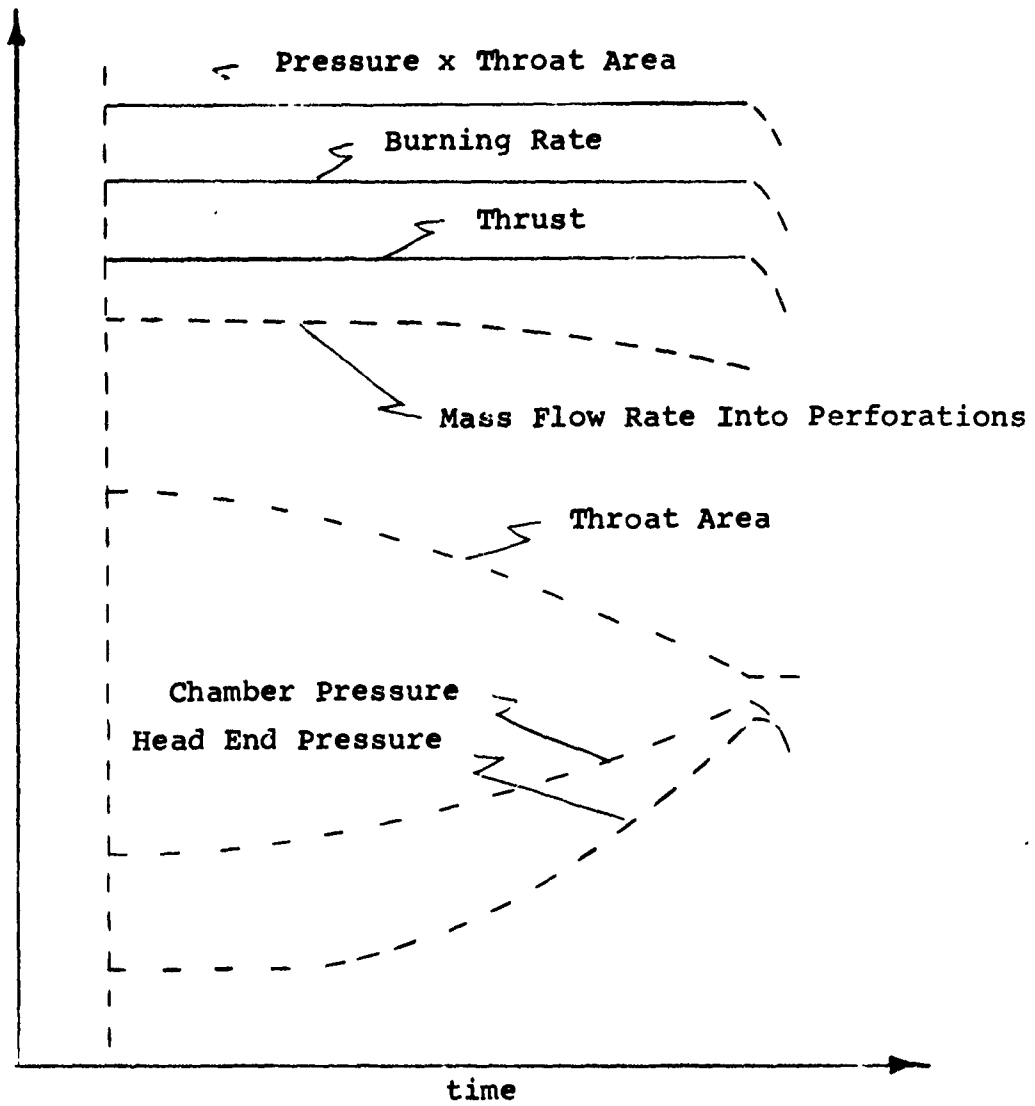


Fig. 27 Transients During Constant Thrust Operation of Rocket Motor with Perforated Propellant Grain.

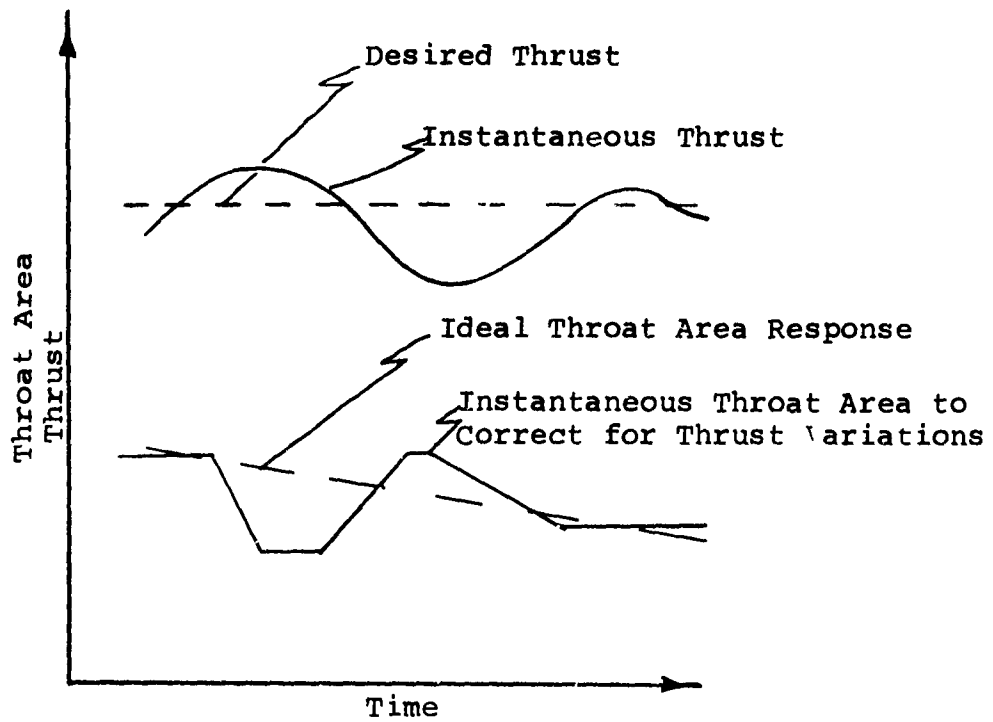
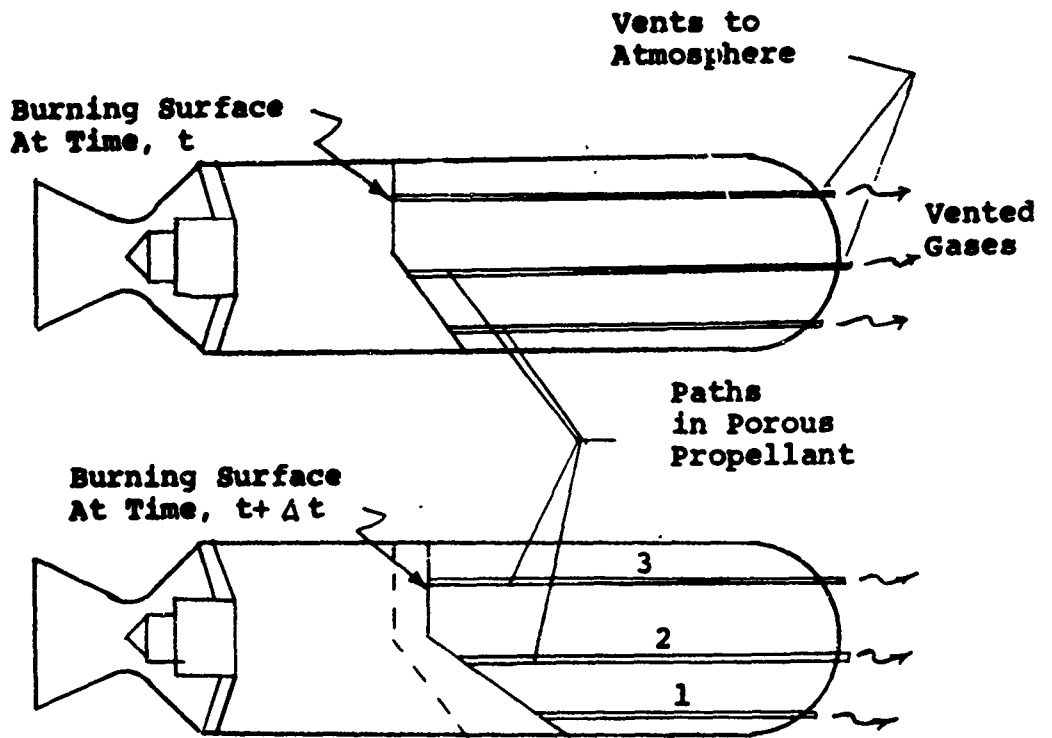
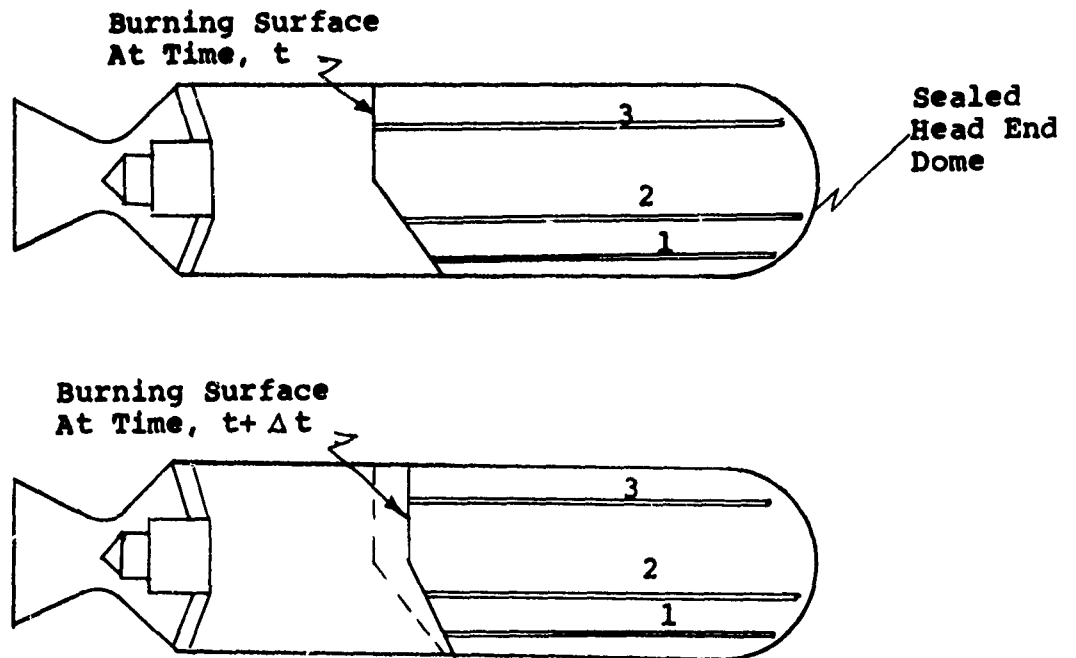


Fig. 28 The Type of Throat Area Response That Will Be Required to Make Continuous Corrections to Thrust.



a) Motor with vented head-end dome (inherently unstable)



b) Motor with sealed head-end dome (inherently stable)

Fig. 29 Response to Non-uniform Burning of Motors With Vented-head Ends and Closed-head Ends.

path length No. 1, then the flow resistance along path No. 1 will be less than along paths Nos. 2 and 3. Accordingly, the mass flow rate into the perforated propellant will be greater in the vicinity of path No. 1, which will further decrease the length of path No. 1. Thus, the situation of non-uniform burning, once it occurs, will become progressively worse. Conversely, if non-uniform burning occurred in the configuration depicted in Fig. 29b, it may tend to correct itself. The head-end dome of the configuration of Fig. 29b is not vented; the perforations are formed in a primarily axial direction without radial gas passages in the grain. In this configuration, when the length of path No. 1 is shortened by non-uniform burning, the pressure in the perforations forming path No. 1 will rise and, thereby, decrease the local pressure differential between the motor chamber and the entrance to path No. 1. As a consequence, the burning rate in the vicinity of path No. 1 decreases and the burning surface becomes less non-uniform. From first appearances, the non-vented, head-end dome configuration of Fig. 29 offers the promise of a rocket motor configuration with self regulating burning rates.

It should be noted that non-uniform burning is commonly observed in end-burning rocket motors and that radial pressure gradients will occur because of the converging axisymmetric flow in the chamber.

B. Analysis

This section presents a system of mathematical equations that account for the important physical processes and the interactions among them. As previously pointed out, the physical situation is complex. Indeed, intuition is of little value in estimating such items as burning rates, practical perforation dimensions, and pressure levels. Assumptions consistent with the physical property accuracy were introduced early in the equation derivations; approximate numerical techniques were used to solve a simplified version of the resulting systems of differential equations.

As indicated in Figure 30, burning rates will be predicted by considering the flow and thermal processes associated with a single perforation. The individual perforations are assumed to be conduits without sharp turns and of circular cross-section. The rocket motor is divided into three interacting flow regions (shown on Fig. 30): Region #1 - upstream of the entrance to the perforation, Region #2 - the entrance section of the perforation (a quasi-steady, developing flow), and Region #3 - the flow region after the hot combustion gases have been cooled (a region of nearly isothermal flow).

The important assumptions are:

General - The fluid is a perfect gas

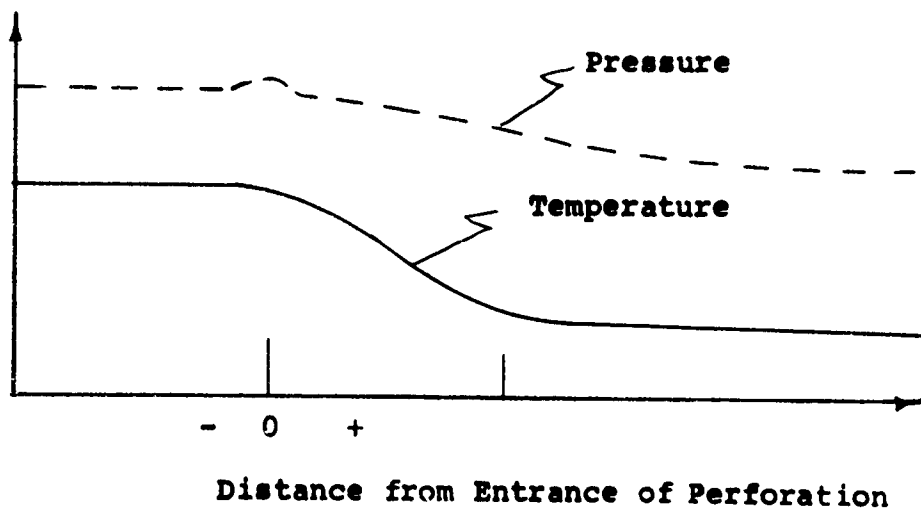
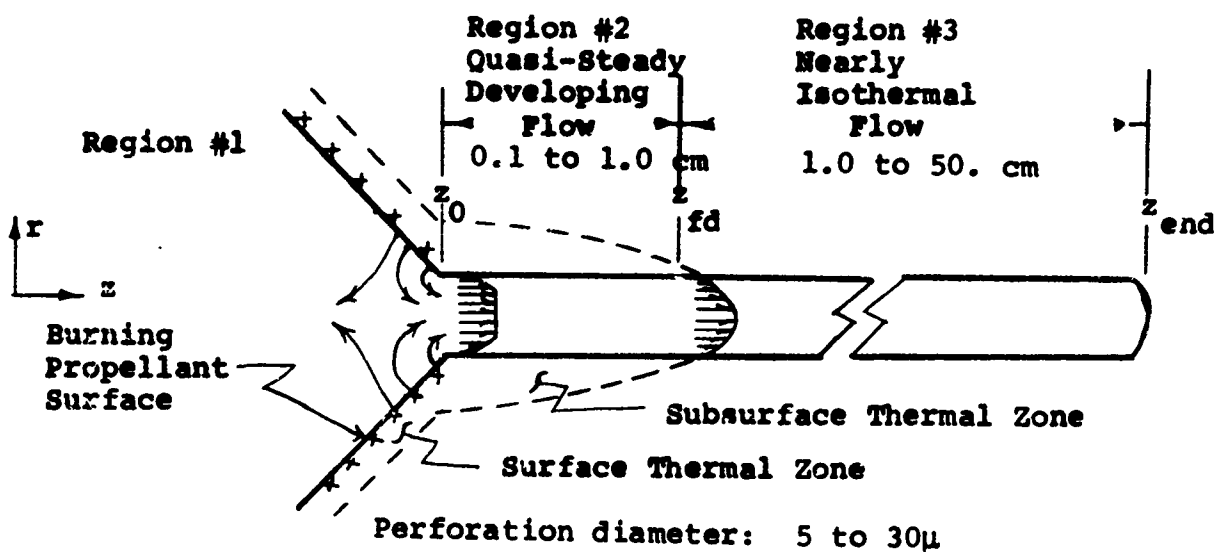


Fig. 30 Idealized Model of Fluid Flow and Thermal Zones in Burning Perforated Propellant Showing a Single Perforation.

Region #1, upstream of entrance to perforation

$\partial P / \partial z$ is small.

Gas temperature is uniform.

Region #2, Entrance region -

Diameter of entrance is much smaller than flame zone thickness

Circular and constant area passage

No sharp turns in passage

Quasi-steady, i.e., pressure transients are slow compared to the time required for a gas molecule to pass through the entrance region.

Axisymmetric and laminar flow

$$u_r \ll u_z$$

$$u_z \gg r$$

Region #3, Region of nearly isothermal flow in propellant grain-

Circular and constant area passage

No sharp turns in passage

Axisymmetric and laminar flow

Velocity profile is parabolic, $u_z = u_{cl} [1 - (r/r_w)^2]$

u_r is small

$$T_g \approx T_i$$

Solid propellant -

Thermal properties do not vary with temperature and time.

Propellant ignites when propellant temperature reaches prescribed ignition temperature, T_{ign}

Surface thermal zone and thermal zones surrounding the perforations are independent of each other.

The thermal zones of adjacent perforations do not interact.

The mass balance in the motor chamber is:

$$\dot{m}_{gen} = \dot{m}_{dis} + \dot{m}_{acc} \quad (26)$$

where:

$$\text{mass generated, } \dot{m}_{gen} = r(t) \rho_p A_b \quad (27)$$

$$\text{mass discharged, } \dot{m}_{dis} = P_c(t) A_t(t) g/c^* + \sum \dot{m}_{\text{into perforations}} \quad (28)$$

$$\begin{aligned} \text{mass accumulated, } \dot{m}_{acc} &= d[\rho_g(t) V_c(t)] / dt \\ &= [V_c dP/dt + P(t) r(t) A_b] / 12.0 RT_g \quad (29) \end{aligned}$$

Pressure and throat area are further constrained by the thrust equation,

$$F = C_F P_c(t) A_t(t)$$

where the thrust coefficient, C_F , is a non-linear function of P_c and A_t .

The equations governing flow in the entrance region (Region #2) are:

$$\text{Continuity} \quad \frac{d}{dz} \int_0^{r_w} \rho_g u_z r dr = 0 \quad (30)$$

$$\text{Momentum} \quad \frac{-r_w^2}{2} \frac{dP}{dz} + r_w \tau_w = \frac{d}{dz} \left(\int_0^{r_w} \rho_g u_z^2 r dr \right) \quad (31)$$

$$\text{Energy} \quad -r_w q = \frac{d}{dz} \left(c_g \int_0^{r_w} \rho_g u_z T r dr \right) \quad (32)$$

A study of the published work on the various types of entrance region flows with large temperature differentials revealed that even with the fluid flow uncoupled from the heat conduction to the propellant, four (coupled) nonlinear partial differential equations must be solved. Accordingly, considerable simplification to the complexity of the mathematical formulation is necessary. A most attractive assumption is to consider that the flow is quasi-steady in the entrance region. This assumption is justified if the cool down time for the hot combustion gases entering the perforation is short compared to the time required for pressure changes in the motor chamber to occur. This is the case because of the high surface area to volume ratio of the perforation, a condition conducive to rapid removal of heat from the gases. Theoretical

descriptions (Eq. 30, 31 and 32) of the steady-state velocity and temperature fields have been accomplished many times in the past. Most of the previous work applies to constant property fluids. Since the temperature differences being considered here are at least 1500K, the fluid densities and viscosities are obviously not constant. Also, existing compressible flow solutions are for either constant heat flux or isothermal wall conditions. In this case the wall temperature and heat flux are necessarily rapidly varying. While recent numerical solutions to Equations 30, 31, and 32 offer the promise of successfully handling the boundary conditions being considered, setting up such a solution is a major undertaking and greatly beyond the scope of this study. Another alternative is to use empirical correlations of friction factors and convective coefficients in tube entrance regions to estimate the pressure and temperature gradients in Region #2. In this manner, since the developing thermal and boundary layer profiles are not solved for, Eqns. 31 and 32 can be integrated as two simultaneous first order ordinary differential equations using numerical techniques.

The equation governing the heat conduction in the propellant adjacent to the entrance region is closely coupled to the equations governing the gas flow in the entrance region. The equation for two-dimensional heat conduction in the propellant (with respect to a fixed coordinate system) is

$$\rho_p c_p \frac{\partial T}{\partial t} = k_p \left(\frac{\partial^2 T}{\partial r^2} + \frac{1}{r} \frac{\partial T}{\partial r} + \frac{\partial^2 T}{\partial z^2} \right) \quad (33)$$

where the boundary conditions are

$$q(z) = -k_p \left(\frac{\partial T}{\partial r} \right) \text{ at } r = r_w \quad (34)$$

$$T = T_i \quad \text{as } r \rightarrow \infty \quad (35)$$

Because of the rapidly varying boundary conditions Eq. 33 must be solved using finite difference techniques. Unfortunately, solutions for 2-D transient heat conduction of the type being considered here require long running times on even the fastest digital computers. Fortunately, the complexity of Equation 33 was reduced so that a relatively simple integral-method, heat conduction solution³⁴ could be used. An order-of-magnitude analysis showed that, for the burning rate regimes of interest the terms $\partial^2 T / \partial z^2$ and $(1/r) (\partial T / \partial r)$ can be neglected.

The equations governing flow in the isothermal portion of the perforated propellant grain (Region #3) are:

Continuity -

$$\frac{r^2}{2} \frac{\partial \rho}{\partial t} + \int_0^{r_w} \frac{\partial \rho u_z}{\partial z} r dr = 0 \quad (36)$$

Momentum -

$$\begin{aligned} \rho \int_0^{r_w} \frac{\partial u_z}{\partial t} r dr + \int_0^{r_w} u_z \frac{\partial u_z}{\partial z} r dr \\ = - \frac{r^2}{2} \frac{\partial p}{\partial z} + \int_0^{r_w} \frac{\partial}{\partial r} \left(r \frac{\partial u_z}{\partial r} \right) dr + \mu \int_0^{r_w} \frac{\partial^2 u_z}{\partial z^2} r dr \end{aligned} \quad (37)$$

where the velocity at any cross section is assumed to be laminar.

Equations 36 and 37 have the boundary conditions

$$P = P_h \quad \text{at} \quad z = z_{\text{end}}$$

when the perforations are vented as shown in Fig. 29a, or

$$u_z = 0 \quad \text{at} \quad z = z_{\text{end}} \quad (38)$$

when the perforations are closed as shown in Fig. 29b.

The calculated burning rate of the perforated propellant is the linear rate (normal to the bulk burning surface) at which the propellant ignition temperature advances along the entrance to the perforation, i.e., the regression rate of the perforation entrance. Keeping in mind that each square inch of burning surface will have a limited number (between 100 and 1000) of perforation openings surrounded by regions of solid propellant, two regression rates must be considered: the regression rate of the perforation entrance and the normal burning rate of the surrounding propellant. On a macroscopic level, the bulk burning rate of the perforated propellant is the regression rate of the perforation entrance, and the normal propellant burning rate has only a second order influence on the bulk burning rate.

Ideally, if homogeneous propellant surrounded each perforation entrance, a conically shaped propellant surface

would form around each perforation. The semivertex angle of the cone would be $\arcsin (r_0/r_{per})$. Actually, since most propellants contain granular oxidizers, the burning surface surrounding the perforations will be a very irregularly shaped pit. For the high burning rate and high performance situation being considered, a mathematical description of the shape of the propellant surface surrounding the perforation is not required in formulating the governing equations.

C. Calculated Results for Perforated Propellants

The three systems of gas phase equations (Equation 26, Equations 30, 31, and 32, and Equations 36 and 37), the heat conduction equation (Equation 33) and their boundary conditions were studied to determine the amount of effort required to obtain a numerical solution. It was concluded that a solution to the equations was beyond the scope of this contract and that any approximate solution would soon be superceded by the closely related research being carried on by K. K. Kuo (a Ph.D. candidate under the supervision of M. Summerfield). Mr. Kuo is developing a mathematical model to study the pressure, velocity, and mass generation rate transients during the ignition of porous propellants and packed beds of propellant grains. The formulation of the aerothermodynamic problem is being approached in a vigorous manner and the solution is being obtained by means of an extensive numerical scheme. When Kuo's solution is available it can be extended to perform analyses of motors containing perforated propellants. Accordingly, additional simplifications were made to the equations present in this report in order to obtain interim results. These simplifications are: 1) the convective heat transfer coefficient was calculated from the empirical correlations of Ref. 35, 2) friction factors were calculated using the empirical correlation of Ref. 36, and 3) the flow in Region #3 was vented and quasi steady. The resulting simultaneous first order differential equations for the flow were solved using the Runge Kutta method. The solution for the gas flow was coupled to the heat conduction solution obtained using Hill's method³⁴.

Calculated results were obtained to investigate the characteristics of burning perforated propellants. Since the results correspond to a range of burning rates and chamber pressurization rates which are much greater than conventionally used in rocket motors, they should be viewed in terms of possible new applications which can take advantage of such high rates. Also, as previously discussed, motors with variable throat area nozzles to compensate for the effects of extremely rapid pressure transients should be considered when searching for perforated propellant applications.

Unless otherwise indicated, the values used in the calculations are those of the Datum Case defined in Table 4. The gases that flow into the perforations are the combustion products of the binder and ammonium perchlorate in a composite propellant that contains 14% aluminum. The aluminum combustion

TABLE 4

Datum Case Values Used in Perforated Propellant Calculations

Diameter of perforation, $D_{per} = 0.002$ cm
Thermal conductivity of propellant, $k_p = 0.00105$ cal/cm K sec
Density of propellant*, $\rho_p = 1.952$ gm/cm³
Specific heat of propellant, $c_p = 0.344$ cal/gm K
Ignition temperature of propellant, $T_{ign} = 713$ K
Gas temperature at entrance to perforation, $T_g = 2547$ K
Specific heat of gas, $c_g = 0.49$ cal/gm K
Average molecular weight of gas, $\bar{m}_g = 22.99$ gm/gm-mole
Ratio of specific heat of gas, $\gamma_g = 1.22$
Chamber pressure, $P_c = 35$ atm
Head-End pressure, $P_h = 20$ atm
Length of perforation, $L = 10.0$ cm

* For reasons explained in the text, the propellant along the perforation was considered to have the same thermal properties as ammonium perchlorate.

is considered not to affect the gases that flow into the perforations since the major portion of the aluminum burns after it leaves the propellant surface and the gases that flow into the small perforations come from the gaseous regions immediately above the burning propellant. The thermal properties of the propellant surrounding the perforation are those of ammonium perchlorate rather than the mean properties of the mixture of aluminum, binder, and ammonium perchlorate. The ammonium perchlorate thermal properties were used since heating ammonium perchlorate to its ignition point is a realistic criterion for ignition along the walls of the perforation. Also, this criterion is further justified by the fact that in many practical propellants the ammonium perchlorate particle dimensions will be larger than the thickness of the thermal zone surrounding the perforations.

Figures 31 and 32 show the gas properties in the entrance region corresponding to a chamber pressure of 34 atm and a mass flow rate into the perforation of 0.00097 gm/sec. The steep pressure and thermal gradients in Fig. 31 are characteristic of entrance region flows. Fig. 32 shows the very large convective heat transfer coefficients near the leading edge of the perforation and the decrease in gas velocity as the gas is cooled.

Burning rates and mass flow rates into the perforation are shown in Fig. 33 as a function of chamber pressure. Note that in the range of P_c covered by the figure the effective pressure exponent for the perforated propellant, n , (for a $r = aP^n$ burning rate law) is approximately one. Also the pressure exponent increases as chamber pressure increases. This indicates that an equilibrium balance of mass generated by the burning propellant surface and the mass discharged through a constant throat area nozzle may not be obtainable.

The effects of perforation diameter on the burning characteristics are of particular interest since perforation diameter can be controlled as part of the propellant grain manufacturing process. The results presented in Fig. 34 show that burning rate increases as perforation diameter increases. The rate of heat transfer to the walls of the perforation increases as perforation diameter increases. The rate of heat transfer to the walls of the perforation increases as diameter increases since the mass flow rate of the hot combustion gases entering the perforation increases as the square of the diameter and the surface area along the perforations increases linearly with diameter. For the range of perforation diameters included in Fig. 34, the convective coefficient varies less than 25% since the changes in mass flow rate and perforation diameter have compensating effects. The net effect is that as perforation diameter increases the hot combustion gases penetrate to a greater depth below the perforation opening and the propellant along the walls of the perforation is heated at a greater rate.

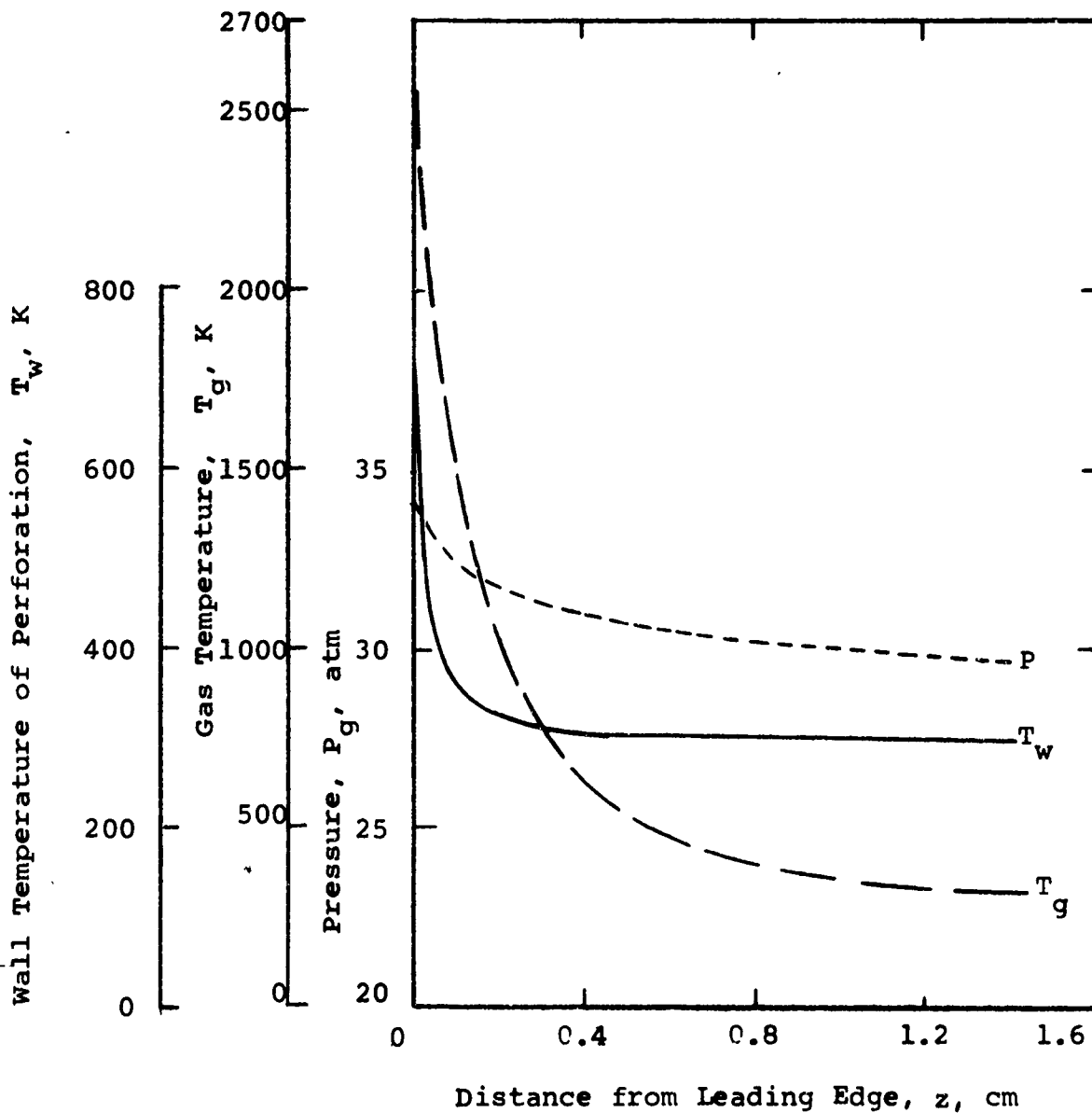


Fig.31 Pressure and Temperatures Along Perforation for Datum Case Conditions

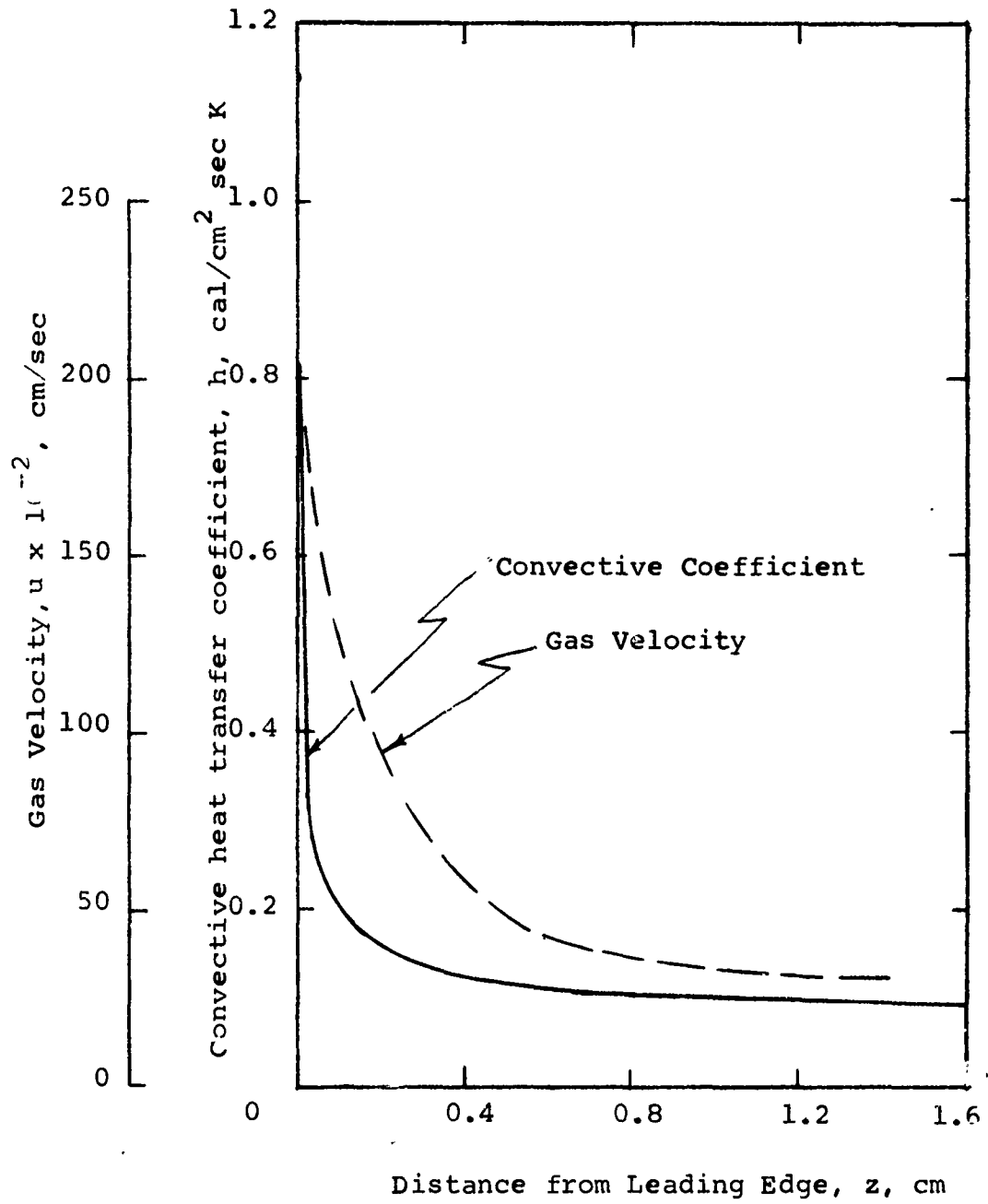


Fig. 32 Gas Velocity and Convective Heat Transfer Coefficient Along Perforation for Datum Case Conditions

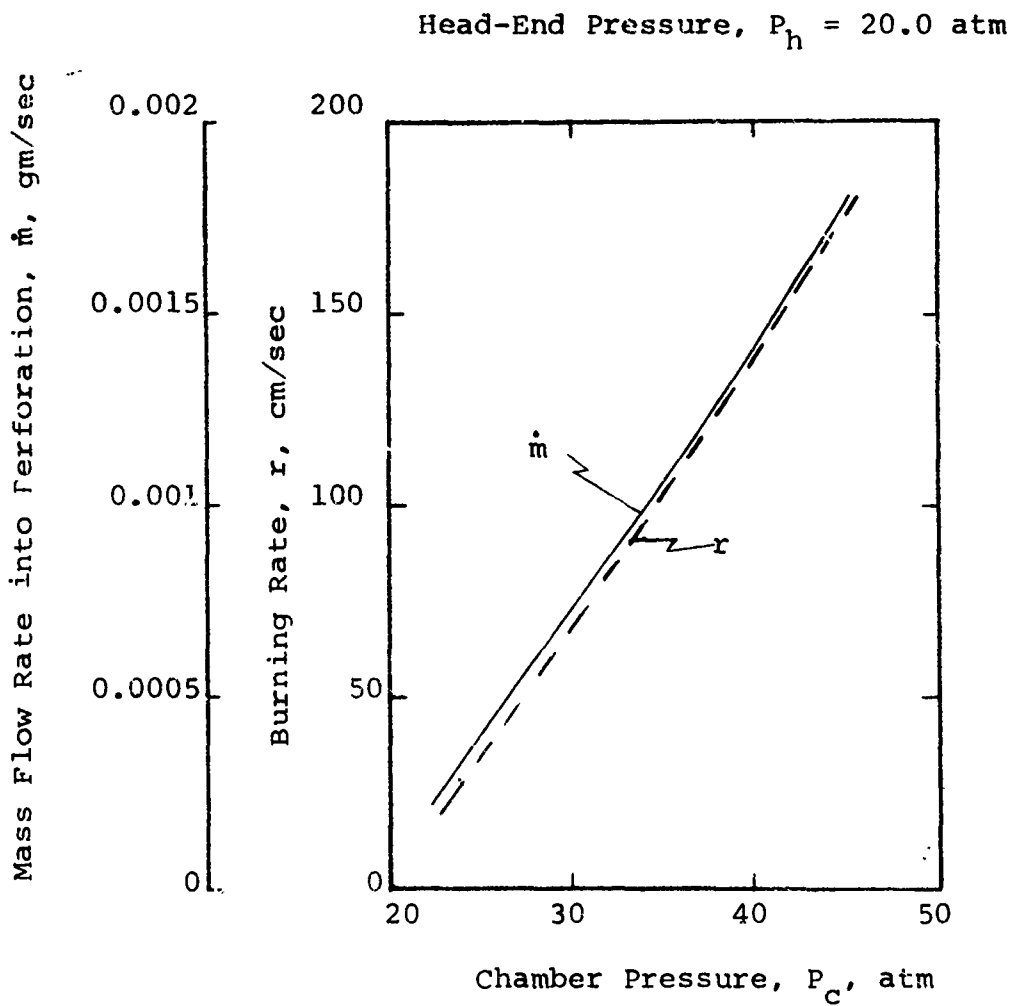


Fig. 33 Perforated Propellant Burning Rate and Mass Flow Rate into Perforation as a Function of Chamber Pressure

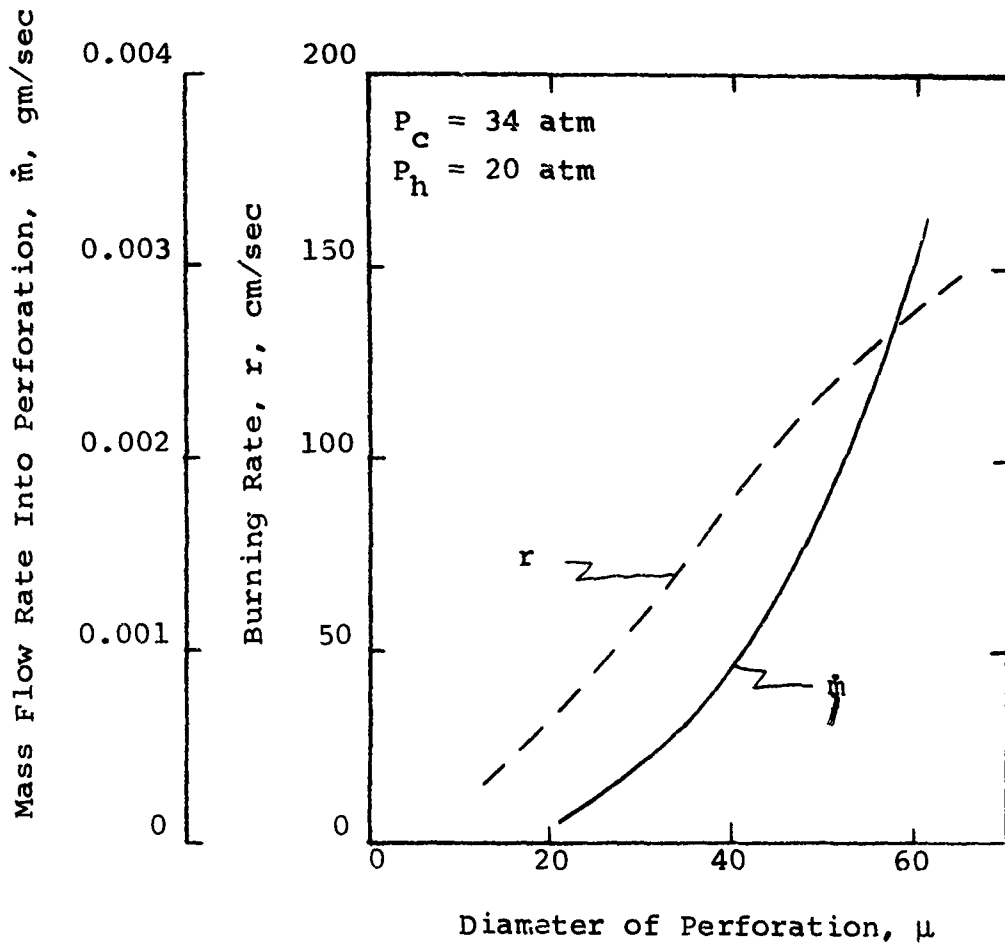


Fig. 34 Effect of Perforation Diameter on Mass Flow Rate and Burning Rate

The total mass flow rate into the perforations is small compared to the gas generated by the burning surface. For example, let us consider the datum case and a propellant with 100 perforation openings per square centimeter of burning surface. Then for a burning rate of 92 cm/sec, the mass flow into the perforations (per unit surface area) is

$$100 \text{ perforation/cm}^2 \times 0.00097 \text{ gm/sec/perforation} = 0.097 \text{ gm/sec cm}^2$$

and the mass from the surface (per unit surface area) is

$$1.72 \text{ gm/cm}^3 \times 92 \text{ cm/sec} = 158 \text{ gm/sec cm}^2$$

Figure 35 shows how burning rate decreases as the pressure differential between the chamber and the head-end is allowed to decrease. Another important variable is the length of the grain. For a given pressure differential between the chamber and the head end the mass flow rate and, thus, the burning rate will increase as the length of the grain decreases. These effects are shown in Fig. 36 with perforation diameter as a parameter.

For the sealed head-end dome case shown in Fig. 29b, the gas flowing into a perforation rapidly pressurizes the volume formed by the perforation and, thus, the mass flow rate rapidly diminishes as the pressure in the perforation approaches the chamber pressure (see Fig. 35). To a good approximation, constant mass flow rate is required to achieve constant burning rate, but to achieve constant flow rate, the chamber pressure must be increased at approximately the same rate as the head end pressure increases. Thus, to consume a 5 cm long grain at 100 cm/sec, the chamber pressure must be increased several thousand psi in 0.05 sec. Thus, the datum case propellant (even after allowing for modifications) is an unlikely candidate for constant burning rate and surface area applications.

A more practical means of utilizing perforated propellants with sealed head-ends is to allow the burning rate to decrease as the increase in head-end pressure reduces the pressure differential between the chamber and the head-end and to obtain part of the pressure level control by means of propellant grains that are designed to burn with rapidly changing surface areas.

The results in Figs. 33 through 36 are initial results and must be interpreted in terms of individual applications. While the predicted burning rates are much higher than conventional burning rates, they are well within the range of interest. Because of the strong influence of grain length and pressure differentials on the burning rate, any system which uses perforated propellants as a means of obtaining command control of burning rate will require complex feed-back control of the head-end pressure and, most likely, a variable throat area nozzle. Also, perforated propellants may be feasible in non-controllable systems that require extremely high burning rates.

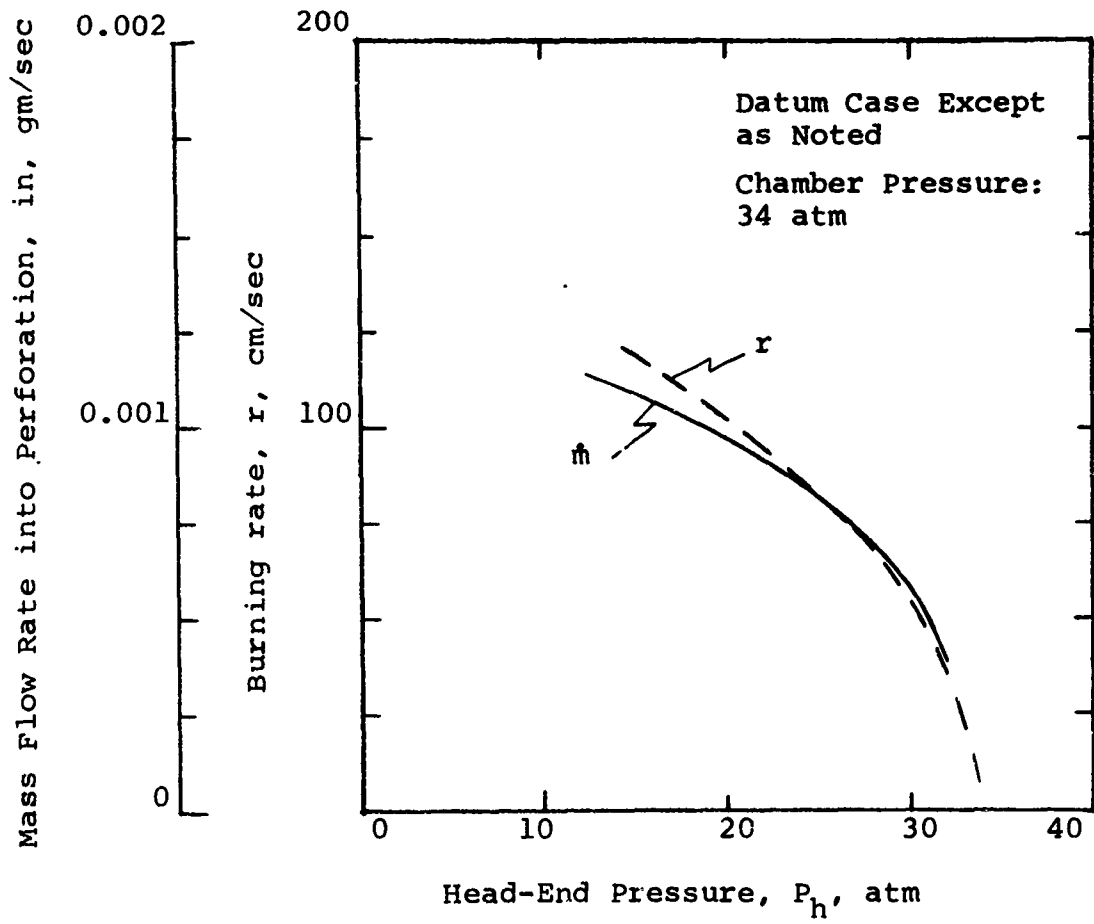


Fig. 35 Burning Rate and Mass Flow Rate as a Function of Head-End Pressure

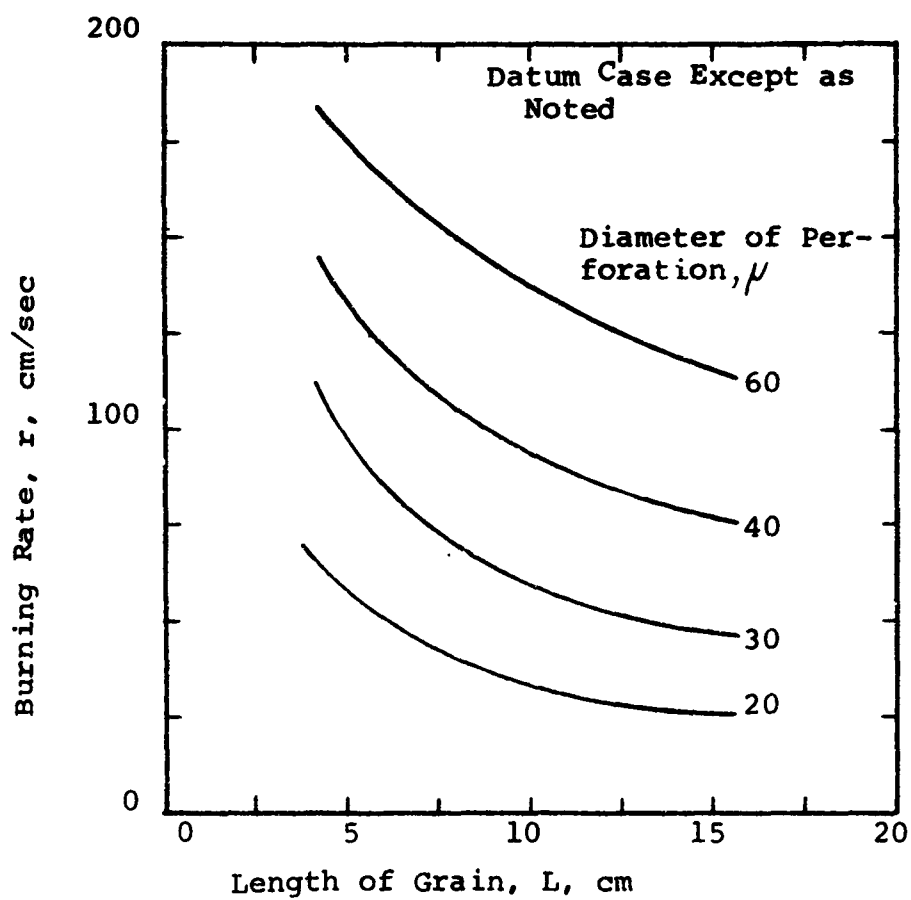


Fig. 36 Burning Rate as a Function of Grain Length

SECTION VI

EMBEDDED POROUS ELEMENT ROCKET MOTOR (EPERM)

A new approach to command control of burning rate emerged as a result of this study to evaluate the feasibility of command control of burning rate. Fig. 37 is a schematic drawing of the concept. The figure shows the major components of an end-burning rocket motor that contains small diameter (< 0.3 cm) porous elements.* The burning rate of the propellant surrounding the porous elements is controlled by regulating the back flow of hot combustion gases through the porous elements. The porous elements provide high-resistance flow paths connecting the combustion chamber to the head-end plenum. The pressure differential between the plenum and the combustion chamber and, thus, the gas flow rate in the porous elements can be precisely controlled by controlling the valve that vents the plenum to the atmosphere. Since the embedded element is designed to rapidly transfer heat from the combustion gases, the combustion gases that reach the head-end plenum are cool.

The EPERM offers the promise of the following features:

- a wide range of burning rates;
- command variation of burning rate suitable for at least 8:1 thrust modulation ratios;
- a light weight, high performance propulsion system (the components associated with the concept are light weight and can be used with high performance propellants and with gas generator propellants).
- a motor which can be manufactured using readily developed techniques.

Analyses to determine the characteristics of the embedded elements indicate that the concept is practical. This section describes the operation of the motor and gives the results of the analyses that have been conducted.

A. Description of Concept

The embedded porous elements could be made from relatively inert materials with ignition temperatures between 800 and 1500K.

* As a convenience, this motor will be referred to as the Embedded Porous Element Rocket Motor or as, simply, EPERM.

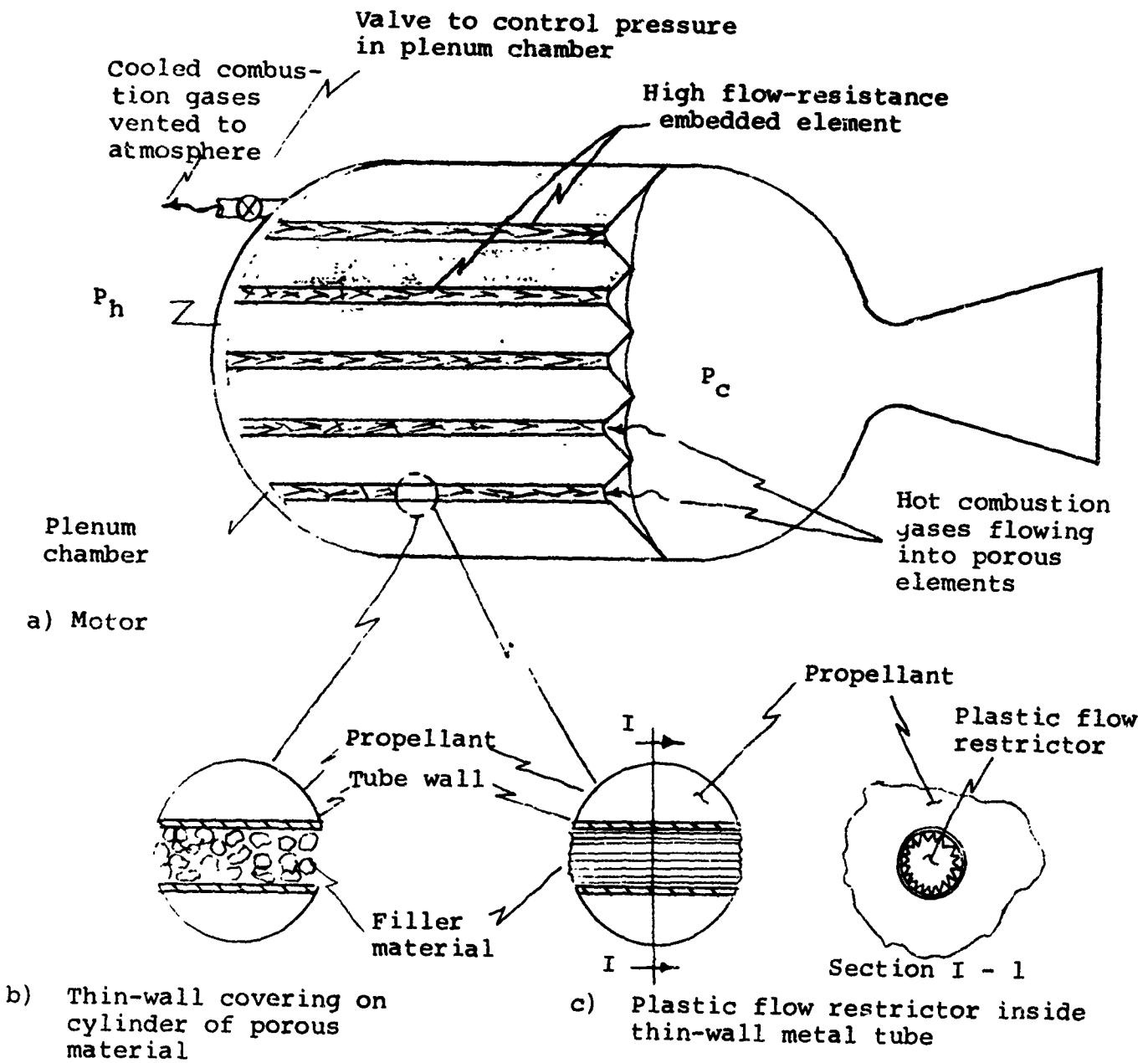


Fig. 37 New Rocket Motor Configuration That Contains Porous Axial Elements That Have Very High Gas-Flow Resistances

The material should possess several properties:

- 1) very high resistance to combustion gas flow;
- 2) low radial thermal resistance to rapidly conduct heat from the combustion gases to the surrounding propellant, i.e., restrict the depth of subsurface heating* ; and
- 3) as the material burns its melt or ash must not plug the flow passages.

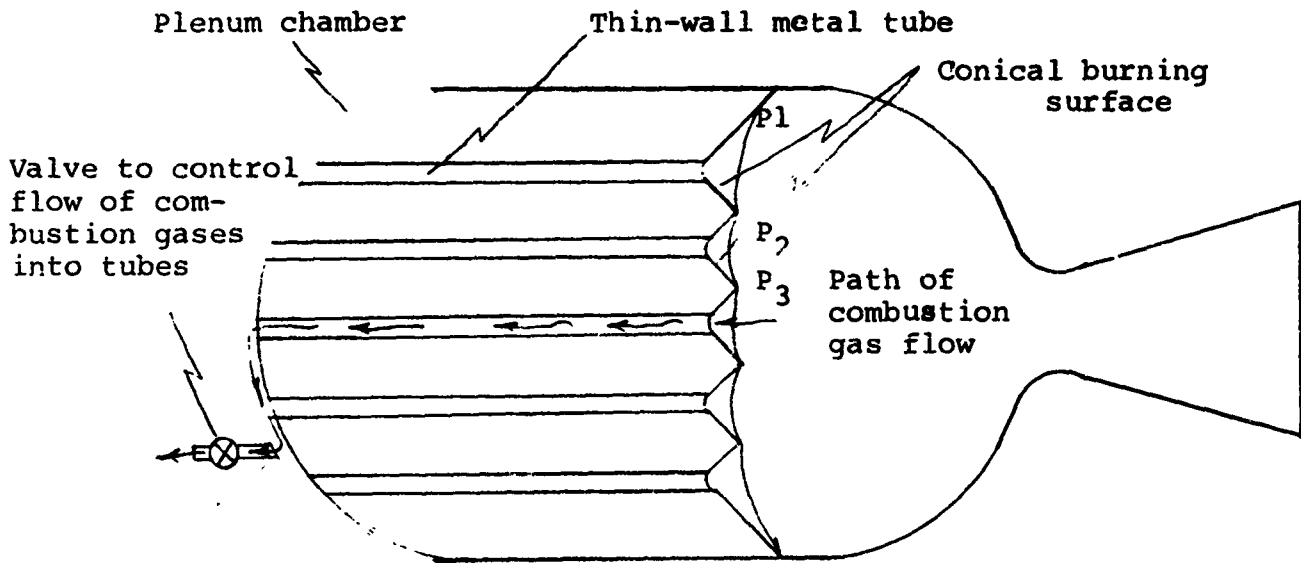
Figs. 37b and 37c show two possible constructions of the porous element. The element in Fig. 37b consists of a pressed or molded porous cylinder covered with a thin (< 0.0025 cm) sheath. Either plastic or aluminum would be suitable materials for the sheath. The element in Fig. 37c is a commercially available metal tube with a plastic flow restrictor inserted in it. The tube could be aluminum and the plastic could be Teflon. Several manufacturing considerations will dictate the construction of the embedded elements: the embedded elements must have sufficient tensile strength so that they can be supported during propellant casting, the outer wall should bond to the propellant, and propellant ingredients must not penetrate the outer circumference and fill the porous passages.

Certain processes in the Embedded Porous Element Rocket Motor are similar to those in two other controllable rocket motor concepts: 1) the controlled combustion of perforated propellants that was considered in Section V of this report 2) the embedded tube rocket motor (see Fig. 38) which was considered by the Thiokol Chemical Corporation^{37,38}. The potential advantages of the EPERM will be pointed out by discussing the distinctive differences between EPERM and the other two controllable rocket motor concepts.

First, EPERM will be compared to the Thiokol embedded tube motor. In the Thiokol concept, control over the flow rate into the embedded tube is achieved in the same manner as just described for the EPERM (see Fig. 38a). Analytical studies demonstrated that the thermal processes were well defined and that propellant burning rates could be predicted by solving the equations for the analytical model shown in Fig. 39. The burning rates were measured at constant pressure conditions; the tube burning rates were very sensitive to small changes in the gas flow rate into the tube (see Figs. 40 and 41). The very large increases in burning rate corresponding to the very small gas flow rates produce two problems that are difficult to solve: First, since the gas flow rates required to heat the tubes are low, the pressure

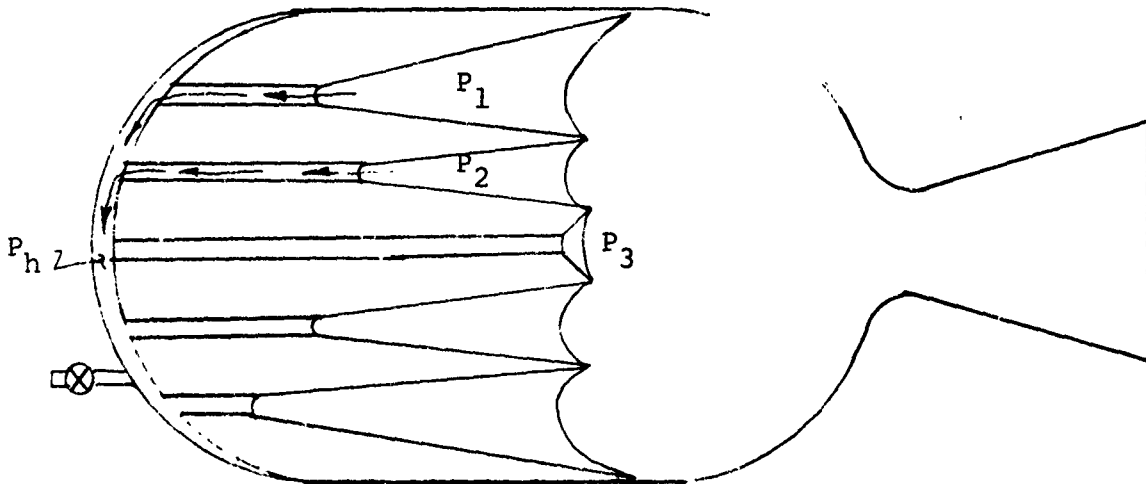
*By restricting the depth of significant subsurface heating to within a few centimeters of the surface, the motor can be throttled back to its basic burning rate. If the propellant were heated to a great depth, all of the heated propellant would have to be consumed before the basic rate of the propellant could be achieved.

NOTE: Tubes are shown greatly oversized
(Typical dimensions: ID, 0.030 in; wall
thickness 0.001 in)



- a) Burning surface if gas flow rates into the individual tubes are equal.

$$P_1 > P_2 > P_3$$



- b) Expected burning surface as a result of nonuniform pressure in the combustion chamber.

Fig.38 Rocket Motor Containing Thin Wall, Metal Tubes Embedded Axially in the Propellant.

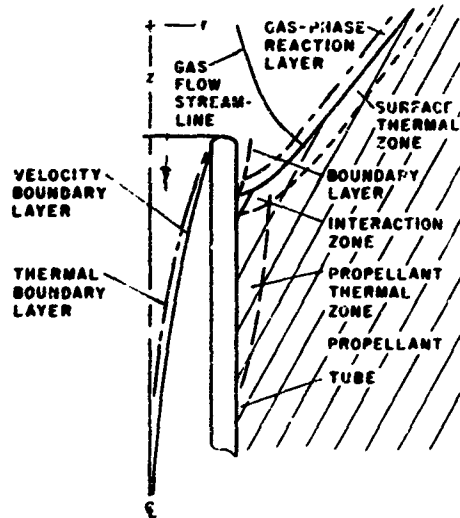


Fig.39 Analytical model for steady-state burning of propellant along an embedded tube with bleed flow. *

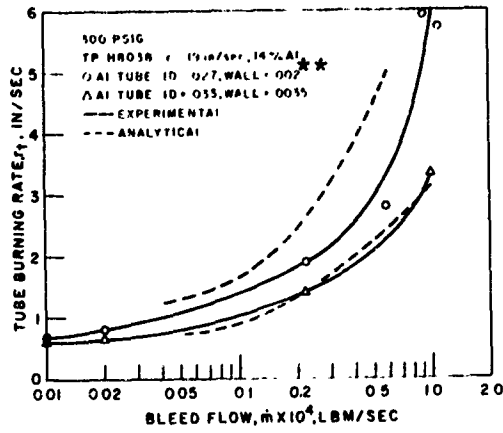


Fig. 40 Analytical and experimental burning rates vs bleed flow. *

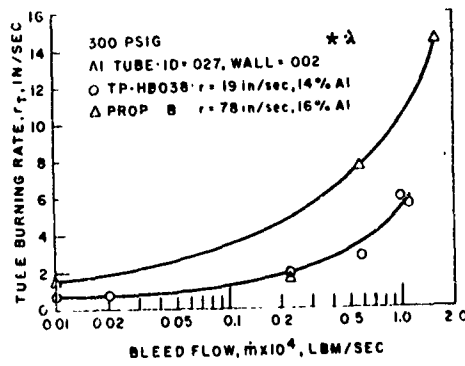


Fig. 41 Effect of propellant composition on tube burning rate. *

* Taken from Reference 37

** All dimensions are in inches

gradients along the tubes are very small (less than 0.1 atm/meter). Thus the radial pressure gradients in end-burning rocket motors* produce large tube-to-tube variations in the pressure differential between motor chamber and the head-end plenum. As indicated in Fig. 38b, the higher pressure differentials and, therefore, the higher tube burning rates occur near the case wall. The cones surrounding the tubes with the higher burning rates are steeper and deeper than the cones surrounding the tubes near the motor center line. The steeper the cone the higher the pressure at the apex of the cone. Also, the shorter tube will have the lowest flow resistance. Thus, the burning rates of the tubes nearest to the case wall progressively increase in an uncontrollable manner.

If the pressure drop along the embedded element is the same order of magnitude as the chamber pressure, the small radial variations in chamber pressure will have only a secondary effect on burning rate and the catastrophic tube burning sequence will not occur. It is hoped that a porous element can be designed to provide the desired pressure drop.

The second problem associated with an embedded tube rocket motor results from the relatively large free volume in the tube. As the chamber pressure is increased, hot combustion gases flow into the tube to equalize pressures in the tube and the combustion chamber. The transient gas flow into the tube corresponding to chamber pressure increases on the order of 500 psi is sufficient to consume the majority of the tube. This effect may also lead to a catastrophic sequence since the higher tube burning rate resulting from hot combustion gases filling the tube further increases the chamber pressure. The smaller gas passages in the higher flow resistance porous elements will have a greatly reduced free volume.

B. Analysis

Since the successful operation of the Embedded Porous Element Rocket Motor (EPERM) depends on achieving equilibrium burning rates over a wide range of chamber pressures, the interactions between the mass flow rates of combustion gases through the porous elements, chamber pressure, and propellant burning rate were analyzed.

Analytical predictions of burning rates and flow characteristics were made for an EPERM that employed porous aluminum elements. The porous aluminum element was selected because data in Ref. 37 can be used to approximate burning rate as a function of gas flow rate into the porous element. The data in Ref. 37 are for burning rate enhancements that result from hot combustion gases flowing through thin wall aluminum tubes. These data were correlated by expressing the burning rate enhancement ratios, r_t/r_{t0} , in terms of the mass flow rate of combustion gas per unit cross-sectional area of the metal tube wall, $\dot{m}/\pi (D_{i,t} + \gamma_w)\gamma_w$.

*In an end-burning motor with a single nozzle, the gas flow results in small but significant pressure differentials in the radial direction.

The assumption was made that a porous aluminum element and a thin wall aluminum tube of equal mass per unit length will produce equal burning rate enhancements if the mass flow rate of the combustion gases through the tube and porous elements are the same. The predicted burning rate enhancements are shown in Fig. 42. Note that the chamber pressure increases will be greater than the increases in burning rate because burning rate, r_b , increases with pressure; thus

$$P \sim (r_e/r_b)^{\frac{1}{1-n}} \quad (39)$$

For purposes of this analysis the porous aluminum element was considered to be made up of aluminum spheres. The Ergun equation as presented in Ref. 39 was expressed in differential form and used to calculate the pressure drops for a range of porous elements. The pressure at the discharge end of a porous element varies with chamber pressure, the mass flow rate, and the diameter of spherical packing used in the porous element.

A knowledge of the pressure differentials along embedded elements and the burning rates of the embedded element as a function of mass flow rate are the important items for establishing the effectiveness of the EPERM. To illustrate the motor parameter variations over an 8:i pressure modulation range, calculations were performed for a particular motor configuration (see Fig. 43). The motor configuration used to obtain the results of Fig. 43 is not an optimum configuration; however, it does demonstrate those characteristics which are necessary for stable rocket motor operation. Without backflow of combustion gases ($\dot{m} = 0$), the equilibrium chamber pressure is 250 psia. Equilibrium chamber pressures above 250 psia are obtained by adjusting the discharge area of the valve which vents the head-end plenum to the atmosphere. If the valve discharge area is increased, the mass flow rate into the porous elements and the pressure drop along the porous elements increase and a higher equilibrium chamber pressure is established. Note that the mass vented through the valve is extremely small compared to the mass generated by a typical rocket motor. Thus the total impulse loss through vented gases is negligible.

Conical burning surface areas will form around each of the embedded elements. The rate at which these conical burning surfaces change their contours and, thus, the pressure response of the EPERM are dependent on the spacing of the embedded elements, the pressure time history of the motor, and the basic propellant burning rate characteristics. The transient development of these conical surfaces must be considered in the control of the EPERM if uniform pressure-time traces are to be achieved^{40, 38}.

C. Calculated Results

A series of calculations was performed to study the characteristics of the motor considered in Fig. 43. Figure 44 shows that for a prescribed \dot{m} , ΔP decreases with increasing chamber pressure.

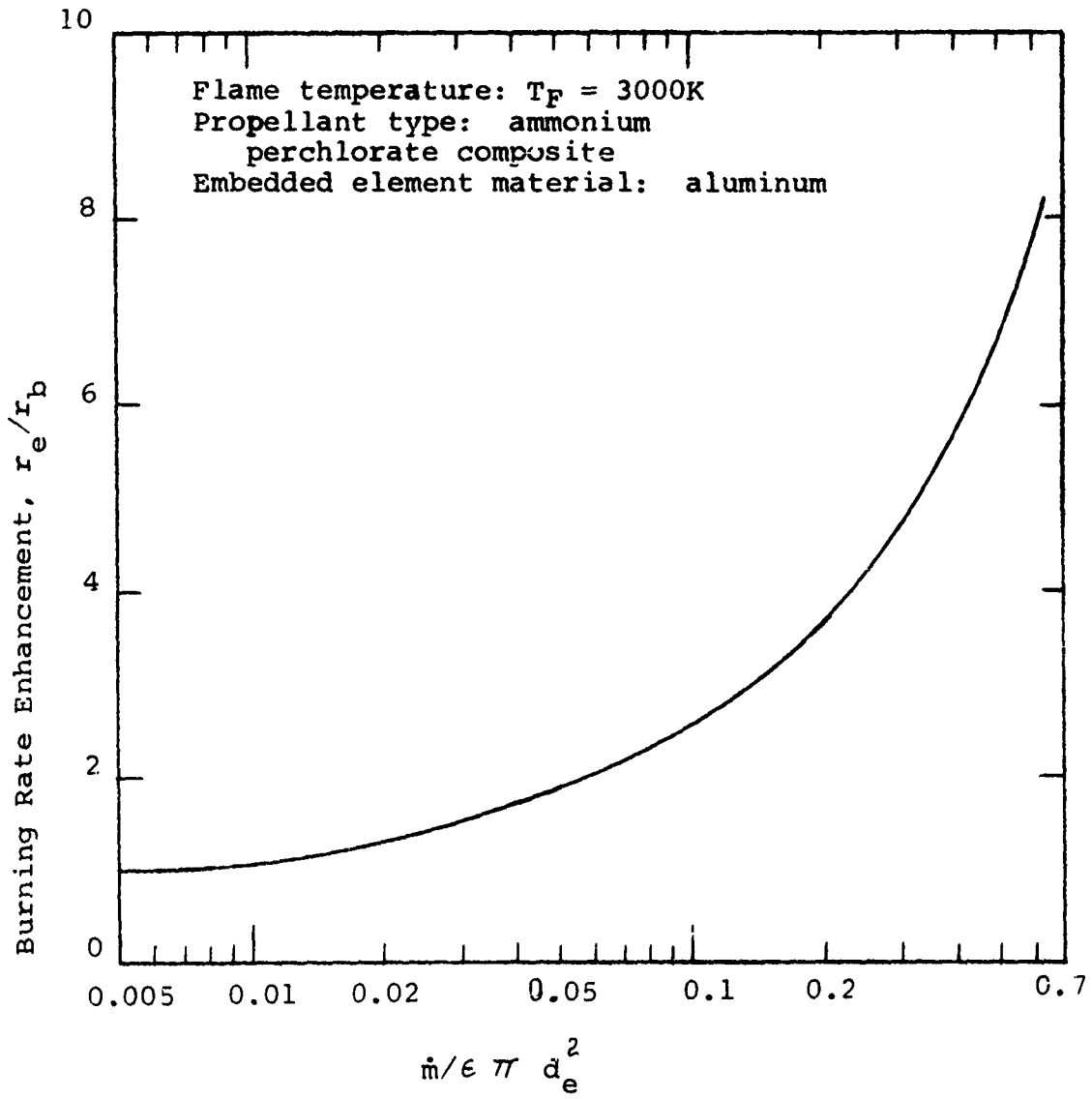


Fig.42 Burning Rate Along Embedded Porous Element as a Function of Mass Flow Rate of Hot Combustion Gases

Chamber pressure without
backflow of combustion
gases: 250 psia

Properties of Embedded
Porous Element

$d_m = 16\mu$

Porosity, $\epsilon = 0.4$

Length = 100 cm

$d_e = 0.05$ cm

Burning Rate Exponent, $n = 0.3$

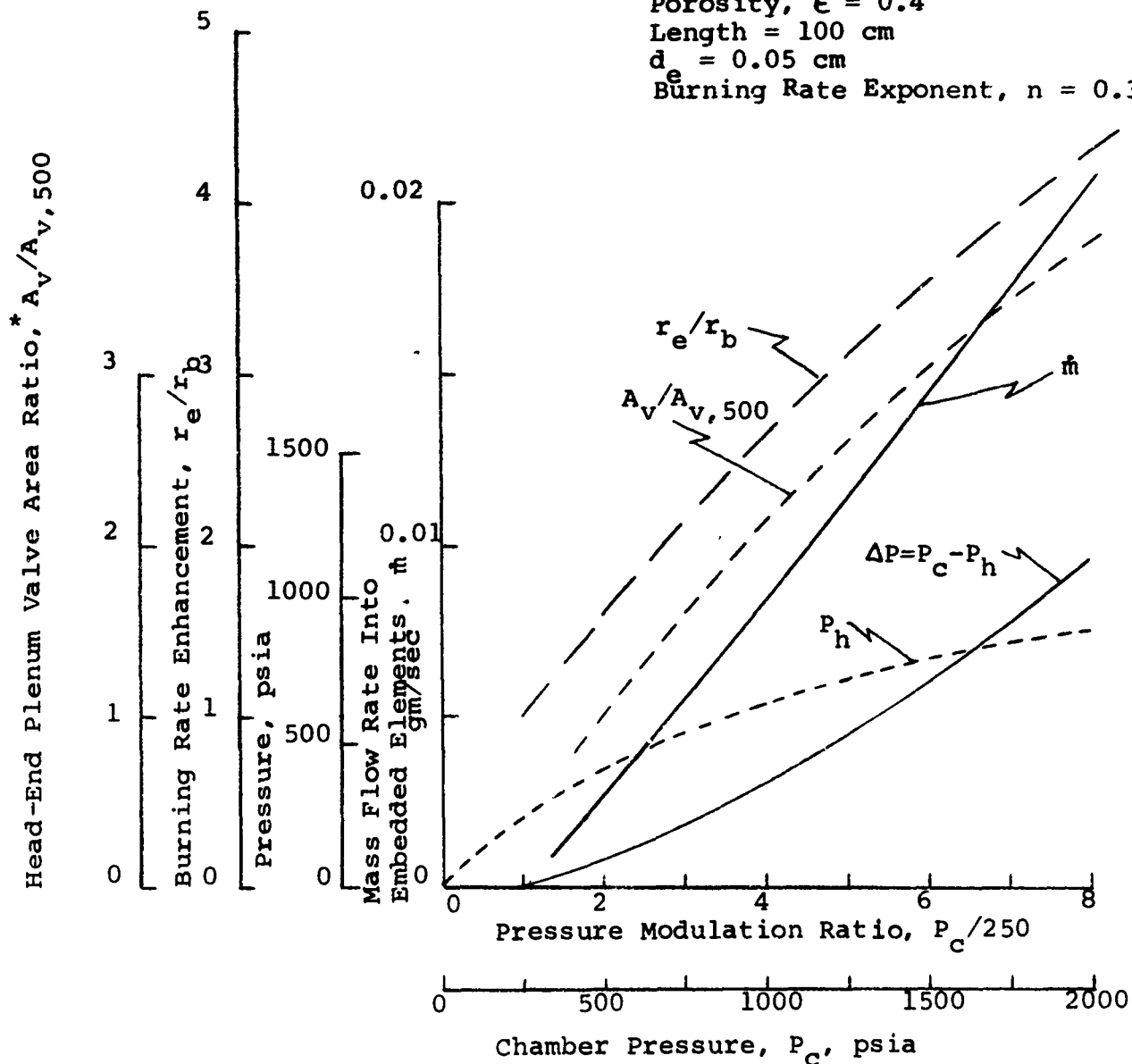


Fig. 43 Parameters of Embedded Porous Element Rocket Motor Up to an 8:1 Pressure Modulation Ratio

* $A_n/A_v,500$ is the discharge area of the head-end plenum valve divided by the discharge area required to achieve 500 psi.

Length = 100 cm
Porosity, $\epsilon = 0.6$
 d_m is Diameter of Spherical Packing

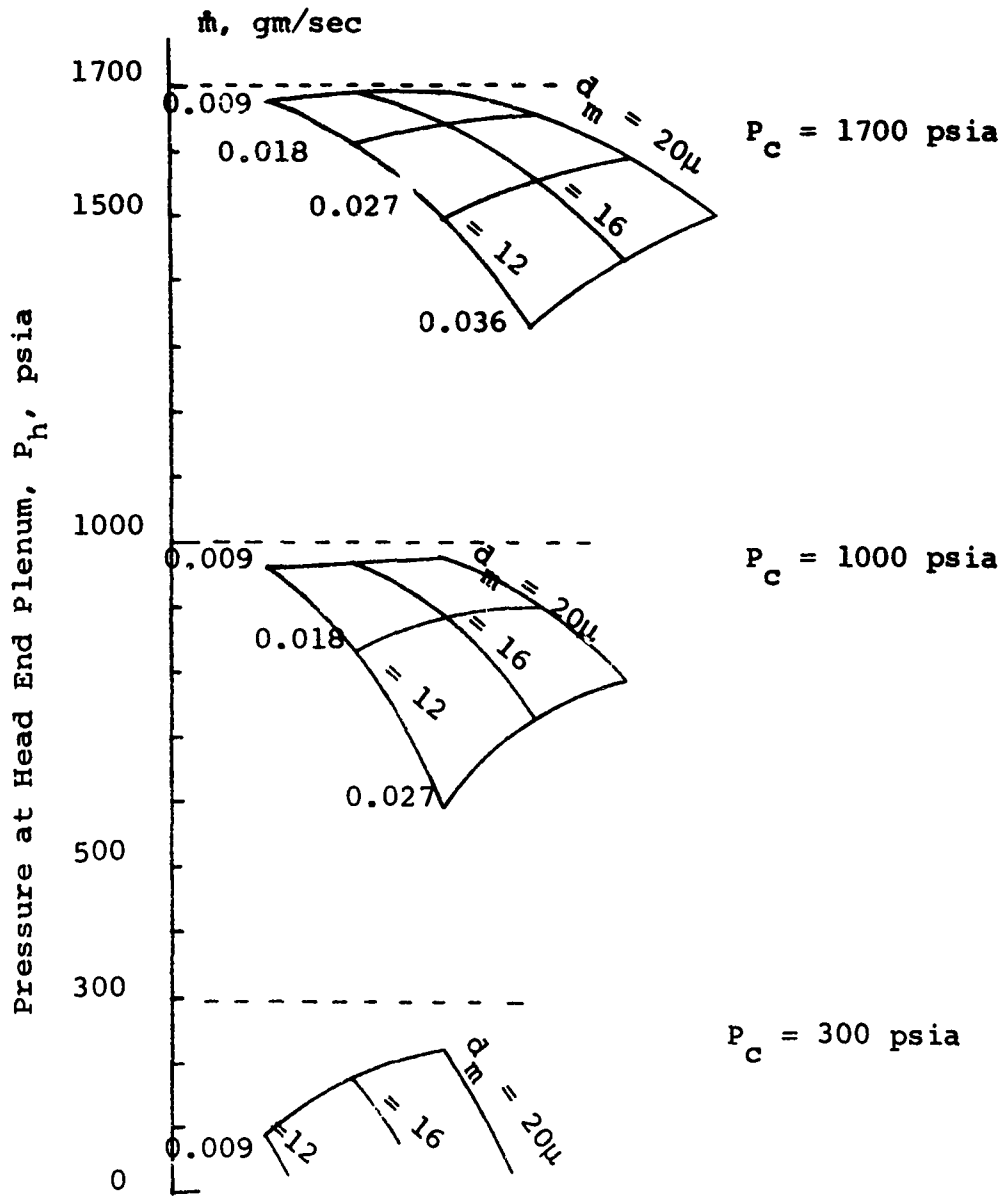


Fig.44 Pressure at the Head End of a Porous Element With Chamber Pressure, Flow Rate, and Spherical Packing Diameter as Parameters

The figure also shows the extent that ΔP is affected by the diameter of the particles in the porous element. Because of the previously discussed interactions among \dot{m} , ΔP , P_c , and P_h , it is of interest to examine the flow characteristics of the embedded elements over a range of equilibrium, motor operation conditions. The shaded portions of Fig. 45, 46, and 47 indicate the pressure drops along the porous elements.

Fig. 45 shows the effect of porosity on the pressure drop along the embedded element and indicates that close tolerances must be maintained over the variation in the porosity of the individual embedded elements when many embedded elements are used in one grain. Note that as porosity decreases from 0.5 to 0.4, significant increases in the pressure drop along the element occur. It is believed that the pressure drops resulting from porosities between 0.4 and 0.5 are sufficiently large to prevent the catastrophic variations in tube burning rates.

Figs. 46 and 47 show the effect of the diameter of the spherical packing on the pressure drop along the embedded element. At the higher pressures and mass flow rates, the diameter of the spherical packing can be an important factor when a low porosity embedded element is required (see Fig. 47). However, if sufficiently large pressure drops can be achieved with lower porosities, then the pressure drop along the element is relatively insensitive to the diameter of the spherical packing.

Figs. 44 through 47 indicate that a porous element with the necessary flow characteristics can be obtained. However, the practical considerations of designing an embedded element with satisfactory flow characteristics over a wide range of motor equilibrium pressures and with acceptable flow variations between individual elements will require careful analyses and development. Many design options are available to provide embedded elements that have the properties to meet the requirements of a particular application. Even though the best designs and configurations can evolve only as a result of rocket motor and strand burner experiments, speculation on some of the desirable characteristics will indicate some of the means of solving potential problems. It can be argued that an all metal embedded element might melt and partially seal off the gas flow path in a random and unpredictable manner. A design which will be less likely to be sealed by melting consists of a thin wall tube filled with either silica or alumina particles. Since the thin wall aluminum tube retaining the particles will burn before either alumina and silica will melt, it is reasonable to expect that the alumina or silica particles will be released and entrained in the flow of combustion gases as they leave the propellant surface. Thus, the entrances of such an embedded element will be continuously removed before melting and plugging can occur. Also, if the embedded element does become plugged by melting or restricted by residues from the gases, the affected portion of the element will be quickly eliminated as the solid propellant burns away and exposes an unaffected portion of the embedded element.

ϵ is Porosity of Embedded Element
Pressure Differential Between Chamber and Head End Plenum

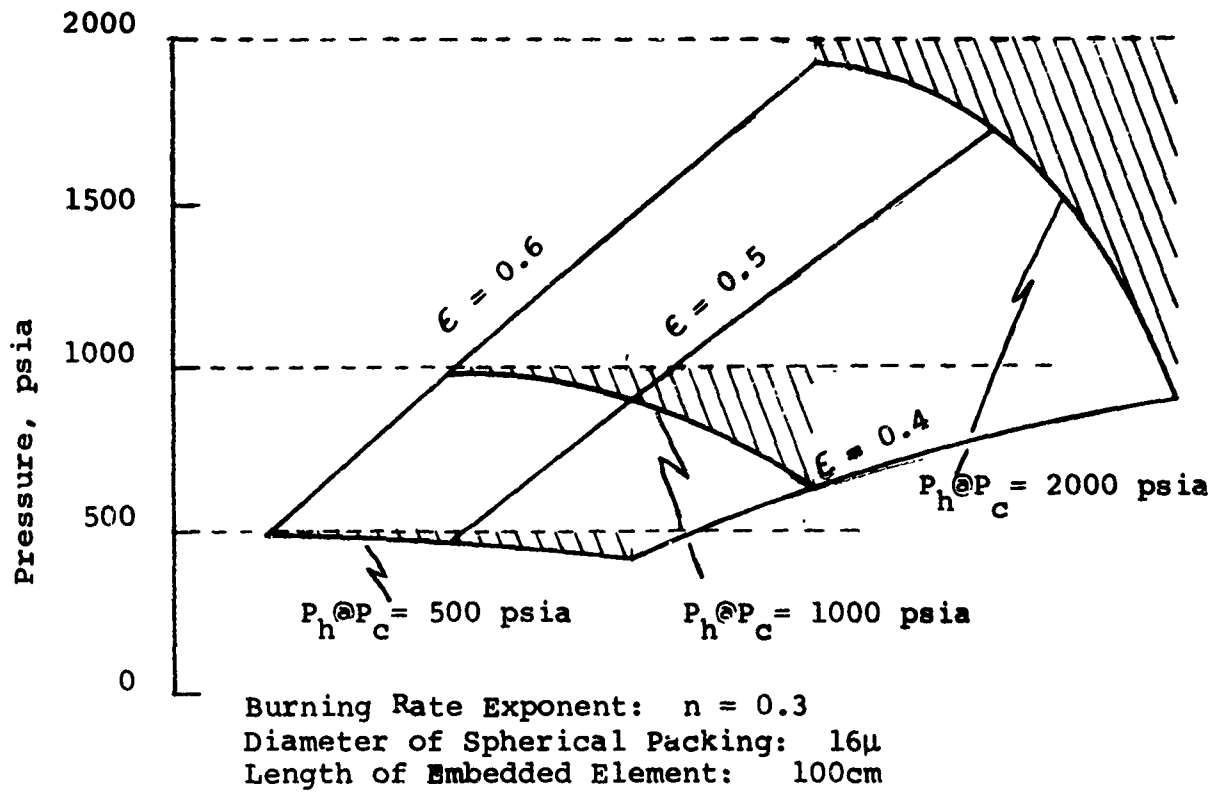


Fig.45 Pressure Differential Between Combustion Chamber and Head End Plenum With Porosity of Embedded Element as a Parameter

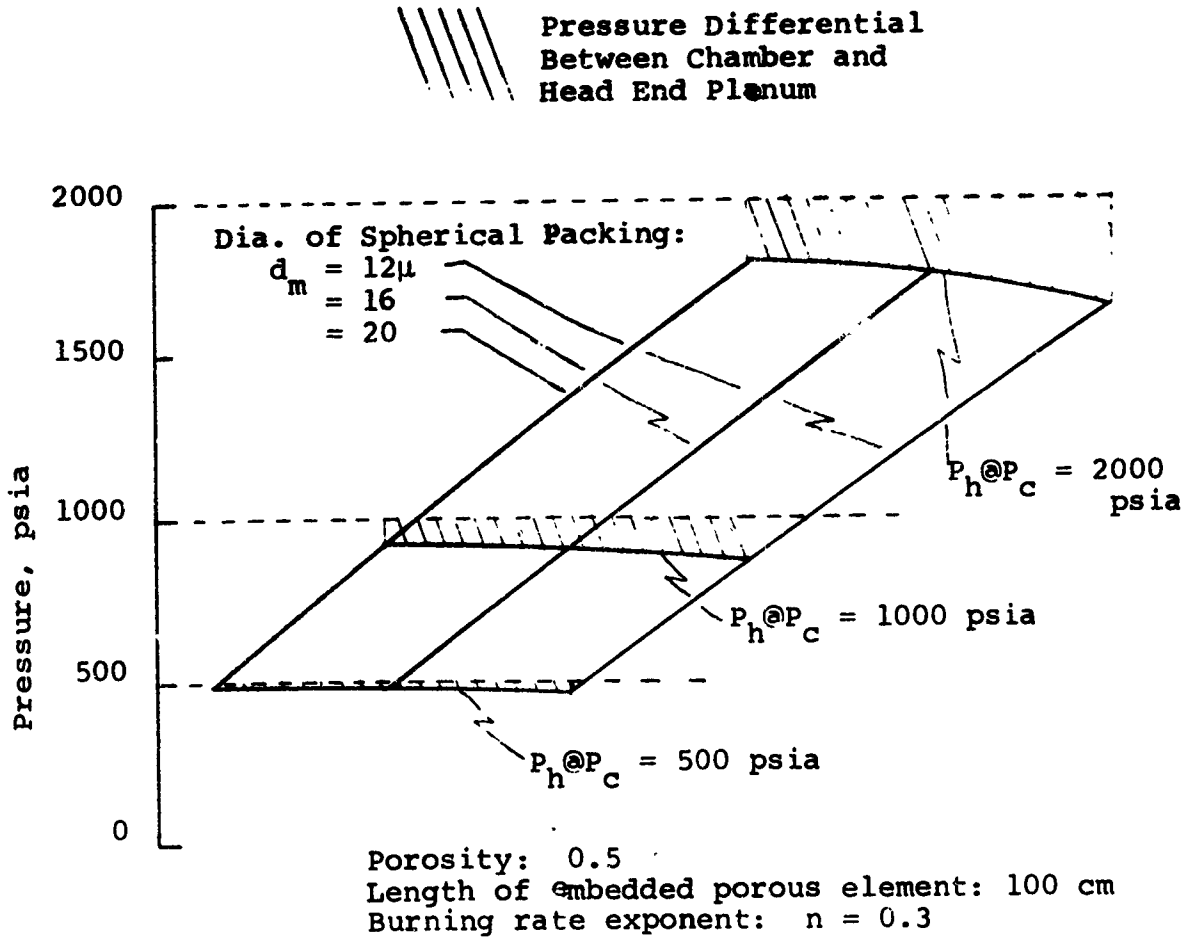


Fig. 46 Pressure Differential Between Combustion Chamber and Head End Plenum With Diameter of Spherical Packing as a Parameter (Porosity = 0.5)

d_m is Diameter of Spherical Packing

Pressure Differential
Between Chamber and
Head End Plenum

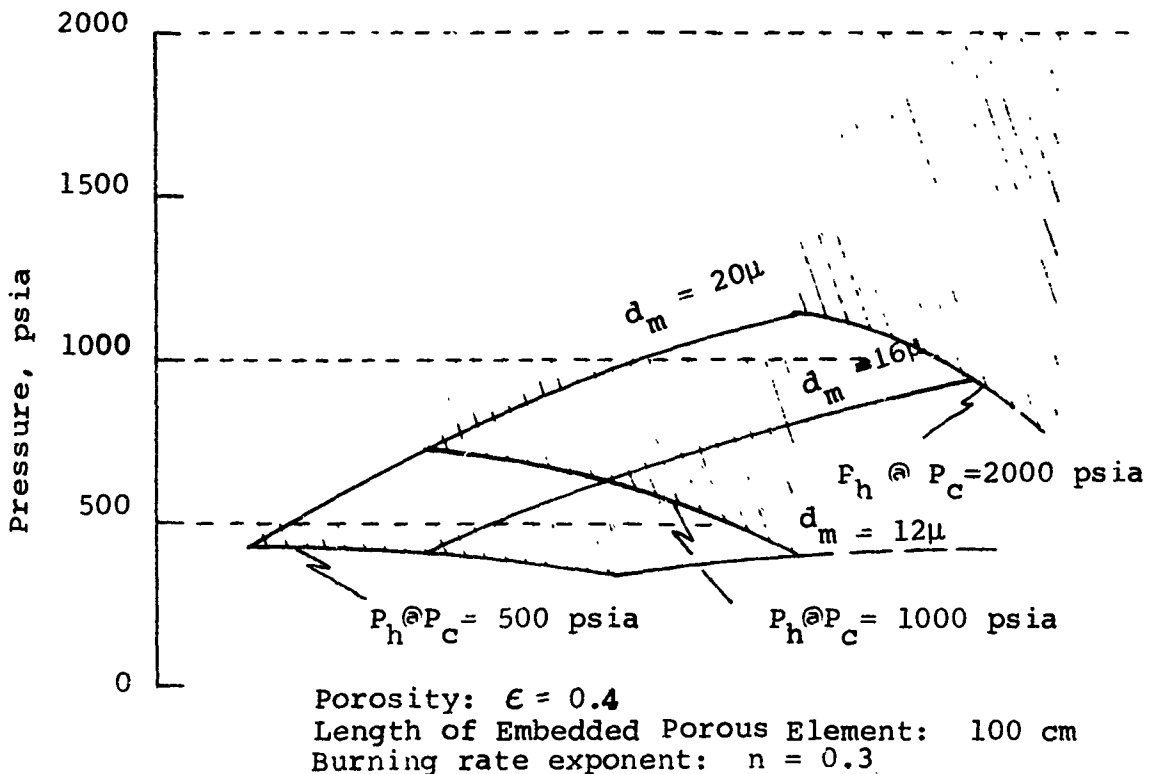


Fig. 47 Pressure Differential Between Combustion Chamber and Head End Plenum With Diameter of Spherical Packing as a Parameter (Porosity = 0.4)

Since some propellants such as gas generator and ducted rocket propellants have very low flame temperatures, inert embedded elements may not be consumed by the influx of combustion gases. An active packing, such as ammonium perchlorate, in an aluminum tube may eliminate this problem.

The results presented in Fig. 43 through 47 are for an embedded element that is 100 cm long. As the embedded element is consumed, the flow resistance and pressure drop along the element decrease. Depending on the duty cycle of the particular rocket motor, a low flow resistance per unit length element which is suitable for high mass flow rates during the initial part of motor operation may not provide sufficient pressure drops during a period of low mass flow rate toward the end of motor operation when the element length is reduced. A means of obtaining pressure drops along the elements that are less dependent on grain length is to use two porous elements in series: a porous element of moderate flow resistance embedded along the full length of the grain and a smaller porous element of higher flow resistance located at the head-end plenum.* Thus, as the longer, embedded porous element is consumed, the higher flow resistance porous element located at the head-end plenum will maintain the required pressure drop.

Based on the preceding analysis and discussion, the EPERM has several attractive features which include:

- a wide range of burning rate control (greater than 8:1)
- a thrust modulation range of greater than 8:1 using conventional low burning rate exponent propellants (i.e., exponents between 0.3 and 0.4)
- compatibility with most solid propellants
- small inert weight penalty.

* The use of high flow resistance elements located at the head-end of the metal tubes used in the Thiokol approach was suggested by G. F. Mangum of the Thiokol Chemical Corporation

BLANK PAGE

SECTION VII

INJECTION OF BURNING RATE CATALYST
VIA THE GAS PHASE

Injection of catalyst into the combustion zones near the burning propellant surface is a potentially attractive method of command control of burning rate. While the mechanisms by which the commonly used iron-containing, burning rate catalysts enhance burning rate are not fully understood, there is sufficient evidence to conclude that the important catalytic reactions occur in the gaseous combustion zones^{41,42} which are less than 200 microns thick at 1000 psi. Also, the more finely the catalyst is dispersed the more effective it is as a rate enhancer^{41,42}. Accordingly, methods which will efficiently and effectively disperse the catalyst in the gaseous combustion zones were sought.

Figure 48 illustrates some of the items that must be considered in evaluating the effectiveness of the catalyst injection method of burning rate control. To insure that the catalyst is uniformly dispersed in the axial direction, an injector such as a piccolo tube injector may be required (see Fig. 48a). If the catalyst is injected at the head-end, the previously discussed problems of displacement and nonuniform density of injected particulate matter also apply to the injected catalyst (see Fig. 4 and 5).

Another consideration is the injector to be used to disperse the catalyst in the combustion zone. There are two conflicting requirements: 1) If the catalyst is to be efficiently used, it must be dispersed as a finely atomized spray in the very thin gaseous combustion zones; and 2) if the catalyst is to be effective, the individual droplets must have sufficient momentum and mass so that they are not completely oxidized before they arrive at the gaseous combustion zones⁴³. If the catalyst is injected as a solid jet to insure that it is not oxidized before it reaches the combustion zones, the jet may locally deluge the burning surface and may not be finely dispersed after it impinges on the surface (see Fig. 48b). In addition, such a jet may locally quench the burning propellant. On the other hand, sprays that disperse the catalyst in the combustion zones (see Fig. 48c) may not be practical since the initial droplet size and velocity of such sprays may result in most of the catalyst being oxidized before it arrives at the gaseous combustion zones.

Of course, the catalyst injection problem is a function of motor size, the degree of burning rate control that is required, motor geometry, and the acceptable performance penalty.

* For ammonium perchlorate composite propellants, the combustion zones of interest are the ammonium perchlorate gas phase decomposition zone and ammonium perchlorate-binder diffusion flame.

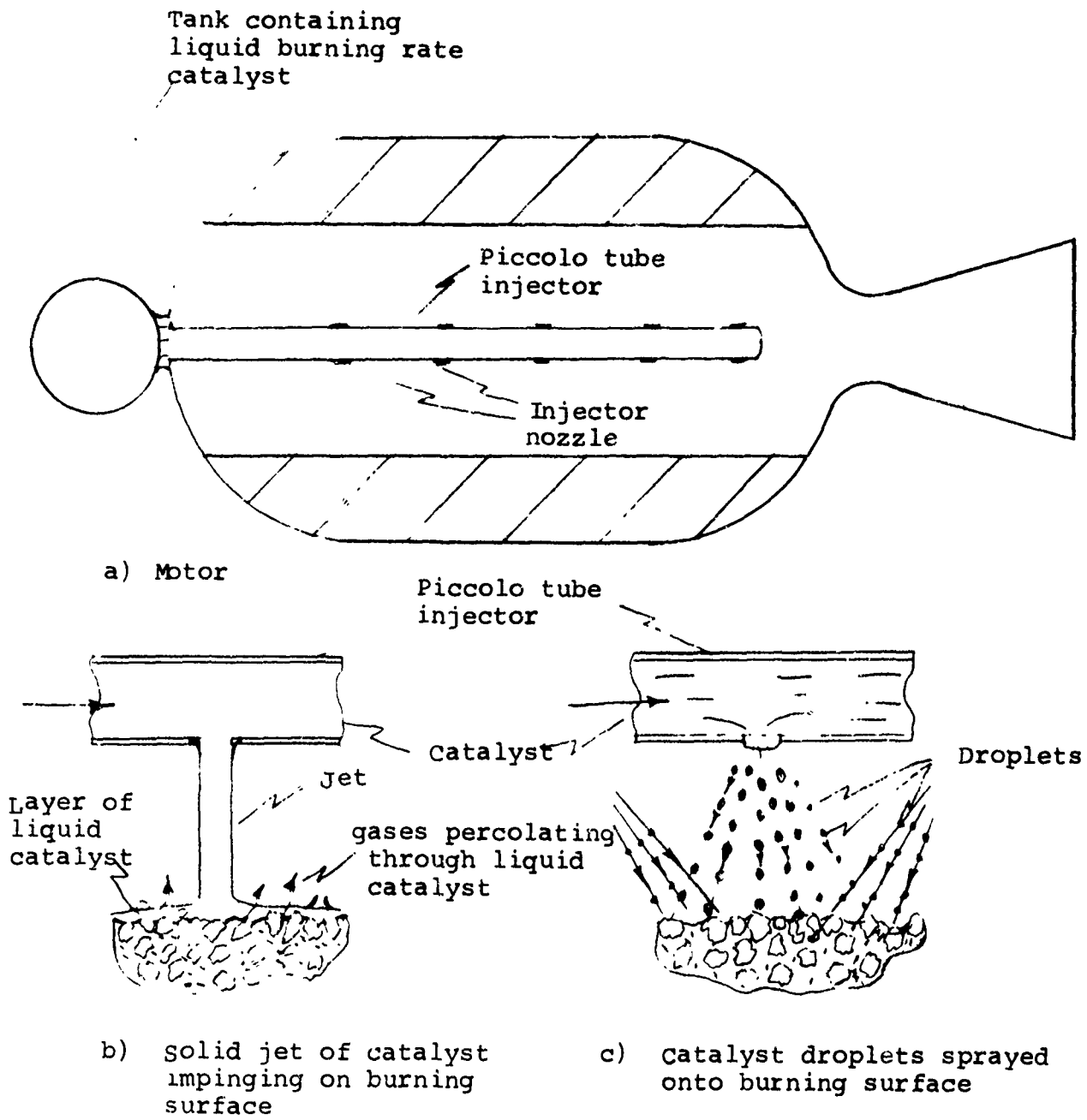


Fig.48 Rocket Motor Configuration to Obtain Uniform Distribution of Injected Catalyst by Means of a Piccolo Tube Injector

It is reasonable to assume that injecting catalysts into the gaseous combustion zones will influence propellant burning rate. However, unless proper attention is given to designing the injector, the experiments to establish the effectiveness of the method may produce negative results.

Consideration was given to establishing a catalyst droplet size and velocity criteria. Studies of liquid rocket and diesel engine injectors and droplet combustion were reviewed. However, the results were so dependent on the droplet composition, composition of the gas through which the droplet passes, and the temperature differentials that the reported results add little to the previously expressed understanding of the droplet penetration problem. Also, before burning rates can be predicted, assumptions must be made concerning the effectiveness of injected catalysts in terms of the effectiveness of catalysts that are dispersed in binders.

Experiments were conducted at the Air Force Rocket Propulsion Laboratory in which catalysts were sprayed onto strands burning in a window bomb. The tests produced no encouraging results even though movies showed that an excess of catalyst had reached the burning surface.

SECTION VIII

RESISTIVE HEATING OF THE PROPELLANT SURFACE

By causing electric current to flow through the solid propellant, the solid propellant can be resistively heated and the heat to the reacting propellant ingredients can be augmented on command. An important consideration in this method is the amount of on-board electrical power required to modify the burning rate. The effectiveness of this method of command control of burning rate will also depend on the extent to which the heating can be localized at the propellant surface.

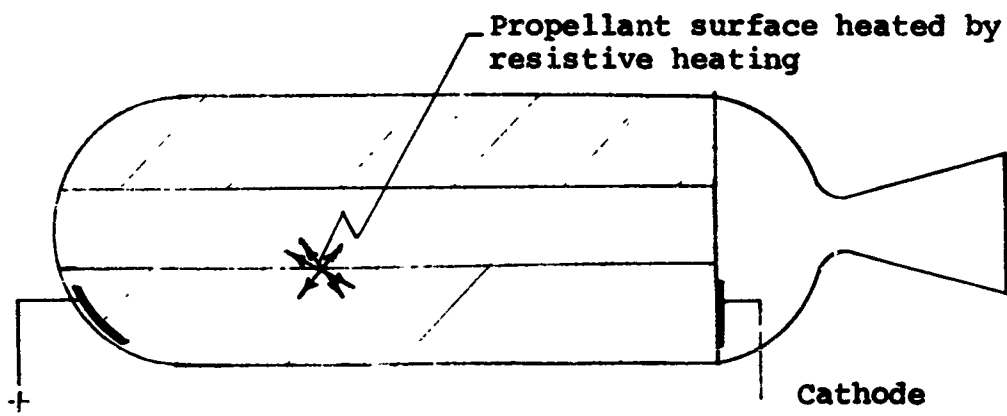
Fig. 49 shows schematically how the current might be applied to run parallel to the propellant surface. It is important that the electrodes not penetrate into the ionized combustion products so that the circuit is not completed through the ionized gases. Fig. 50 (a summary taken from Ref. 44) illustrates the general trend of decreasing electrical resistance with increasing temperature for some non-metallic substances. Also shown on Fig. 50 are propellant electrical resistances measured by Petersen and Payne⁴⁵. The resistivity of ammonium perchlorate was measured by Voelkle⁴⁶ and was found to rapidly decrease as temperature was increased from 25 to 225C.

A decrease in resistance with increasing temperature is the proper trend to concentrate the heating at the hot propellant surface if the potential is applied laterally across the grain. Fig. 49 shows the thermal gradient through a propellant corresponding to 1000 psi. Note that, because of the large temperature variations, the resistance near the surface decreases rapidly, and correspondingly there is a concentration of power dissipation at the surface. From first indications, it appears that with proper design and innovation, resistive heating might provide the desired surface heating, but very large voltages (megavolts) may be required. The question is whether additives that will reduce the resistivity can be found to allow the use of moderate voltages.

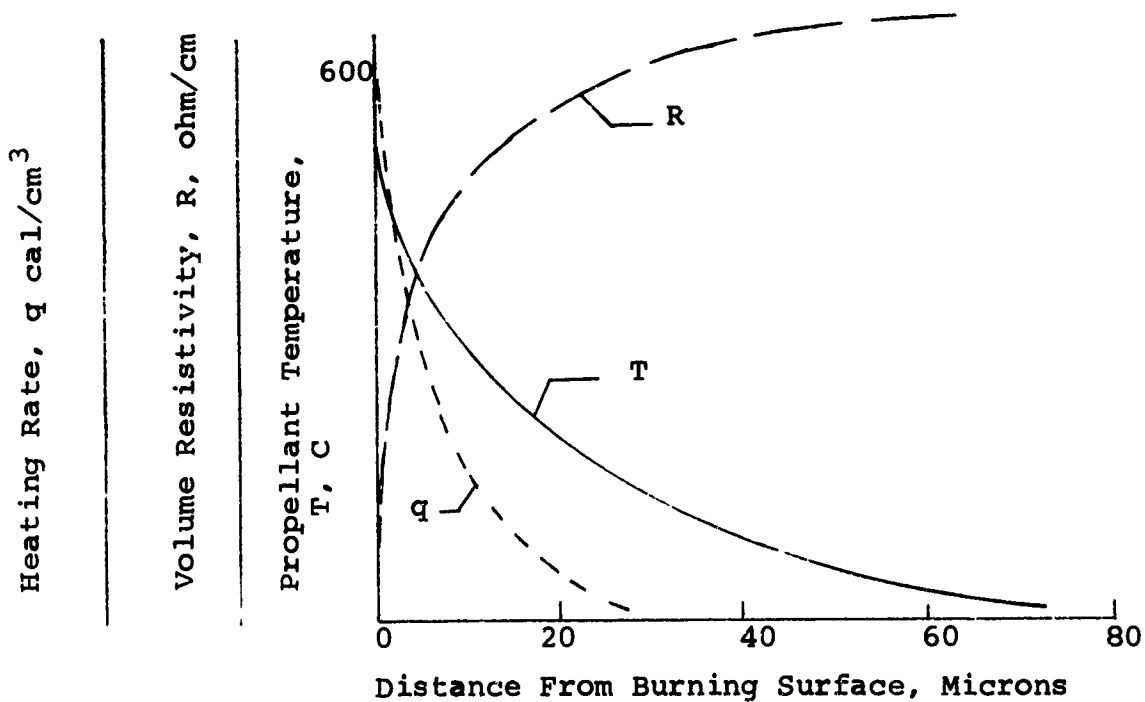
A series of resistive heating experiments were conducted by W. A. Wood⁴⁷ in which the current was passed through the propellant strand perpendicular to the burning surface. The propellant strands were pressed and used a binder material with a relatively low resistance⁴⁸. Wood stated that these experiments produce no encouraging results and that the results were complicated by strand break-up. When Wood tried to pass the current parallel to the burning surface, arcing occurred through the ionized combustion products.

It is interesting to note that electrical resistance measurements can be used to determine the cure fraction of propellants and polymers⁴⁹.

Calculation of the voltage required to achieve a particular deposition of energy will require a careful consideration of how



a) Schematic showing how circuit can be formed along the burning surface



b) Variation of electrical resistance and resistive heating with distance from burning surface

Fig. 49 - Resistive Heating of Propellant Surface

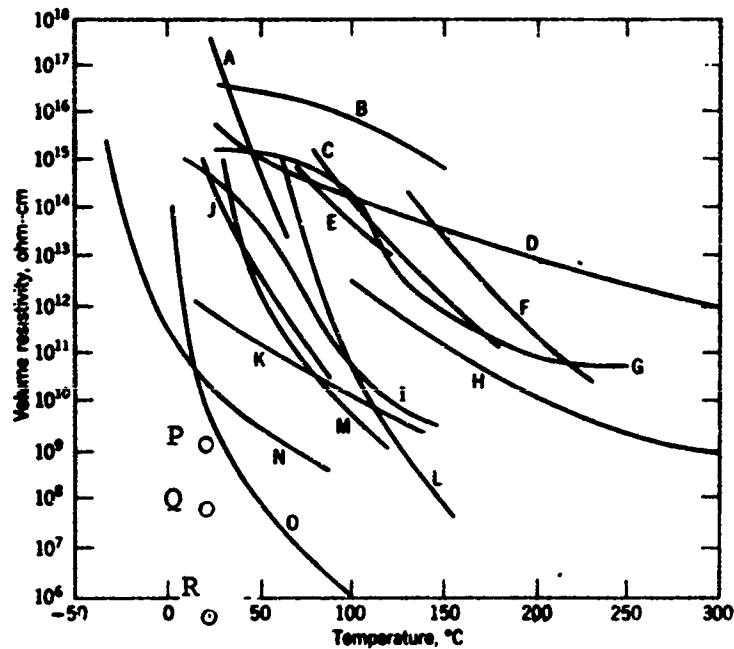


Fig. 50- Effect of temperature on volume resistivity of various plastics. (From Ref. 44 and 45)

- A = low-density polyethylene
- B = polycarbonate foil (Makrofol N, Bayer)
- C = polyester-glass fabric laminate
- D = solventless silicone resin
- E = epoxy casting resin (Epocast #3, Furane)
- F = poly(ethylene terephthalate)
- G = silicone rubber
- H = molded silicone resin
- I = plasticized cellulose acetate butyrate foil (Trifol BW, Bayer)
- J = plasticized poly(vinyl chloride)
- K = soft polyurethan foam (Moltoprene, Bayer), density = 30 kg/m^3
- L = epoxy resin
- M = cast epoxy resin (Araldite 502, Ciba)
- N = polyurethan elastomer (Vulkollan, Bayer)
- O = polyamide
- P = UTP3001 propellant (Ref. 45)
- Q = TPH-1011 AP composite propellant (Ref. 45)
- R = C-112 propellant double base propellant (Ref. 45)

resistance varies with temperature up to propellant surface temperatures and the preferential paths the current will take through the binder and the oxidizer crystals. Also, since the effect is not exactly a surface effect, the resistive heating has to be considered over a finite thickness. The voltage required for a given deposition of energy can be estimated only after the thermal resistance of burning propellant has been measured.

Predictions of the effect of resistive heating on burning rate must account for the complex interplay between the increased mass generation rate resulting from the resistive heating and the changes in the gas phase produced by the increased rate of mass generation at the propellant surface. These considerations are very similar to those discussed when the effects of radiative heating were considered (see pages 14 through 16).

For steady state burning and by assuming that no current flows through the combustion gases, the increased energy transferred to the propellant by resistive heating can be expressed in terms of an equivalent increase in initial propellant temperature. The resistive heating is

$$\Delta q_{\text{elect}} A_b = 4.18 E^2 / R \text{ cal/sec} \quad (40)$$

Under steady state burning conditions, the electrical heating produces an effect equivalent to increasing the initial propellant temperature by an amount

$$\Delta T_i = \Delta q_{\text{elect}} / r \rho c_p \quad (41)$$

and a corresponding increase in flame temperature

$$\Delta T_F = c_p \Delta T_i / c_g \quad (42)$$

The increase in c^* that corresponds to the increase in initial temperature is the well known ballistic parameter, $\partial \ln c^* / \partial T_i$, which occurs in Eq. 12.

Applying the method that was used to predict the effect of radiative heating produces the following result analogous to Eq. 14

$$P/P_0 = r/r_0 = \exp \left[\frac{1}{1-n} (\sigma_p + \partial \ln c^* / \partial T_i) (\Delta q_{\text{elect}} / r \rho c) \right] \quad (43)$$

For most propellants, the value of $\partial \ln c^* / \partial T_i$ is less (approximately 0.005%/K) than the accuracy to which σ_p is known. Accordingly the effect of $\partial \ln c^* / \partial T_i$ was not considered in this analysis.

Figs. 51 and 52 are results of a parametric study to show the range of burning rate control that can be obtained if large amounts of electrical power are available. The results apply to typical high energy propellants and are meaningful for both non-metallized and metallized propellants. The temperature sensitivity value of 0.135%K is typical of many composite propellants that are in wide use. The results of Figs. 51 and 52 show that increasing burning rate exponents has a strong influence on the burning rate enhancement.

As expected formulating propellants with burning rates that are unusually sensitive to changes in initial temperature is extremely attractive. Figs. 51 and 52 includes results for propellants with temperature sensitivities of 0.135 and 0.27%K, respectively.

An important consideration is the basic burning rate of the propellant. The lower burning rate propellants are influenced to a greater extent by thermal radiation. This is explained in part by Eq. 41 which shows that the increase in initial temperature is inversely affected by burning rate. The results of Figs. 51 and 52 indicate that the use of electrical heating as a means of burning rate control will be more effective for the slower burning rate propellants.

The burning rate predictions, Figs. 51 and 52 indicate that burning rate control (by means of electrical heating) is achievable but that for conventional size motors very large power supplies will be required to obtain even small increases in burning rate. The following items tend to increase the degree to which burning rate is increased:

- 1) increasing temperature sensitivity of burning rate
- 2) increasing the pressure exponent of burning rate
- 3) decreasing the basic propellant burning rate

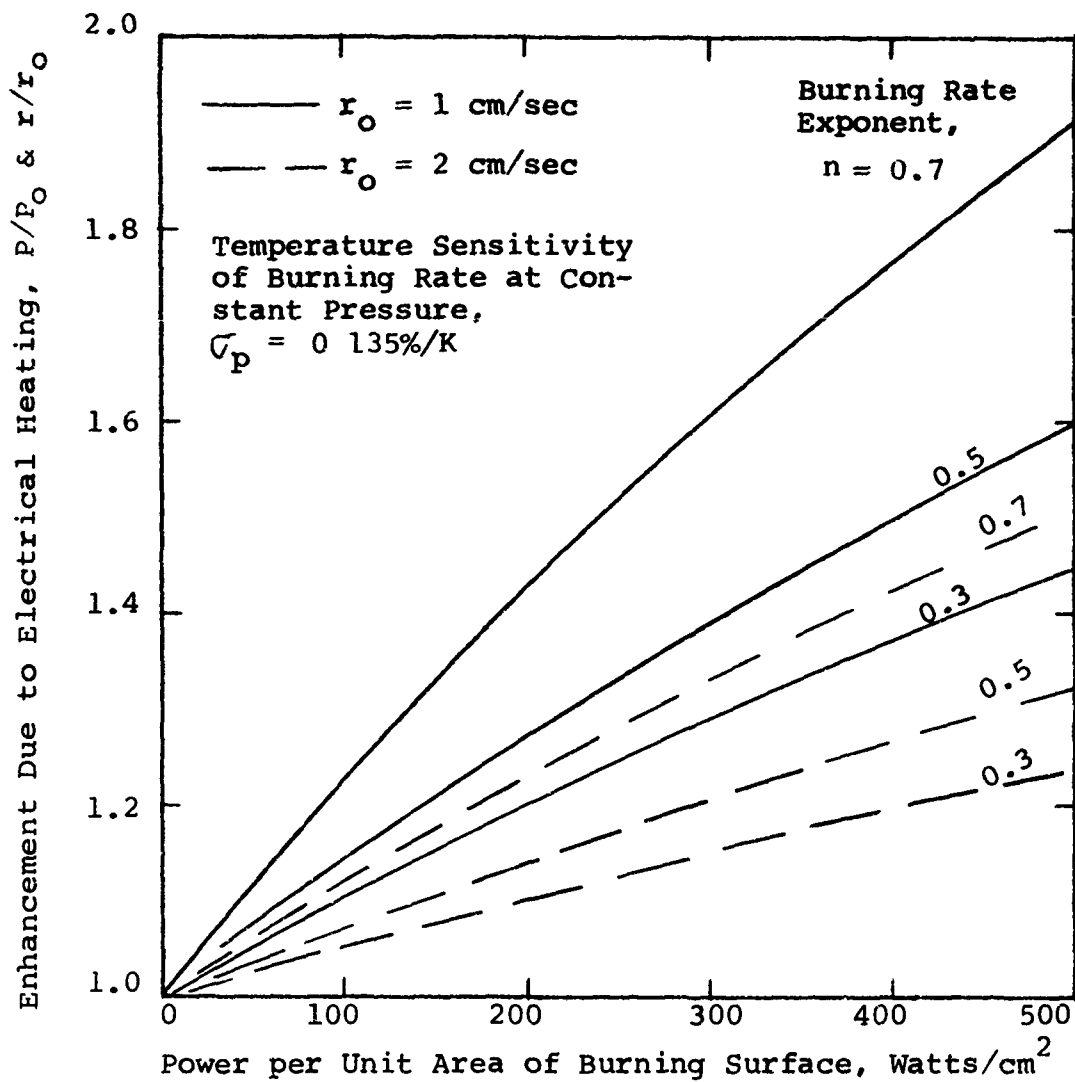


Fig. 51 Effect of Electrical Heating on Propellant Burning Rate for Propellants with Typical Temperature Sensitivity of Burning Rate.

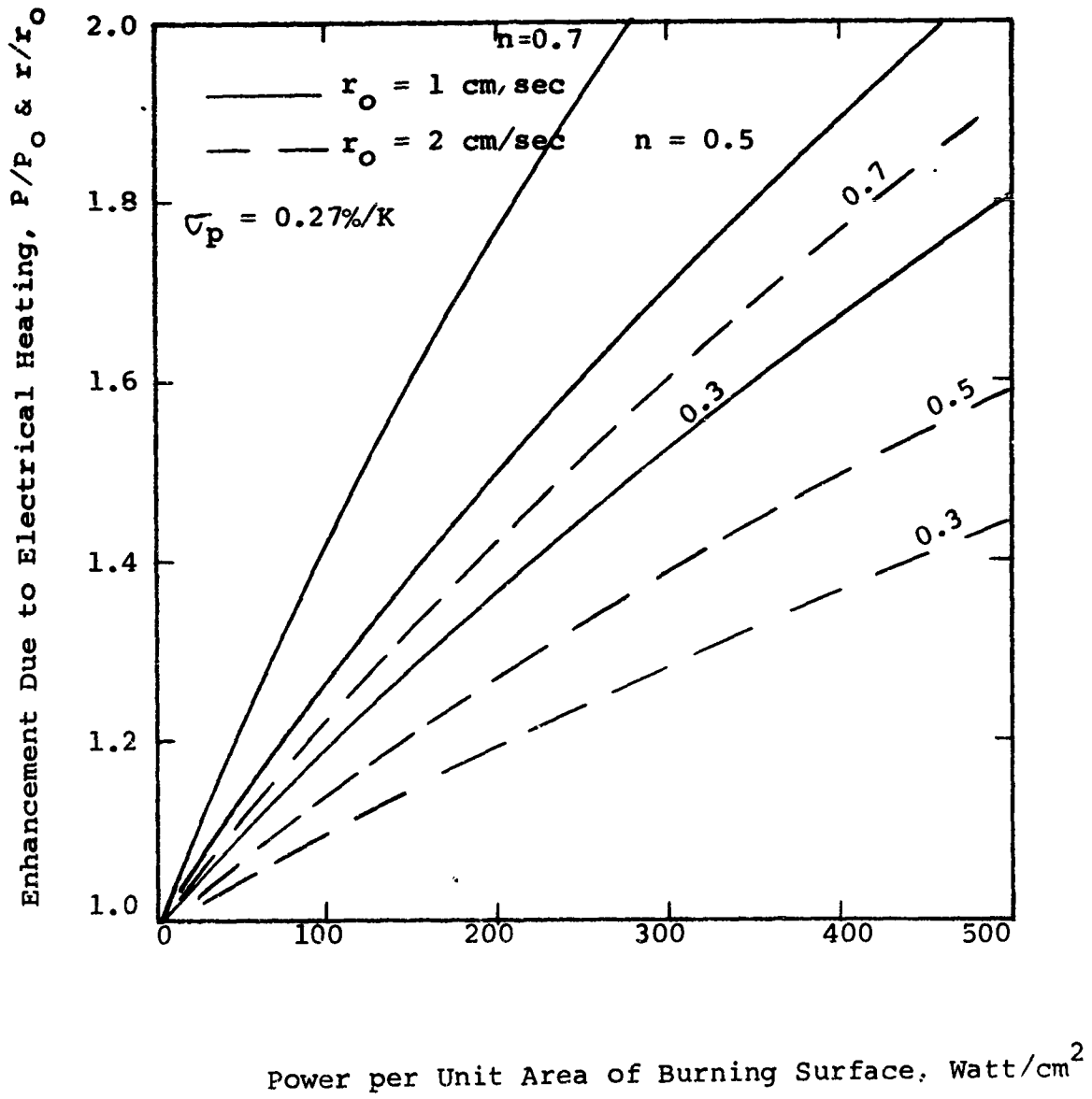


Fig. 52 Effect of Electrical Heating on Propellant Burning Rate for Propellants with Moderately High Temperature Sensitivity of Burning Rate

SECTION IX

OTHER METHODS OF BURNING RATE CONTROL

A. Partial Quench of a Propellant Near Its Extinguishment Point

Recently, it was noted⁵⁰ that reduction of AP loading and reduction of AP particle size cause some propellants either to extinguish at intermediate pressures (800-1200 psi) or to decrease in burning rate beyond some pressure limit. This effect was observed to occur when binders that melt during the pyrolysis process were used. The presence of thick molten fuel layers on propellant surfaces with readily melt-able binders indicates that the molten fuel layers are causing temporary localized extinctions. These temporary localized extinctions are imagined to occur because of coating of the AP particles by the molten binder. The net effect of the temporary localized extinctions is to cause reductions in mean burning rate or, in some cases, extinction.

It is conceivable that propellants that demonstrate intermittent burning characteristics will be very responsive to small amounts of quenchants, when operated near the pressure where such local extinctions begin to occur. Thus, by injecting either particulate or liquid quenchants, large changes in burning rate may be obtained. Similarly, it would be interesting to combine the use of these propellants with some of the other burning rate control concepts. Possibly a propellant operating near its extinction point can be easily excited to a higher burning rate by ultrasonic energy or by injection of particulate matter to concentrate the thermal radiation.

One of the big questions to be answered concerning this concept is: Even though intermittent burning characteristics have been demonstrated repeatedly in strand burners, will these basic characteristics occur also in internally perforated motors? The axially directed gas flow parallel to the surface may alter these effects completely. Some experiments are needed.

B. Self-Heating Through Vibration

While it is well known that materials can be heated by vibration, it is unlikely that sufficient energy to achieve the desired result can be efficiently mounted in a rocket motor. A disadvantage of this approach is that vibrational heating would be concentrated where the vibration amplitude is greatest and not at the propellant surface. Also, once the propellant is heated, the propellant would have to be cooled to depress the burning rate.

C. Induced Unstable Burning as a Means of Increasing Mean Burning Rate

Some forms of combustion instability appear to produce a uniform and reproducible shift in rocket motor pressure level. Such instability can be initiated by small explosive charges set off in the rocket motor chamber⁵¹. The charges produce cyclic non-linear pressure and velocity waves in the longitudinal mode in the motor cavity. Examination of motors which have experienced such DC shifts in pressure indicates that the propellant burning rate is markedly increased at the location of the pressure node⁵². Thus, the use of DC shift as a command mode of burning rate control would be complicated by the premature exposure of the rocket motor case at the position of the pressure node. Also, feasibility of the control of the amplitude of the instability is an open question. Of course, if for a particular application a rocket motor can be designed so as to have extra insulation at the vicinity of the pressure node, then this concept may be worthy of consideration.

D. Disruption of Metal Film on Burning Propellant Surface

High-speed motion pictures⁵³ of burning metalized propellants and the examination of extinguished metalized propellants indicate that metal fuel additives absorb an appreciable amount of energy at the propellant surface. The important exothermic heat release by metal combustion occurs after the metal leaves the surface. The photographic studies of Crump⁵³ have resulted in a qualitative understanding of how aluminum additives behave on the propellant surface. Photographs show the aluminum melting on the surface and then coalescing to form large agglomerates of molten aluminum. The molten aluminum agglomerates are covered by oxides. These agglomerates are 100 to 300 microns in diameter as they leave the propellant surface. On the basis of systematic measurements of the average agglomerate size as a function of several propellant parameters, Crump concluded that each agglomerate was made, for the most part, of the aluminum particles present in the space between the adjacent AP particles.

An understanding of how much heat is transferred to the propellant surface is useful in understanding how metal additives affect burning rate. Approximately 270 calories are required to heat and melt each gram of aluminum fuel additive. Nonaluminized AP composite propellants require a net heat feedback of approximately 100 cal/gm from the granular diffusion flame to raise the propellant to the surface temperature of about 550 C and decompose the AP and binder. Since photographic evidence reveals that only a small fraction of aluminum burns at the propellant surface, the aluminum at the propellant surface

can be thought of as a ballast which deprives the binder and AP of some of the heat feedback from the flame. Recent results⁶ supporting this view show that aluminum additives on the order of 15% by weight decreased the burning rate by as much as 10%, when the comparison is made on the basis of a constant AP/binder ratio.

Two burning rate influencing effects may result from disrupting the metal film at the propellant surface. First, a local disruption and agitation of the aluminum particles prior to coalescing would tend to stir the oxidizer and fuel vapors. Such mechanical stirring would hasten the gaseous reaction between the oxidizer and fuel vapors and increase the energy feedback to the burning surface. Secondly, if a means could be devised to force the aluminum from the propellant surface at an accelerated rate, perhaps before melting, more heat from the gas phase would be available to heat and vaporize the oxidizer and binder.

More study will be required to determine to what extent the aluminum film or agglomerates can be moved about, stirred, or otherwise affected by various energy sources. Watermeier⁵⁴ measured aluminum oxide particle movements produced by pressure oscillations imposed normal to the burning surface. If oscillations were imposed parallel to the burning surface, it is possible that the desired effect of stirring the fuel and oxidizer vapors can be achieved. Analytical predictions of the pressure oscillation frequency required to achieve stirring in the granular diffusion flame were presented in Section III. One criterion for good stirring would be that the aluminum particles go through at least one oscillation prior to passing through the thin granular diffusion flame zone.

Methods which will cause aluminum to leave the surface on command are not apparent.

E. Dielectric Heating

Electromagnetic energy at radio frequencies is used to efficiently heat many materials in industrial applications⁵⁵. These materials include some which are very poor electrical conductors referred to as dielectrics. The heating process is termed dielectric heating and may be applicable to solid propellants. Advantages of dielectric heating for industrial applications are: it is efficient, does not throw off wasted heat, can be accurately controlled with reasonably simple devices, and can be used selectively. Two ranges of radio frequencies are generally considered for dielectric heating: radio frequency heating at 1 to 200 megacycles/sec and microwave heating above 890 megacycles/sec. When high-frequency energy is applied, the material between the electrodes is heated fairly uniformly throughout its volume. In microwave heating the energy is applied by horns or wave guides and its effect decreases to very

low values at some point below the surface. The depth of penetration depends upon the frequency and on the material being used. Thus, it appears that microwave heating may have some potential as a means of burning rate control.

Exactly how microwave heating can be employed is not clear at this time. Possibly, the microwave horn can be positioned at the head end of the rocket motor and directed in a programmed manner at various portions of the burning surface. The program would be designed to compensate for the attenuation caused by geometry and varying distance along the grain. Possibly, missile systems employing onboard radar could utilize a portion of the radar circuitry.

F. Resistive Heating of Wire Network Buried in the Propellant

An array of wires cast in the propellant can be heated electrically to control the mass discharge of the rocket motor, either by ejecting bits of propellant through subsurface ignitions or by locally enhancing the burning rate. One possible scheme is to fabricate ladders of resistors, whereby the resistor nearest the burning surface has the lowest resistance. The resistance of the resistors is arranged to progressively increase in the direction away from the burning surface. If voltage is applied to such a ladder, the resistor nearest the surface will heat up most rapidly. As the propellant burning surface approaches the propellant heated by a particular resistor, the local rate will increase over the unheated level. If the heating rate of the resistor is high enough, the hot resistors will cause progressive subsurface ignitions.

While this approach will probably produce irregular burning surfaces, it may be possible to apply it in some end burning rocket motors. It is probably best suited for rocket motors where nonuniform increases in pressure are acceptable. The complexity required to achieve uniform and continuous burning rate control appears to be prohibitive.

G. Electrical and Electromagnetic Effects on Solid Propellant Flames

The effects of electric fields on combustion, flames, and hot gases have been the subject of a large number of research papers. (See, for example, Gaydon and Wolfhard⁵⁶, Flames, pp. 313-317). There is a well-developed field of research on ionization in flames and high temperature gases⁵⁶⁻⁶⁰ and the Proceedings of the Combustion Institute regularly include a section on the electrical properties of flames. Several reasons have been offered as to why electric fields should increase burning rate. The ionic wind can possibly generate turbulence and mixing of the reacting gases and affect the burning propellant in a similar manner as described for acoustic energy. Also,

the ionic wind can increase the heat transfer to the propellant surface by forcing the reacting charged particles to the propellant surface. This latter effect depends on the polarity of the field.

One of the first demonstrations that electrical fields can affect solid propellant burning was reported by Mayo, Watermeier, and Weinberg⁵⁹. They examined two methods: varying the normal burning rate and varying the rate of flame spread over the propellant surface. The latter was considered as a means of controlling the total mass generation rate by varying the rate at which flames can be made to propagate into small crevices in the propellant. Ionic winds were used to increase and decrease the flame spread rate. By making the propellant one electrode, the flame spreading rates were increased. By using an electrode contacting the flame, the flame spread rate was decreased. In simple systems at atmospheric pressure, increases of about 200 to 1 and decreases of approximately 10 to 1 were achieved. Weinberg and co-workers⁵⁷⁻⁵⁹ predicted that larger effects should be possible at rocket motor pressures.* However, only small changes (less than 10% decrease) in the normal burning rate resulted from the extremely high voltages of 25kV. Stones⁶⁰ conducted similar experiments and also concluded that the effect is small.**

This concept was the subject of a program being conducted by the Air Force Rocket Propulsion Laboratory⁴⁵ in which the results of past investigations were examined and series of experiments were conducted. When strands of double-base propellants were subjected to 15 kilovolts normal to the burning surface, a 3 to 10% reduction in burning rate was obtained.

H. Electric Currents to Enhance the Decomposition of Certain Propellant Ingredients

It is well known that electric currents can enhance the decomposition rate of certain materials. Some of these materials may be of interest as propellant ingredients.

The Dow Chemical Company investigators⁶¹ discussed the effect of electrical fields on the thermal stability of aluminum hydride, AlH_3 . As a semi-conductor, aluminum hydride possesses two bands, one a non-conducting band and the other a conducting band. At a given temperature, the electron movement between the two bands is a steady-state exchange. The Dow investigators noted that this equilibrium is changed by

* Such large changes in the flame spread rate can not be expected under conditions where the flame spread rates are dominated by other external stimulus such as high gas velocities from an ignitor.

** As this report was being completed, it was brought to our attention that Stones reported more encouraging results in a subsequent report.⁶⁹

the presence of an electrical field since the probability of the electrons falling back to the non-conducting band is reduced and the motion in the reverse direction is unaffected. An indication that the above process is operative is implied by experiments to determine the effect of an electrical field (45 volts DC) on the thermal stability of AlH_3 -1451 at the elevated temperature of 100 C. The tests revealed that 40% decomposition occurred in four hours with the electrical field and in ten hours without the electrical field. Higher voltages applied at burning surface temperatures may produce a usable degree of burning rate control. However, it is most tenuous to assume that an effect observed at very low decomposition rates, especially at 100 C, will be prominent at rocket motor pressures and rates⁶². Thus experiments conducted at rocket motor pressures and burning rates will be required to evaluate the effectiveness of this approach.

I. Acceleration Forces to Alter Propellant Combustion

The effect of acceleration on burning rate is the subject of much recent research.⁶³⁻⁶⁸ Acceleration forces normal to and into the burning surface affect metallized propellants by increasing the extent to which metal fuel additives agglomerate on the burning surface. Since these metal agglomerates are local, increases in the burning rate (can be in excess of 100%) are generally local and produce irregular or conical pits in the burning surface. The mechanism by which acceleration forces normal to and into the propellant surface increases the burning rate of nonmetallized propellants is not fully understood. However, these increases are small compared to the increases in metallized propellants. The effects of acceleration forces normal to and out of the burning surface are not fully evaluated because of the complex nature of the interactions produced by the density gradients in the gas phase and the removal of non-gaseous products and reactants from the surface.

66

Crowe conducted experiments where tungsten particles were introduced into the propellant. Radial accelerations force the tungsten particles against the propellant surface. Since the tungsten did not react to form oxides, it remained unaltered on the propellant surface. In a similar manner, dense nonreactive particles of special geometry could be injected into the combustion chamber of a spinning rocket motor. At high radial acceleration, these particles will be retained on the surface. If the radial acceleration rates are sufficiently high, cones will form in the propellant surface. While this technique seems feasible for increasing burning rate, it may not be cancellable, that is, it may not be possible to reverse the effect, particularly if cones form in the burning surface. Also, there will be serious problems in developing methods to uniformly disperse the particles along the burning surface.

Figure 53 is a schematic drawing of a rocket motor that utilizes acceleration* forces away from the burning surface to control burning rate. A propellant rod is positioned along

* Spinning of the rocket motor components may introduce tangential gas flows in the motor chamber and vortex flows in the nozzles. Such flows can impart roll torques to a missile system.

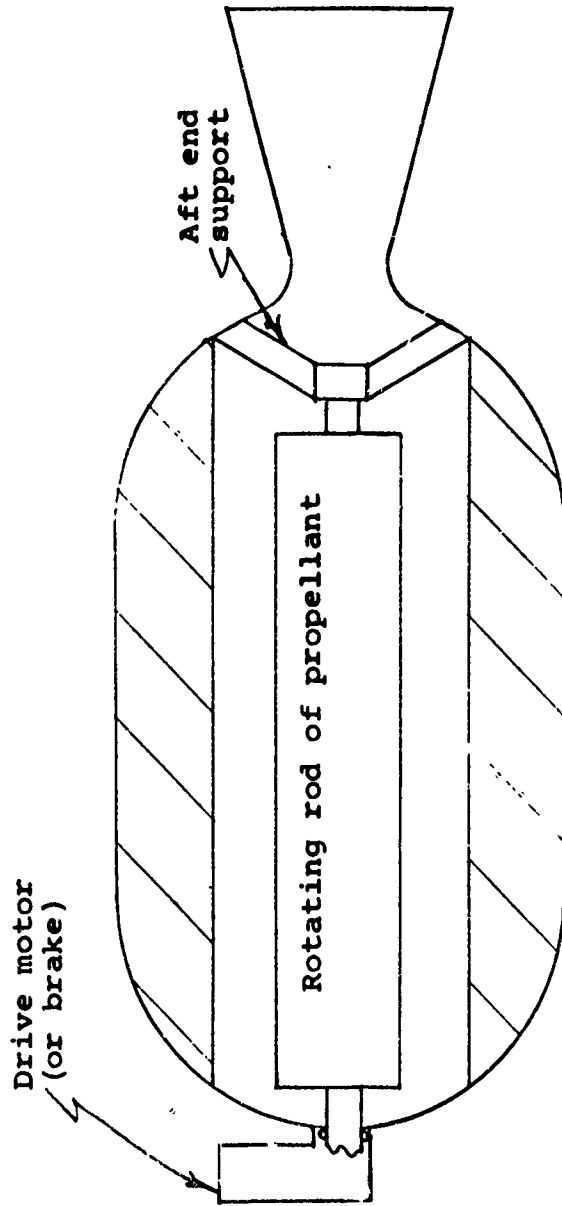


Fig.53 - Schematic Design Showing Propellant Rod Which Can be Either Rotated or Oscillated About its Longitudinal Axis in the Combustion Chamber.

the internal perforation on the motor centerline. The rocket motor also contains an internal-burning propellant charge. The propellant rod can be made to rotate by means of vanes in the entrance region of the nozzle. The rotation rate of the rod can be controlled by an adjustable brake positioned at the head end. An alternate means of rotating the rod is to use a motor-driven drive at the head-end.

Figure 54 shows how rotation of the rod may affect the propellant burning surface. Figure 54a shows the relatively large aluminum agglomerates on the propellant surface when the rod has not rotated. Based on photographs of burning metallized propellants⁵³, it appears that aluminum agglomerates must reach a certain size before they can be lifted from the burning surface by the evolving gases. Accordingly, it seems reasonable that the centrifugal forces acting on the agglomerates will tend to remove them from the burning surface sooner in their growth and thereby reduce the agglomerate size. Figure 54b and 54c show successively smaller agglomerates corresponding to higher radial accelerations. This might affect the surface gasification rate by changing the heat balance at the propellant surface.

A variation of the spinning propellant rod would be to rapidly oscillate the rod and, in effect, shake the aluminum agglomerates free. This may have an advantage, in that a vortex flow in the nozzle would be avoided and, as a result, roll torques would not be produced.

An additional consideration in the rotating rod approach is that, at sufficiently high rotation rates, erosive burning-type effects may occur.

Rotating rod experiments should be an excellent diagnostic experiment to determine the effects of aluminum agglomeration on propellant burning. Such experiments were conducted by King and McHale⁶³ and decreases in burning rate up to 12% were observed. However, as indicated in Table 5, the effect was more pronounced for nonmetallized propellants. It is not clear that the King and McHale experiments give an accurate evaluation of the concept since the thin propellant disks burned in their tests could have been cooled by entraining the cool N_2 used to pressurize the bomb.

J. Utilization of Photochemical Processes

The Dow Chemical Company investigators⁶¹ noted in their studies of aluminum hydride, AlH_3 , propellants that radiant energy and electrical fields produced visible signs of decomposition similar to those observed at elevated temperatures. At elevated temperatures AlH_3 -1451 usually changes to an off-white or gray after only a few tenths of a percent decomposition. With further decomposition, the color of AlH_3 -1451 changes to black.

* It should be noted that the King and McHale experiments did not produce simple results since some of their experiments revealed increases in burning rate up to 8% at the higher acceleration levels (see Table 5).

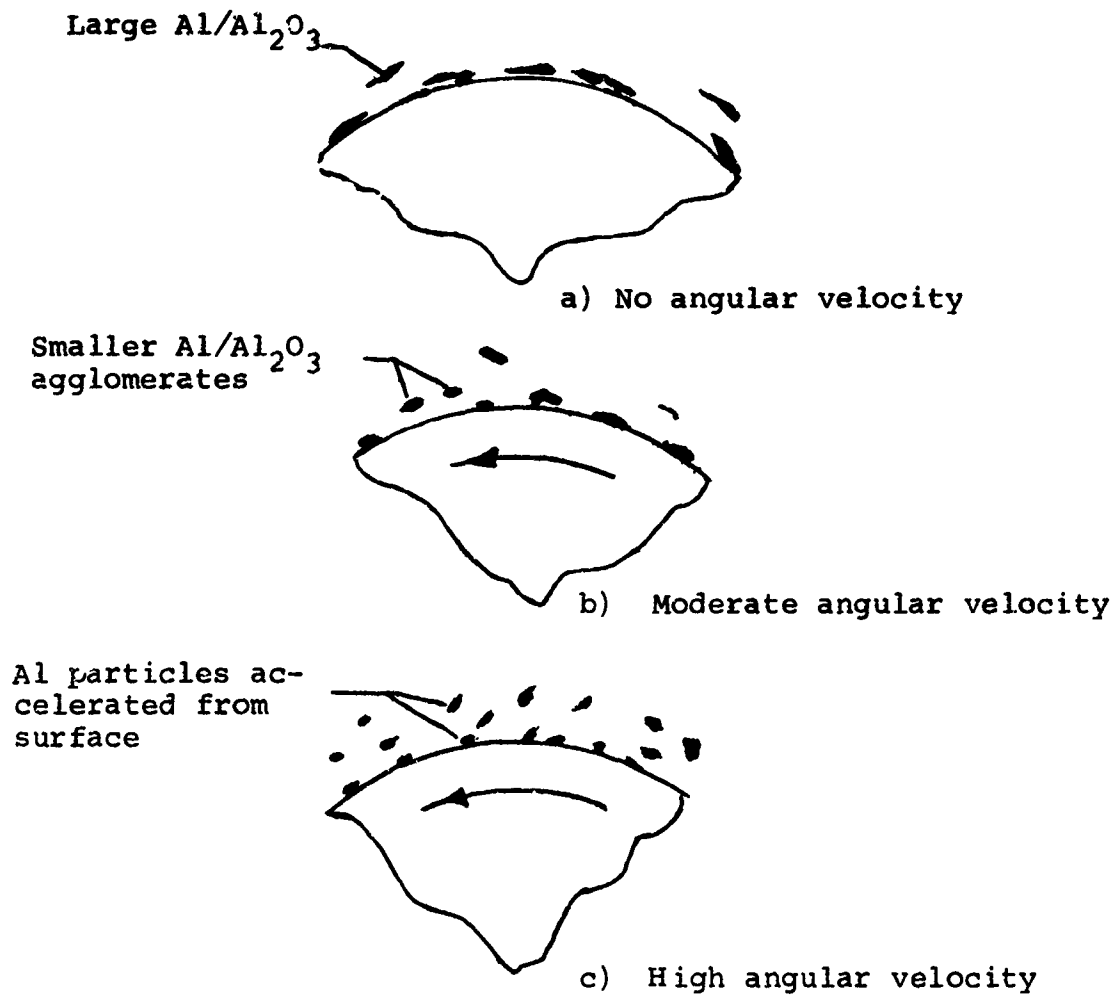


Fig. 54 - Effect of Propellant Rod Angular Velocity on Removal of Aluminum and Aluminum Oxide from Propellant Surface.

TABLE 5

EFFECTS OF OUTWARD-DIRECTED RADIAL ACCELERATION
FIELDS ON BURNING RATES*

| <u>Propellant</u> | <u>Pressure, atm</u> | <u>Burning Rate Augmentation \dot{r}/r_0</u> | <u>Acceleration Level, g</u> |
|--|----------------------|---|----------------------------------|
| AP composite propellant using CTPB binder | 10 | 0.80 | 550 |
| | 25 | 0.80 | |
| | 50 | 0.81 | |
| | 10 | 0.71 | 1400 |
| | 25 | 0.87 | |
| | 50 | 0.65 | |
| AP composite propellant using CTPB binder and catalyzed with copper chromite | 10 | 0.86 | 750 |
| | 30 | 0.86 | |
| | 50 | 0.94 | |
| | 10 | 0.68 | 1800 |
| | 30 | 0.87 | |
| | 50 | 1.1 | |
| Aluminized AP composite propel- lant using CTPB binder | 10 | 0.90 | 700 |
| | 30 | 1.02 | |
| | 50 | 1.08 | |
| | 10 | 0.92 | 1800 |
| | 30 | 0.98 | |
| | 50 | 0.88 | |

* Taken from Ref. 63

The Dow investigators found that ultraviolet irradiation, visible light irradiation, electron bombardment, and gamma irradiation of AlH_3 -1451 changed its color from white to light brown or black. The Dow investigators offered an explanation for this effect in terms of the crystal structure and speculated that the thermodynamic temperature imparted locally to AlH_3 -1451 by irradiation with visible, ultraviolet, or gamma-rays, could easily exceed 60 C which is probably above the threshold temperature for the onset of decomposition of the hydride. Thus, it is expected that the more energetic forms of radiation will increase this excitation. Qualitative observations indicate that ultraviolet light is more likely to accelerate decomposition than visible light. After the AlH_3 has been excited by an external source, further decomposition will require less external energy.

The observed results only suggest that various sources of external radiation may affect on command the burning rate of some propellant ingredients. The evaluation of this method must be based on experiments conducted under rocket motor type conditions so that the various competing modes of decomposition are accounted for.

SECTION X
CONCLUSION

Twenty possible methods of command control of burning rate have been investigated. According to the broad guidelines for the study, the methods were evaluated primarily in terms of their effectiveness as means of command control of burning rate rather than in terms of the general practicality of the individual concept. During the study, it became increasingly apparent that the practicality of each concept must be evaluated in terms of particular rocket motor and gas generator requirements.

The results of the study are summarized in Table 6 which includes the range of pressure level control that can be expected from each of the concepts and summarizes the features of each concept.

It is difficult to single out the most promising concepts because the word promising also must imply that the concept is practical for a particular application. Of the several concepts that require the propulsion system to be designed around a particular mechanical approach, the Embedded Porous Element Rocket Motor (EPERM) offers attractive potential. Much of the study was devoted to investigating methods which could produce command control of burning rate for existing rocket motors. Of these concepts, the only one which has been demonstrated and offers promise, is the control of burning rate by means of acoustic energy beamed onto the burning propellant surface by a generator excited by a combustion gas source. Also, further study of the use of the electric fields and radiation sources to control the decomposition of special propellant ingredients may produce important results.

TABLE 6

Methods of Obtaining Command Control of Burning Rate

-Conclusions and Summary -

| Approach | Range of Pressure Level Control | Objectionable or Impractical Characteristics to be Overcome | Advantages, Potential Applications, or Comments |
|--|--|---|---|
| Injection of particulate matter in gas phase to intensify radiation | 10 to 50% depending on propellant exponent and temperature sensitivity | Particle clouds will not produce uniform heating and are rapidly discharged from the motor | Practical for very small degree of vernier control |
| Insertion of radiation source heated by combustion gas to concentrate radiative energy | 10 to 50% depending on propellant exponent and temperature sensitivity | Source must withstand chamber conditions and be adjustable | Practical means of inserting and/or controlling source is not proven |
| Insertion of radiation source heated by outside power supply | 10 to 50% depending on propellant exponent and temperature sensitivity | Relatively large voltage per change in burning rate is required | Practical for small motors with electrically heated radiation sources in the combustion chamber |
| Control of solid propellant by acoustic energy | 5% w/o He Flow 3:1 with high sonic velocity driver gas | Effect varies as propellant configuration changes during burning and requires a driver gas with a high sonic velocity | Low chamber pressure motor with low burning rate non-metallized propellants show greatest potential. May have particular promise when used with propellant ingredients that are porous. |

Continued on next page....

TABLE 6 (continued)

| Approach | Range of Pressure Level Control | Objectable or Impractical Characteristics to be Overcome | Advantages, Potential Applications, or Comments |
|---|---|---|---|
| a) Opposing surfaces of two similar propellants b) An inert ram and a propellant | < 10% 10:1 | Requires time for burning surface to adjust to steady state conditions Inert ram limits flame temperature. | Gas generators where drive mechanism does not produce an objectionable weight penalty |
| Opposing fuel rich and oxidizer rich surfaces | Very wide range because of very low idle pressure | | Attractive for gas generators where an off or idle mode is required |
| Perforated propellant grains | 20:1 | Stability of combustion process has not been established. Control of chamber pressure may not be feasible | Should be considered for ultra-high acceleration boosters and eject motors not requiring a carefully controlled pressure-time history |
| Embedded porous element rocket motor (EPERM) | 8:1 | Best suited for end burning configuration; element variation is potential problem | High performance sustainer motors appear to be obtainable with low developmental risk |
| Injection of burning rate catalyst | | Catalyst can not be delivered to the portion of the combustion zone where catalysts normally act | |
| Resistive heating of propellant surface | 2:1 | Relatively large wattage per change in burning rate is required | May be attractive for systems that have large on-board electrical power supplies |

Continued on next page...

TABLE 6 (continued)

| Approach | Range of Pressure Level Control | Objectionable or Impractical Characteristics to be Overcome | Advantages, Potential Applications, or Comments |
|---|---------------------------------|--|--|
| Partial quench of propellant near its extinguishment point | | Limited to a special class of low energy propellants with narrow burning rate range | |
| Self heating through vibration | < 5% | Vibrational heating does not produce local heating effects | |
| Induced unstable burning as means of increasing mean burning rate | | Burning rate increases are centered at the pressure node | Might be considered for systems that can tolerate nonuniform propellant burn out |
| Disruption of metal films on burning surface | < 5% | No practical method has been suggested for disrupting the metal film | |
| Electromagnetic radiation (dielectric heating) | ? | Complex apparatus would be required to achieve uniform heating | |
| Resistive heating of wire network buried in propellant | > 2:1 | Increasing burning rate at each individual wire will cause non-uniform increases in pressure | Pulse type operation may be achievable |
| Electrical and electromagnetic effects on solid propellant flames | 10 to 20% | Requires large voltages and careful placement of electrodes | |

Continued on next page....

TABLE 6 (continued)

| Approach | Range of Pressure Level Control | Objectionable or Impractical Characteristics to be Overcome | Advantages, Potential Applications, or Comments |
|--|---------------------------------|---|--|
| Electric currents to enhance decomposition of certain propellant ingredients | ? | Potentially attractive for some of the less common propellant ingredients | |
| Acceleration forces to alter propellant combustion | | Requires spinning components which may introduce undesirable vortex effects | |
| Utilization of photochromic processes | ? | | Potentially attractive for some of the less common propellant ingredients. |

REFERENCES

1. Zennin, A. A., Glaskova, A. P., Leipunskyi, O. I., and Bobolev, V. K., "Effects of Metallic Additives on the Deflagration of Condensed Systems", Twelfth Symposium (International) on Combustion, The Combustion Institute, Pittsburgh, 1959, pp. 27-35.
2. Chao, G. T. Y., Leslie, J. C. and Mancus, H. V., "A Direct Measuring Radiation Calorimeter for Determining Propellant Gas Emissivity", Journal of Spacecraft and Rockets, Vol. 3, No. 6, June 1966, pp. 928-930.
3. Blair, D. W. and Lake, W., "Solid Propellant Flame Zone Radiation", AIAA Journal, Vol. 7, No. 9, Sept. 1969, pp. 1808-1810.
4. Blair, D. W., Bastress, E. K., Hermance, C. E., Hall, K. P., and Summerfield, M., "Some Research Problems in the Steady-State Burning of Composite Solid Propellants", Solid Propellant and Rocket Research, Progress in Astronautics and Rocketry Series, Vol. 1, Academic Press, New York, 1960, pp. 183-206.
5. Hottel, H. C. and Sarofim, A. F., Radiative Transfer, McGraw-Hill, New York, 1967, pp. 199-235.
6. Hart, G. H., Steinz, J. A., and Summerfield, M., "The Burning Mechanism of Aluminized Composite Propellants", Apr. 1969, to be submitted for publication.
7. Zeleznik, F. J. and Gordon, S., A General IBM 704 or 7090 Computer Program for Computation of Chemical Equilibrium Composition, Rocket Performance and Chapman-Jouguet Detonation, NASA TN D-1454, 1962.
8. Stull, R. V. and Plass, G. N., "Emissivity of Dispersed Carbon Particles", Journal of the Optical Society of America, Vol. 50, No. 2, Feb. 1960, pp. 121-129.
9. Hottel, H. C. and Sarofim, A. F., ibid pp. 243-247.
10. Taback, H. J., Day, E. E., and Browne, T. P., "Combustion Termination of Solid Rocket Motors", Journal of Spacecraft and Rockets, Vol. 2, No. 3, May-June 1965, pp. 332-337.
11. Gessner, F. R., Burning Rate Control of Solid Propellants, U. S. Patent 3,133,410, filed Aug. 15, 1960.
12. Gessner, F. R., Personal communication, 2 July, 1969.
13. Glick, R. L., "Temperature Sensitivity of Solid Propellant Burning Rate", AIAA Journal, Vol. 5, No. 3, March 1967 pp. 586-587.

14. Summerfield, M., Sutherland, G. S., Webb, M. J., Taback, H. J., and Hall, K. P., "Burning Mechanism of Ammonium Perchlorate Propellants", Solid Propellant Rocket Research, Progress in Astronautics and Rocketry Series, Vol. 1, Academic Press, New York, 1960, pp. 141-182.
15. Krier, H., T'ien, J. S., Sirignano, W. A., and Summerfield, M., "Non-steady Burning Phenomena of Solid Propellants: Theory and Experiments", AIAA Journal, Vol. 6, No. 2, Feb. 1968, pp. 178-185.
16. Summerfield, M., "Control of Solid Propellant Burning Rates by Acoustic Energy", ARS Journal, Vol. 29, Oct. 1959, pp. 791-792.
17. Rod, R. L., Combustion Control Systems, U.S. Patent 3,066,482, Filed 2 Feb. 1959; issued 4 Dec. 1962 (assigned to Acoustica Associates, Inc.)
18. Povinelli, L. A., "Study of Composite Solid Propellant Flame Structure Using a Spectral Radiation Shadowgraph Technique", AIAA Journal, Vol. 3, No. 9, Sept. 1965, pp. 1580-1584.
19. Derr, R. L. and Osborn, J. R., "An Experimental Investigation of the Gaseous Phase Reaction Zone in a Composite Solid Propellant", TM-67-6, Sept. 1967, Jet Propulsion Center, Purdue University, Lafayette, Indiana.
20. Yamazaki, K., Hayashi, M. and Iwama, A., "The Effect of Sound Waves on the Burning Velocity of a Solid Propellant", Int. Chem. Eng., Vol. 5, No. 1, 1965, pp. 156-190.
21. Elias, I., Cheung, H., and Cohen, N. S., "Acceleration of Burning Rate of Composite Propellants by Sound Waves", AIAA Journal, Vol. 3, No. 6, June 1965, pp. 1167-1168.
22. Hall, K. P., Bastress, E. K., and M. Summerfield, Burning Rate Control Factors in Solid Propellants, Initial Progress Report, Princeton University Aeronautical Engineering Report No. 446-a, April 1959.
23. Hall, K. P., Bastress, E. K., and M. Summerfield, Burning Rate Control Factors in Solid Propellants, Third Quarterly Status Report, Princeton University Aeronautical Engineering Report No. 446-c, March 1960.
24. Elias, Isidor, Investigation of Solid Propellant Burning Rate Control by Acoustic Means, Report No. D0574 Acoustic Associates, Inc. September 1963.
25. Elias, Isidor, "Sonic Combustion Control", Sound, Vol. 2, No. 6, Nov.-Dec. 1963, pp. 8-12.

26. Manfred, R. K., Lista, E. L., O'Neill, P., "Fast-Burning Propellants Containing Porous Ammonium Perchlorate", 3rd ICRPG/AIAA Solid Propellant Conference, June 1968.
27. Stang, P. L., personal communication, 17 Oct. 1969.
28. Marston, C. H., Controlled Hot Gas Generation from Solid Propellant, Ph.D. Thesis, Massachusetts Institute of Technology, 1962.
29. Stokes, B. B., Ram Design Evolution for Control of Solid Propellant Hot Gas Generation, MSME Thesis, Massachusetts Institute of Technology, 1963.
30. Mann, R. W., Marston, C. H., and Stokes III, B.B., "Control of Solid Propellant Combustion", Journal of Spacecraft and Rockets, Vol. 3, No. 8, Aug. 1966, pp. 1196-1201.
31. Paul, Igor, Solid Propellant Burning Rate Control Through Mechanical Variation of Heat Transfer from the Combustion Flame, Ph.D. Thesis, Massachusetts Institute of Technology, 1964.
32. Shapiro, A. H., The Dynamics and Thermodynamics of Compressible Fluid Flow, Vol. I, The Ronald Press, N. Y. 1953.
33. Saderholm, C. A., "A Characterization of Erosive Burning for Composite H-Series Propellants", Presented at the 1964 AIAA Solid Propellant Rocket Conference.
34. Hill, P. R., A Method of Computing the Transient Temperature of Thick Walls From Arbitrary Variation of Adiabatic Wall Temperature and Heat Transfer Coefficient, NACA TR 1372.
35. Shapiro, A. H., Siegel, R., and Kline, S. J., "Friction Factor in the Laminar Entry Region of a Smooth Tube", Proceedings of the Second U. S. National Congress of Applied Mechanics, ASME, 1954, pp. 733-741.
36. Rohsenow, W. M. and Choi, H. Y., Heat Mass and Momentum Transfer, Prentice-Hall Inc., Englewood Cliffs, N.J. 1961 p. 166.
37. Caveny, L. H. and Sawyer, T. T., "Solid-Propellant Burning Along a Tube Heated by Combustion Gas Influx", AIAA Journal, Vol. 6, No. 11, Nov. 1967, pp. 2004-2010.
38. Caveny, L. H., Glick, R. L., and Sawyer, T. T., "Heated Tube Method for Command Variation of Thrust (U)", ICRPG/AIAA Solid Propulsion Conference, CPIA Publ. No. 111, Vol. II, (June 1966), pp. 3-19, Confidential, also, The Investigation and Demonstration of a Unique Method of Command Thrust Modulation, Final Report, Thiokol Chemical Corporation, Huntsville, Alabama, Control No. C-66-12A, March 1966, Confidential.

39. Bird, R. B., Stewart, W. E., and Lightfoot, E. N., Transport Phenomena, Wiley, New York, 1960, pp. 196-200.
40. Helman, D. and Spiegler, E., "Propulsion With Chord Grains", Israel Journal of Technology, Vol. 3, No. 1, 1965, pp. 38-49.
41. Flanigan, D. A., Investigation of Mechanism of Solid Propellant Burning Rate, Final TR AFRPL-TR-67-18, Jan. 1967, Thiokol Chemical Corp., Huntsville, Ala.
42. Pittman, C. U., "The Location and Mode of Action of Burning Rate Catalysts in Composite Propellant Combustion", AIAA Journal, Vol. 7, No. 2, Feb. 1969, pp. 328-333.
43. Flanigan, D. A., personal communication, 8 Aug. 1969.
44. Mathes, K. N., "Electrical Properties", Encyclopedia of Polymer Science and Technology, 1st ed., Vol. 5, John Wiley & Sons, New York, 1966, pp. 528-628.
45. Petersen, R. E. and Payne, C. E., Effects of Electrostatic Fields on Solid Propellant Burn Rate, Technical Report AFRPL-TR-69-40, Air Force Rocket Propulsion Laboratory, Edwards, California, Feb. 1969; also "Electrostatic Field Control of Solid Propellant Burning Rate", Proceedings of 4th ICRPG Solid Propulsion Meeting, CPIA Publ. No. 188, Vol. 1, pp. 247-262.
46. Voelke, H. P., "Thermal Decomposition and Electrical Resistance of Ammonium Perchlorate Under High Pressure", Proceedings of 2nd Combustion Conference CPIA Publ. No. 105, May 1966, pp. 313-318.
47. Wood, W. A., personal communication, 5 February 1970.
48. Wood, W. A., "Published Comments on propellant resistivity", Proceedings of Second ICRPG Combustion Conference, CPIA Publ. 105, May 1966, p. 457.
49. Warfield, R. W. and Rosen, A. H., "Hardening of Solid Propellants", ARS Journal, Vol. 32, No. 11, Nov. 1962, pp. 1748-1749.
50. Steinz, J. A., Stang, P. L., and Summerfield, M., "The Burning Mechanism of Ammonium Perchlorate-Based Composite Solid Propellants", AIAA Paper No. 68-658, June 1968; also, Steinz, J. A., Ph.D. Dissertation, Feb. 1969, Princeton University, Princeton, N. J.

51. Dickinson, L. A., "Command Initiation of Finite Wave Axial Combustion Instability in Solid Propellant Rocket Engines", ARS Journal, Apr. 1962, pp. 643-644.
52. Crump, J. E. and Price, E. W., "Effect of Acoustic Environment on the Burning Rate of Solid Propellants", AIAA Journal, Vol. 2, No. 7, July 1964, pp. 1274-1278.
53. Crump, J. E., "Aluminum Combustion in Composite Propellants", Proceedings of Second ICRPG Combustion Conference, CPIA Publ. 105, May 1966, pp. 321-329.
54. Watermeier, L. A., Aungst, W. P., and Pfaff, S. P., "An Experimental Study of the Aluminum Additive Role in Unstable Combustion of Solid Propellants", Ninth Symposium (International) on Combustion, Academic Press, New York, 1963, pp. 316-326.
55. Rothstein, M., "Dielectric Heating", Encyclopedia of Polymer Science and Technology, 1st ed., Vol. 5, John Wiley & Sons, New York, 1966, 1-23.
56. Gaydon, A. G. and Wolfhard, H. G., Flames - Their Structure, Radiation and Temperature, Chapman and Hall, Ltd., London, 1960,
57. Payne, K. G. and Weinberg, F. J., "A Preliminary Investigation of Field-Induced Ion Movement in Flame Gases and its Applications", Proceedings of the Royal Society of London, Vol. 250, Apr. 1959, pp. 316-336.
58. Lawton, J. and Weinberg, F. J., "Maximum Ion Currents from Flames and the Maximum Practical Effects of Applied Electric Fields", Proceedings of the Royal Society of London, Vol. 277, Feb. 1964, pp. 468-497.
59. Mayo, P. J., Watermeier, L. A., and Weinberg, F. J., "Electrical Control of Solid Propellant Burning", Proceedings of the Royal Society of London, Vol. 284, 1965, pp. 488-498.
60. Stones, J. L., "Effects of Electrostatic Fields on the Combustion of Solid Propellants", Proceedings of 2nd. Combustion Conference CPIA Publ. No. 105, May 1966, pp. 449-460.
61. Brower, F. M., et al, High Energy Propellant Ingredient Research and Development, Final Technical Report AFRPL - TR-67-37, The Dow Chemical Company, Jan. 67, pp. 54-55.
62. Caveny, L. H. and Pittman, C. U., "Contribution of Solid-Phase Heat Release to AP Composite-Propellant Burning Rate", AIAA Journal, Vol. 6, No. 8, Aug. 1968, pp. 1461-1467.

63. King, M. K., McHale, E. T., "An Optical Bomb Study of the Combustion of Solid Propellants in High Acceleration Fields" Atlantic Research Corporation, July, 1969.
64. Sturm, E. J. and Reichenbach, R. E., "An Experimental Study of the Burning Rates of Aluminized Composite Solid Propellants in Acceleration Fields", presented at the 1968 ICRPG/AIAA 3rd Solid Propulsion Conference, Atlantic City, New Jersey, 4-6 June, 1968, AIAA Paper No. 68-529.
65. Northam, G. B., Effects of Steady-State Acceleration on Combustion Characteristics of an Aluminized Composite Solid Propellant, NASA TN D-4914, December, 1968.
66. Crowe, C. T. and Willoughby, P. G., "Effect of Spin on the Internal Ballistics of a Solid Propellant Rocket Motor", AIAA Preprint No. 66-523, presented at the AIAA 4th Aerospace Sciences Meeting (West Coast), June 27-29, 1966
Also, "Investigation of Particle Growth and Ballistics Effects on Solid Propellant Rockets", United Technology Center Rept. UTC 2128-FR, June, 1968
67. Anderson, J. B. and Reichenbach, R.E., "An Investigation of the Effect of Acceleration on the Burning Rate of Composite Propellants", AIAA Journal, Vol. 6, No. 2, 1968 pp. 271-277.
68. Glick, R. L., Hodge, B. K., and Caveny, L. H., "Effect of Acceleration on the Burning Rate of Composite Propellants", Thiokol Chemical Corporation, AIAA Paper 67-470, July, 1967.
69. Stones, J. L., The Effects of Electrostatic Fields on the Combustion of Solid Propellant and the Use of Absorption Liners in Solid Propellant Rocket Motors, Ministry of Aviation Contract No. PD/31/014/R1, Dept. of Fuel Technology and Chemical Engineering, University of Sheffield, England, January 1967.

DOCUMENT CONTROL DATA - R & D

(Security classification of title, body of abstract and indexing annotation must be entered when the overall report is classified.)

| | | | |
|--|--|---|--|
| 1. ORIGINATING ACTIVITY (Corporate author) Princeton University Department of Aerospace and Mechanical Sciences Princeton, New Jersey 08540 | | 2a. REPORT SECURITY CLASSIFICATION UNCLASSIFIED | |
| | | 2b. GROUP N/A | |
| 3. REPORT TITLE A Feasibility Study of Command Control of Solid Propellant Burning Rate | | | |
| 4. DESCRIPTIVE NOTES (Type of report and inclusive dates) Final Report | | | |
| 5. AUTHOR(S) (First name, middle initial, last name) Leonard H. Caveny and Martin Summerfield | | | |
| 6. REPORT DATE February 1970 | 7a. TOTAL NO. OF PAGES 112 | 7b. NO. OF REFS 68 | |
| 8a. CONTRACT OR GRANT NO F04611-69-C-0067 | 9a. ORIGINATOR'S REPORT NUMBER(S) AMS Report No. 893 | | |
| b. PROJECT NO | 9b. OTHER REPORT NO(S) (Any other numbers that may be assigned this report) AFRPL - TR - 69-249 | | |
| c. | | | |
| d. | | | |
| 10. DISTRIBUTION STATEMENT This document is subject to special export controls and each transmittal to foreign governments or foreign nationals may be made only with prior approval of AFRPL(RPORT/STINFO), Edwards, California 93523 | | | |
| 11. SUPPLEMENTARY NOTES | | 12. SPONSORING MILITARY ACTIVITY Air Force Rocket Propulsion Laboratory Edwards, California 93523 | |
| 13. ABSTRACT Analytical studies of twenty methods of command control of burning rate were performed to help establish which methods are most likely to be effective. Any method which offers a $\pm 5\%$ or greater throttleability is of interest. Since the study was not directed at a particular application, problems of implementation were not considered in detail. The approaches which received the greatest attention include: thermal radiation by injected particles and inserted intensifiers, acoustic energy, penetration of thermal wave by back flow of combustion gases into either perforated propellants or embedded porous elements, injection of burning rate catalysts, rammed propellant surfaces, and resistive heating. Other methods which were surveyed include: partial quenching, heating through vibration, induced unstable burning, dielectric heating, resistive wire networks, electrical and electromagnetic effects on flames and ingredient decomposition, acceleration forces, and utilization of photochemical processes. The thermal radiation methods should produce 10-50% increases in pressure level, but a practical radiation source is not apparent. The penetration of thermal waves into perforated propellants offers a wide range of control ($>10:1$), but feasibility of controlled burning is not established. The embedded porous element approach should produce $> 8:1$ control in high performance systems with reasonable developmental risks. Injection of catalysts is dependent on finding a method of delivering micron size particles to the propellant reaction zones. Two propellants of dissimilar composition when rammed together, may produce a very wide range of control. Radiation and electrical methods which accelerate the decomposition of some propellant ingredients are largely untried and offer potential. The results emphasize that the merit and practicality of each method is largely dependent on the application. | | | |

| 14 KEY WORDS | LINK A | | LINK B | | LINK C | |
|----------------------------|--------|----|--------|----|--------|----|
| | ROLE | WT | ROLE | WT | ROLE | WT |
| Solid propellant | | | | | | |
| Propellant combustion | | | | | | |
| Burning rate control | | | | | | |
| Thrust modulation | | | | | | |
| Controllable rocket motors | | | | | | |
| Burning rate augmentation | | | | | | |
| Thermal radiacion | | | | | | |
| Porous propellants | | | | | | |